ChemistryOPEN

Supporting Information

De Novo Modular Development of a Foldameric Protein–Protein Interaction Inhibitor for Separate Hot Spots: A Dynamic Covalent Assembly Approach

Éva Bartus, Zsófia Hegedüs, Edit Wéber, Brigitta Csipak, Gerda Szakonyi, and Tamás A. Martinek*[a]

open_201700012_sm_miscellaneous_information.pdf

Table of contents

Supplementary text

Design and synthesis of the folded fragment library

To achieve a quasi-equimolar library composition, double coupling of sub-stoichiometric amounts of the acylating amino acid mixtures (0.8 equivalent)[1] were used in positions 2 and 5, utilizing a long coupling time and microwave irradiation. The foldameric fragments were identified via HPLC-MS/MS measurements (Table S1-4), and the estimated library purities were in the range of ~69% to ~84% with acceptable equimolarity (Supplementary Fig. 1).

Mapping the hot spot regions of the model protein

CaM was immobilized through a His-tag, which was incubated with the folded fragment libraries. After washing away the unbound fragments, the CaM-foldamer complexes were eluted and analysed using HPLC-MS. The integrated peaks were referenced to the control library and expressed in percentages, which provided an interaction map of CaM (Fig. 2b and Supplementary Fig. 2).

Supplementary materials and methods

Synthesis and purification of the folded fragment libraries

Foldamer libraries were synthesized using a CEM Liberty 1 microwave peptide synthesizer by the manual addition of amino acids. The four sub-libraries consisted of aromatic and β^3-*h*Met (**L1)**; charged (**L2**); apolar (**L3**) and non-charged, polar (**L4**) amino acid side-chains.

Rink Amide PS resin was used for solid support and HATU (1-[bis(dimethylamino)methylene]-1H-1,2,3-triazolo[4,5-b]pyridinium 3-oxid hexafluorophosphate) was used as a coupling reagent. Fmoc-(1*S*,2*S*)-ACHC ((1*S*,2*S*)-Fmoc-2-aminocyclohexane carboxylic acid) was applied in excess of 3 equivalents at 75 °C for 30 min. β^3- amino acid mixtures were double coupled using 0.8 equivalents at 75 °C for 45 min. 16 different β^3-amino acids were coupled in position 5 and 4 different amino acids in the position 4, which yielded 64 different components in each sublibrary. The deprotection solution was 2 % piperidine 2 % DBU (1,8-diazabicycloundec-7-ene) in DMF (*N,N*-dimethylformamide), deprotection were carried out for 10 min at 75 °C. The foldamer mixture was cleaved by 90 % TFA (trifluoroacetic acid), 5 %

DTT (dithiothreitol), 5 % water, then the TFA was evaporated and the resin washed with acetic acid and water. The mixture was lyophilized. The library was purified by using RP-HPLC (Phenomenex Luna C18, 250x10 mm column). Fractions were analysed by MS and each fraction that contained library members was pooled together. Library components were identified by HPLC-MS based on molecular weight and retention time estimated by hydrophobic properties of the peptides. Purity analysis was based on quantification of the total library members and impurities by integration of the HPLC-MS chromatograms.

Synthesis purification of the pure foldamer sequences

Foldameric sequences were synthesized manually using standard solid-phase peptide synthesis with Fmoc chemistry. Tentagel R RAM resin was used as solid support and HATU as coupling reagent. Amino acids and coupling reagents were used in excess of 3 equivalents and with shaking at room temperature for 3 h. Deprotection was carried out using a DMF solution containing 2 % DBU and 2 % piperidine. Cleavage was performed with TFA/H_2O/DTT/TIS (triisopropylsilane) (90:5:2.5:2.5), which was followed by precipitation in ice-cold diethyl ether. The resin was washed with acetic acid and water, filtered, then lyophilized. Peptides were purified by RP-HPLC on a C18 column (Phenomenex Jupiter, 10x250 mm). The HPLC eluents were 0.1% TFA in water and 0.1% TFA, 80% ACN in water. Purity was confirmed by analytical RP-HPLC and ESI MS measurements.

Synthesis and purification of heterodimer 18

Chloroacetylated **12** was synthesized on a solid support with C-terminal 4-methyltrityl (Mtt)-protected lysine. The Mtt protecting group was eliminated with a treatment of AcOH/TFE/DCM (2:1:7) for 1 h. Chloroacetic acid was coupled to the ε-amino group of lysine in excess of 5 equivalents with DCC/HOAt activation. The crude peptide (**12-Lys(ClAc)**) was cleaved from the resin with a mixture of TFA/H_2O/TIS (92:5:3) and followed by precipitation in ice-cold diethyl ether. The resin was washed with acetonitrile and water, then filtered and lyophilized. Crude peptide was purified by RP-HPLC on a C18 column (Phenomenex Luna, 250 x 10.00 mm). The purified **12-Lys(ClAc)** was completely dissolved in 0.1 M Tris buffer (pH = 8.2) with acetonitrile as a co-solvent. Previously purified **9-SH** was dissolved in the same buffer in 1.5 molar excess and added to the reaction mixture under continuous stirring (Supplementary Fig. 6.). After overnight incubation at room temperature, the mixture was

injected directly onto a C18 HPLC-column and purified. Purity was confirmed by analytical RP-HPLC and ESI-MS measurements.

CaM expression, isotope labeling and purification

Calmodulin (CaM) (*bovine*) gene was cloned into pET28a vector. The sequenced plasmid was then transformed to competent *E. Coli* cells (BL21 DE3) for protein expression. Cells were grown on LB liquid media at 37 °C until OD600 = 0.5, then expression of CaM was induced by adding 200 μM IPTG and was carried out overnight (~19 hours) at 22 °C. After centrifugation, cell pellets were resuspended in Ni-NTA Lysis Buffer (50 mM NaH_2PO_4, 300 mM NaCl, 10 mM imidazole, pH 8.0) and were lysed by sonication with addition of 1 μM Leupeptin, 0.1 μg/ml Pepstatin A and 20 μM PMSF. The cleared lysate was first purified using a Ni-NTA filled column according to the manufacturer's protocol (Expression and purification of proteins using 6×Histidine-tag): After equilibration of the Ni-NTA column, lysate was added for a short incubation on ice (30 min), washed with Ni-NTA Wash Buffer (50 mM NaH_2PO_4, 300 mM NaCl, 20 mM imidazole, pH 8.0), and finally CaM was eluted with small volumes of Ni-NTA Elution buffer (50 mM NaH_2PO_4, 300 mM NaCl, 250 mM imidazole, pH 8.0).The clear fractions were concentrated using Amicon Ultra Filter Device (10K) and the buffer was changed to 20 mM HEPES, pH 7.0. The His-tag was removed with an overnight Thrombin digestion at 4 °C leaving 9 extra amino acid (GSHMARSNS) on the N terminus of the protein. Thus, the molecular weight of the protein was 17765.58 g/mol, which was confirmed by ESI-MS measurements.

In order to remove additional cleavage fragments after thrombin treatment CaM was purified by using RP-HPLC on a C4 (Phenomenex, Jupiter 250x10 mm) column, using a gradient of 40-70% B over 60 minutes at 4 ml min^{-1} flow rate with A: 0.1% TFA/ H_2O and B: 0.1% TFA in 20% H_2O, 80% ACN. After lyophilization, the protein was subjected to dialysis in 20 mM, pH 7.0 HEPES buffer in order to remove TFA traces and ensure correct folding. Purity and folding was assessed by HPLC-MS, native ESI-MS and NMR measurements. CaM concentration was measured by using BCA assay (Thermo Scientific, Pierce) utilizing the manufacturer's protocol.

Tryptophan fluorescence blue-shift measurements. Fluorescence experiments were carried out using a Hitachi F-2500 fluorescence spectrophotometer (PMT voltage: 700 V, response: 0.08 s) at room temperature, in 20 mM HEPES, pH= 7.4 and 150 mM NaCl, containing 1 mM

$CaCl_2$ or 5 mM EDTA. Tryptophan excitation was performed at 295 nm to minimize contributions of CaM tyrosines to the emission spectra. Emission spectra were recorded from 305 to 400 nm and the excitation and emission bandwidths were set at 5 nm. For determination of K_D, 1 ml of 0.2 μM foldamer solutions were titrated with CaM from stocks 2-100 μM, so that the final added volume was < 2% of the total volume. The fluorescence intensity at 330 nm was monitored, and the results from three replicates were analyzed using one site-specific binding nonlinear regression analysis (GraphPad Prism 5.03). Nonspecific binding between the foldamers and CaM was measured in the presence of EDTA, and this titration was subtracted from total binding from the same titrations in $CaCl_2$.

Native gel electrophoresis

Native gel electrophoresis was run under non-denaturing condition that is suitable for the detection of protein-protein interactions or complex formation. The gel was prepared from 1.2 ml 30 % acryl-amide (Serva), 3 ml 2 × Gel buffer (480 mM glycine, 50 mM Tris), 1.8 ml distilled water, 60 μl 10 % APS (ammonium peroxydisulfate) and 2.5 μl TEMED (*N*,*N*,*N*′,*N*′-Tetramethylethane-1,2-diamine). After polymerization, the gel was pre-run for 30 minutes, using 200 V voltage at 4 °C (Running buffer: 240 mM glycine, 25 mM Tris). CaM Samples were prepared in pH 7.0 20 mM HEPES buffer containing 30 mM $CaCl_2$ using 100 μM protein concentration. The foldamer was added in different equivalents from a 1 mM stock solution prepared in DMSO. 10 μl of the samples were mixed with 2 μl 50 % glycerol, loaded into the pockets and followed by 30 minutes long run with the same settings as the pre-run. The gel was then treated with Coomassie Brilliant Blue G250 dye for 30 minutes and destained with a methanol and acetic-acid containing solution.

CaM-Sepharose pulldown experiments

A pulldown experiment was performed by using CaM-Sepharose 4B resin. 700 μl (1 mg/ml) resin washed 3 times with buffer A (20 mM HEPES, pH=7.4, with 150 mM NaCl and 2 mM $CaCl_2$) and saturated with TRPV1-CT_{15} at 200 μM concentration for 30 min at room temperature. After the incubation, unbound peptide was completely washed with buffer A and separated into 7 equivalent volume portions (7 x 100 μl) Each portion was incubated with different concentrations of **18** (0-100 μM) for 30 min at room temperature and the eluted mixtures were collected and measured with HPLC-MS. Resin portions were washed several times with buffer A to remove unbounded peptides. The final elution was carried out by buffer B (20 mM HEPES pH=7.4, 150 mM NaCl and 2 mM EDTA). Samples were measured with

HPLC-MS, using 5-80 % during 15 min gradient elution (flow rate: 0.7 ml/min; selective ion monitoring mode m/z= 706-708 and m/z=899-901).

LC-MS methods and parameters

HPLC/ESI-MS analysis was used to characterize the samples from the pull-down assay and the composition of DCL. LC-MS analysis was performed with a Thermo Scientific Dionex UltiMate 3000 HPLC system interfaced to an LTQ ion trap mass spectrometer (Thermo Electron Corp., San Jose, CA, USA). Samples were injected onto an Aeris Widepore XB-C18 (250 x 4.6 mm) analytical HPLC column using gradient elution 5-80 % solution B during 25 minutes. For pull-down samples, eluent composition was 0.1 % acetic acid in distilled water (Solution A) and 0.1 % acetic acid in acetonitrile (solution B) and DCL samples were measured at 50 °C column temperature with 0.1 % formic acid in distilled water used for solution A and 0.1 % formic acid in acetonitrile for solution B. Mass spectra were acquired in full scan mode from 200 to 2000 m/z range. For overlapping peaks, selective reaction monitoring (SRM) was used.

MS data analysis

Thermo Xcalibur 2.2 software was used for peak identification and integration. The 83 % of the foldameric fragments could be resolved independently, *via* HPLC-MS/MS measurements based on molecular weight, MS fragmentation pattern and retention time considering the relative hydrophobicity of the side-chains. (Table S1-4). The majority of the unresolved peaks were foldamers that contained β^3-*h*Ile or β^3-*h*Leu in position 5. These were integrated and averaged. A representative raw file for each sub-library was utilized to create a processing method where each sample component was associated to a chromatographic peak based on the previously identified mass (m/z) and retention time (Supporting Table S1-S4). Using ICIS peak detection algorithm the general detection and integration criteria were smoothing points: 5, baseline window: 80, area noise factor: 5, peak noise factor: 10. Using these processing setups, all raw data files were reprocessed together and analyzed. Errors in peak identification during the automatic processing were corrected manually.

Solution NMR experiments for structural analysis of the peptides

Peptides were dissolved in 20 mM pH 7.0 d_{18}-HEPES (90% H_2O, 10% D_2O) containing 0.02 % NaN_3 and 30 mM $CaCl_2$ at a concentration of 90-500 μM, depending on the solubility of the compound. NMR experiments were performed at 298 K. All spectra were acquired with the excitation sculpting solvent suppression pulse scheme with 2048 time domain points and 256 increments. 2D TOCSY measurements were performed with homonuclear Hartman–Hahn transfer with a mixing time of 80 ms (DIPSI2 sequence). 2D ROESY spectra were recorded with a mixing time of 400 ms. The number of scans varied between 8 and 64, depending on the concentration of the sample. In order to assess the bound conformation of the ligands, 0.02 equivalent CaM was added to the samples and 2D NOESY spectra were recorded with a mixing time of 150 ms. Control NOESY spectra were recorded in the absence of the protein.

NMR – ^{15}N HSQC titration experiments

^{15}N-HSQC titration NMR experiments were carried out on a Bruker Avance III 600 MHz spectrometer equipped with a 5 mm CP-TCI triple-resonance cryoprobe. ^{15}N/^{13}C CaM (purchased from Creative Biolabs) was dissolved in 20 mM pH 7.0 d_{18}-HEPES buffer (90 % H_2O, 10 % D_2O) containing 30 mM $CaCl_2$ and 0.02 % NaN_3. Reference 2D heteronuclear ^{15}N-HSQC spectrum was acquired for the ligand-free CaM at a concentration of 45 μM at 30 °C with 256 increments and 16 scans. Foldamers **2** and **3** were added to the ^{15}N/^{13}C CaM sample in solid form (aliquoted and lyophilized from solutions) and ^{15}N-HSQC spectra were measured again in the presence of **2** or **3**, resulting in a series of CaM spectra with 0.5, 1.0, 1.5, 2.0, 3.0 and 4.0 equivalent peptides. Chemical shift assignment was based upon literature data and verified by standard triple-resonance NMR experiments. Processing was carried out by using Topspin 3.5 (Bruker) and processed data were analysed with Sparky 3.114 (T. D. Goddard and D. G. Kneller, SPARKY 3, University of California, San Francisco). The chemical shift perturbation (CSP) values were calculated by using the formula $[(\Delta\delta(^1H))^2 + 0.14*(\Delta\delta(^{15}N))^2]^{1/2}$.

Supplementary Figures and Tables

Table S1. Characterization data of L1

β^3-amino acid		Detected peaks			MS^2 fragment ions			Pull down assay	
2nd	5th	$[M+H^+]^{1+}$	$[M+2H^+]^{2+}$	Rt (min)	b4	y4	y3	Detected ion	Remark
F	A	764.67	382.75	14.50	537.32	478.34	353.26	$[M+H^+]^{1+}$	
F	D	808.56	404.75	13.07	537.32	522.33	397.25	$[M+H^+]^{1+}$	
F	E	822.58	411.75	13.10	537.32	536.34	411.26	$[M+H^+]^{1+}$	
F	F	840.58	420.76	16.52	537.32	554.36	429.28	$[M+H^+]^{1+}$	
F	I	806.67	403.77	16.79	537.32	520.38	395.30	$[M+H^+]^{1+}$	average integral of FI, FL
F	K	821.58	411.28	10.07	537.32	535.39	410.31	$[M+2H^+]^{2+}$	
F	L	806.67	403.77	16.79	537.32	520.38	395.30	$[M+H^+]^{1+}$	average integral of FI, FL
F	M	824.67	412.75	15.27	537.32	538.34	413.26	$[M+H^+]^{1+}$	
F	N	807.58	404.25	12.22	537.32	521.34	396.26	$[M+H^+]^{1+}$	
F	Q	821.58	411.26	12.36	537.32	535.35	410.27	$[M+H^+]^{1+}$	
F	R	849.67	425.28	10.12	537.32	563.40	438.32	$[M+2H^+]^{2+}$	
F	S	780.58	390.75	12.64	537.32	494.33	369.25	$[M+H^+]^{1+}$	
F	T	794.67	397.75	13.26	537.32	508.34	383.26	$[M+H^+]^{1+}$	
F	V	792.67	396.76	16.11	537.32	506.36	381.28	$[M+H^+]^{1+}$	
F	W	879.67	440.27	16.36	537.32	593.37	468.29	$[M+H^+]^{1+}$	
F	Y	856.67	428.76	14.57	537.32	570.36	445.28	$[M+H^+]^{1+}$	
M	A	748.67	374.74	13.17	521.30	478.34	353.26	$[M+H^+]^{1+}$	
M	D	792.67	396.74	12.05	521.30	522.33	397.25	$[M+H^+]^{1+}$	
M	E	806.67	403.74	12.21	521.30	536.34	411.26	$[M+H^+]^{1+}$	
M	F	824.67	412.75	15.43	521.30	554.36	429.28	$[M+H^+]^{1+}$	
M	I	790.67	395.76	15.54	521.30	520.38	395.30	$[M+H^+]^{1+}$	average integral of MI, ML
M	K	805.67	403.27	9.36	521.30	535.39	410.31	$[M+2H^+]^{2+}$	
M	L	790.67	395.76	15.54	521.30	520.38	395.30	$[M+H^+]^{1+}$	average integral of MI, ML
M	M	808.56	404.74	14.30	521.30	538.34	413.26	$[M+H^+]^{1+}$	
M	N	791.67	396.24	11.30	521.30	521.34	396.26	$[M+H^+]^{1+}$	
M	Q	805.67	403.25	11.51	521.30	535.35	410.27	$[M+H^+]^{1+}$	
M	R	833.47	417.27	9.45	521.30	563.40	438.32	$[M+2H^+]^{2+}$	
M	S	764.67	382.74	11.69	521.30	494.33	369.25	$[M+H^+]^{1+}$	
M	T	778.67	389.74	12.24	521.30	508.34	383.26	$[M+H^+]^{1+}$	
M	V	776.67	388.75	14.84	521.30	506.36	381.28	$[M+H^+]^{1+}$	
M	W	863.67	432.26	15.33	521.30	593.37	468.29	$[M+H^+]^{1+}$	
M	Y	840.58	420.75	13.43	521.30	570.36	445.28	$[M+H^+]^{1+}$	
W	A	803.50	402.26	14.28	576.33	478.34	353.26	$[M+H^+]^{1+}$	
W	D	847.67	424.25	13.18	576.33	522.33	397.25	$[M+H^+]^{1+}$	
W	E	861.66	431.26	13.11	576.33	536.34	411.26	$[M+H^+]^{1+}$	
W	F	879.67	440.27	16.06	576.33	554.36	429.28	$[M+H^+]^{1+}$	
W	I	845.75	423.28	16.27	576.33	520.38	395.30	$[M+H^+]^{1+}$	average integral of WI, WL
W	K	860.75	430.78	10.31	576.33	535.39	410.31	$[M+2H^+]^{2+}$	
W	L	845.75	423.28	16.27	576.33	520.38	395.30	$[M+H^+]^{1+}$	average integral of WI, WL
W	M	863.67	432.26	15.09	576.33	538.34	413.26	$[M+H^+]^{1+}$	
W	N	846.67	423.76	12.45	576.33	521.34	396.26	$[M+H^+]^{1+}$	
W	Q	860.75	430.76	12.52	576.33	535.35	410.27	$[M+H^+]^{1+}$	
W	R	888.75	444.79	10.35	576.33	563.40	438.32	$[M+2H^+]^{2+}$	
W	S	819.67	410.25	12.81	576.33	494.33	369.25	$[M+H^+]^{1+}$	
W	T	833.47	417.26	13.20	576.33	508.34	383.26	$[M+H^+]^{1+}$	
W	V	831.67	416.27	15.71	576.33	506.36	381.28	$[M+H^+]^{1+}$	
W	W	918.67	459.77	15.93	576.33	593.37	468.29	$[M+H^+]^{1+}$	
W	Y	895.67	448.27	14.36	576.33	570.36	445.28	$[M+H^+]^{1+}$	
Y	A	780.67	390.75	12.72	553.32	478.34	353.26	$[M+H^+]^{1+}$	
Y	D	824.67	412.75	11.82	553.32	522.33	397.25	$[M+H^+]^{1+}$	
Y	E	838.67	419.75	11.94	553.32	536.34	411.26	$[M+H^+]^{1+}$	
Y	F	856.67	428.76	14.46	553.32	554.36	429.28	$[M+H^+]^{1+}$	
Y	I	822.58	411.77	14.60	553.32	520.38	395.30	$[M+H^+]^{1+}$	average integral of YI, YL
Y	K	837.67	419.28	9.33	553.32	535.39	410.31	$[M+2H^+]^{2+}$	
Y	L	822.58	411.77	14.60	553.32	520.38	395.30	$[M+H^+]^{1+}$	average integral of YI, YL
Y	M	840.58	420.75	13.52	553.32	538.34	413.26	$[M+H^+]^{1+}$	
Y	N	823.67	412.25	11.16	553.32	521.34	396.26	$[M+H^+]^{1+}$	
Y	Q	837.67	419.26	11.32	553.32	535.35	410.27	$[M+H^+]^{1+}$	
Y	R	865.75	433.28	9.34	553.32	563.40	438.32	$[M+2H^+]^{2+}$	
Y	S	796.67	398.75	11.49	553.32	494.33	369.25	$[M+H^+]^{1+}$	
Y	T	810.67	405.75	11.86	553.32	508.34	383.26	$[M+H^+]^{1+}$	
Y	V	808.56	404.76	14.02	553.32	506.36	381.28	$[M+H^+]^{1+}$	
Y	W	895.67	448.27	14.51	553.32	593.37	468.29	$[M+H^+]^{1+}$	
Y	Y	872.58	436.76	12.96	553.32	570.36	445.28	$[M+H^+]^{1+}$	

Table S2. Characterization data of L2

β^3-amino acid		Detected peaks			MS^2 fragment ions			Pull down assay	
2nd	5th	$[M+H^+]^{1+}$	$[M+2H^+]^{2+}$	Rt (min)	b4	y4	y3	Detected ion	Remark
D	A	732.47	366.74	11.31	505.29	478.34	353.26	$[M+H^+]^{1+}$	
D	D	776.46	388.73	11.20	505.29	522.33	397.25	**y4**	
D	E	790.47	395.74	11.49	505.29	536.34	411.26	$[M+H^+]^{1+}$	
D	F	808.49	404.75	13.04	505.29	554.36	429.28	$[M+H^+]^{1+}$	
D	I	774.51	387.76	13.04	505.29	520.38	395.30	$[M+H^+]^{1+}$	average integral of DI, DL
D	K	789.52	395.26	9.06	505.29	535.39	410.31	$[M+2H^+]^{2+}$	
D	L	774.51	387.76	13.04	505.29	520.38	395.30	$[M+H^+]^{1+}$	average integral of DI, DL
D	M	792.47	396.74	12.16	505.29	538.34	413.26	$[M+H^+]^{1+}$	
D	N	775.47	388.24	10.51	505.29	521.34	396.26	$[M+H^+]^{1+}$	
D	Q	789.48	395.24	10.70	505.29	535.35	410.27	**y4**	
D	R	817.53	409.27	9.04	505.29	563.40	438.32	$[M+2H^+]^{2+}$	
D	S	748.46	374.73	10.88	505.29	494.33	369.25	$[M+H^+]^{1+}$	
D	T	762.47	381.74	11.11	505.29	508.34	383.26	**b4**	average integral of ES, DT
D	V	760.49	380.75	12.48	505.29	506.36	381.28	$[M+H^+]^{1+}$	
D	W	847.50	424.25	13.32	505.29	593.37	468.29	$[M+H^+]^{1+}$	
D	Y	824.49	412.75	11.72	505.29	570.36	445.28	$[M+H^+]^{1+}$	
E	A	746.48	373.74	11.54	519.30	478.34	353.26	$[M+H^+]^{1+}$	
E	D	790.47	395.74	11.23	519.30	522.33	397.25	$[M+H^+]^{1+}$	
E	E	804.48	402.74	11.40	519.30	536.34	411.26	$[M+H^+]^{1+}$	
E	F	822.50	411.75	13.15	519.30	554.36	429.28	$[M+H^+]^{1+}$	
E	I	788.52	394.76	13.15	519.30	520.38	395.30	$[M+H^+]^{1+}$	average integral of EI, EL
E	K	803.53	402.27	9.21	519.30	535.39	410.31	$[M+2H^+]^{2+}$	
E	L	788.52	394.76	13.15	519.30	520.38	395.30	$[M+H^+]^{1+}$	average integral of EI, EL
E	M	806.48	403.74	12.34	519.30	538.34	413.26	$[M+H^+]^{1+}$	
E	N	789.48	395.24	10.70	519.30	521.34	396.26	**b4**	
E	Q	803.49	402.25	10.95	519.30	535.35	410.27	$[M+H^+]^{1+}$	
E	R	831.54	416.27	9.21	519.30	563.40	438.32	$[M+2H^+]^{2+}$	
E	S	762.47	381.74	11.03	519.30	494.33	369.25	**b4**	average integral of ES, DT
E	T	776.48	388.74	11.20	519.30	508.34	383.26	**b4**	
E	V	774.50	387.75	12.62	519.30	506.36	381.28	$[M+H^+]^{1+}$	
E	W	861.51	431.26	13.56	519.30	593.37	468.29	$[M+H^+]^{1+}$	
E	Y	838.50	419.75	11.88	519.30	570.36	445.28	$[M+H^+]^{1+}$	
K	A	745.53	373.27	9.09	518.35	478.34	353.26	$[M+2H^+]^{2+}$	
K	D	789.52	395.26	9.33	518.35	522.33	397.25	$[M+2H^+]^{2+}$	
K	E	803.53	402.27	9.28	518.35	536.34	411.26	$[M+2H^+]^{2+}$	
K	F	821.55	411.28	10.31	518.35	554.36	429.28	$[M+2H^+]^{2+}$	
K	I	787.57	394.29	10.19	518.35	520.38	395.30	$[M+2H^+]^{2+}$	average integral of KI, KL
K	K	802.58	401.79	7.60	518.35	535.39	410.31	$[M+2H^+]^{2+}$	
K	L	787.57	394.29	10.19	518.35	520.38	395.30	$[M+2H^+]^{2+}$	average integral of KI, KL
K	M	805.53	403.27	9.69	518.35	538.34	413.26	$[M+2H^+]^{2+}$	
K	N	788.53	394.77	8.76	518.35	521.34	396.26	$[M+2H^+]^{2+}$	
K	Q	802.54	401.77	8.85	518.35	535.35	410.27	$[M+2H^+]^{2+}$	
K	R	830.59	415.80	7.40	518.35	563.40	438.32	$[M+2H^+]^{2+}$	average integral of RK, KR
K	S	761.52	381.26	8.86	518.35	494.33	369.25	$[M+2H^+]^{2+}$	
K	T	775.53	388.27	9.03	518.35	508.34	383.26	$[M+2H^+]^{2+}$	
K	V	773.55	387.28	9.80	518.35	506.36	381.28	$[M+2H^+]^{2+}$	
K	W	860.56	430.78	10.64	518.35	593.37	468.29	$[M+2H^+]^{2+}$	
K	Y	837.55	419.28	9.45	518.35	570.36	445.28	$[M+2H^+]^{2+}$	
R	A	773.54	387.27	9.19	546.36	478.34	353.26	$[M+2H^+]^{2+}$	
R	D	817.53	409.27	9.47	546.36	522.33	397.25	$[M+2H^+]^{2+}$	
R	E	831.54	416.27	9.34	546.36	536.34	411.26	$[M+2H^+]^{2+}$	
R	F	849.56	425.28	10.49	546.36	554.36	429.28	$[M+2H^+]^{2+}$	
R	I	815.58	408.29	10.32	546.36	520.38	395.30	$[M+2H^+]^{2+}$	average integral of RI, RL
R	K	830.59	415.80	7.34	546.36	535.39	410.31	$[M+2H^+]^{2+}$	average integral of RK, KR
R	L	815.58	408.29	10.42	546.36	520.38	395.30	$[M+2H^+]^{2+}$	average integral of RI, RL
R	M	833.54	417.27	9.81	546.36	538.34	413.26	$[M+2H^+]^{2+}$	
R	N	816.54	408.77	8.84	546.36	521.34	396.26	$[M+2H^+]^{2+}$	
R	Q	830.55	415.78	8.91	546.36	535.35	410.27	$[M+2H^+]^{2+}$	
R	R	858.60	429.80	7.65	546.36	563.40	438.32	$[M+2H^+]^{2+}$	
R	S	789.53	395.27	8.94	546.36	494.33	369.25	$[M+2H^+]^{2+}$	
R	T	803.54	402.27	9.08	546.36	508.34	383.26	$[M+2H^+]^{2+}$	
R	V	801.56	401.28	9.91	546.36	506.36	381.28	$[M+2H^+]^{2+}$	
R	W	888.57	444.79	10.74	546.36	593.37	468.29	$[M+2H^+]^{2+}$	
R	Y	865.56	433.28	9.55	546.36	570.36	445.28	$[M+2H^+]^{2+}$	

Table S3. Characterization data of L3

β^{3}-amino acid		Detected peaks			MS^2 fragment ions			Pull down assay	
2nd	5th	$[M+H^+]^{1+}$	$[M+2H^+]^{2+}$	Rt (min)	b4	y4	y3	Detected ion	Remark
A	A	688.48	344.74	12.00	461.30	478.34	353.26	$[M+H^+]^{1+}$	
A	D	732.47	366.74	11.34	461.30	522.33	397.25	$[M+H^+]^{1+}$	
A	E	746.48	373.74	11.42	461.30	536.34	411.26	$[M+H^+]^{1+}$	
A	F	764.50	382.75	14.20	461.30	554.36	429.28	b4	
A	I	730.52	365.76	14.38	461.30	520.38	395.30	b4	average integral of AI, AL
A	K	745.53	373.27	8.93	461.30	535.39	410.31	$[M+H^+]^{1+}$	
A	L	730.52	365.76	14.38	461.30	520.38	395.30	$[M+H^+]^{1+}$	average integral of AI, AL
A	M	748.48	374.74	13.20	461.30	538.34	413.26	$[M+H^+]^{1+}$	
A	N	731.48	366.24	10.66	461.30	521.34	396.26	$[M+H^+]^{1+}$	
A	Q	745.49	373.25	10.84	461.30	535.35	410.27	$[M+H^+]^{1+}$	
A	R	773.54	387.27	8.93	461.30	563.40	438.32	$[M+H^+]^{1+}$	
A	S	704.47	352.74	10.95	461.30	494.33	369.25	$[M+H^+]^{1+}$	
A	T	718.48	359.74	11.39	461.30	508.34	383.26	$[M+H^+]^{1+}$	
A	V	716.50	358.75	13.82	461.30	506.36	381.28	$[M+H^+]^{1+}$	
A	W	803.51	402.26	14.28	461.30	593.37	468.29	b4	
A	Y	780.50	390.75	12.38	461.30	570.36	445.28	$[M+H^+]^{1+}$	
I	A	730.52	365.76	14.54	503.34	478.34	353.26	b4	
I	D	774.51	387.76	12.79	503.34	522.33	397.25	$[M+H^+]^{1+}$	
I	E	788.52	394.76	12.95	503.34	536.34	411.26	$[M+H^+]^{1+}$	
I	F	806.54	403.77	16.56	503.34	554.36	429.28	$[M+H^+]^{1+}$	
I	I	772.56	386.78	16.90	503.34	520.38	395.30	$[M+H^+]^{1+}$	average integral of II, IL, LI, LI
I	K	787.57	394.29	9.84	503.34	535.39	410.31	$[M+H^+]^{1+}$	
I	L	772.56	386.78	17.22	503.34	520.38	395.30	$[M+H^+]^{1+}$	average integral of II, IL, LI, LI
I	M	790.52	395.76	15.49	503.34	538.34	413.26	$[M+H^+]^{1+}$	
I	N	773.52	387.26	11.92	503.34	521.34	396.26	$[M+H^+]^{1+}$	
I	Q	787.53	394.27	12.10	503.34	535.35	410.27	$[M+H^+]^{1+}$	
I	R	815.58	408.29	9.91	503.34	563.40	438.32	$[M+H^+]^{1+}$	
I	S	746.51	373.76	12.39	503.34	494.33	369.25	b4	
I	T	760.52	380.76	13.13	503.34	508.34	383.26	$[M+H^+]^{1+}$	
I	V	758.54	379.77	16.50	503.34	506.36	381.28	b4	
I	W	845.55	423.28	16.62	503.34	593.37	468.29	$[M+H^+]^{1+}$	average integral of IW, LW
I	Y	822.54	411.77	14.49	503.34	570.36	445.28	y4	
L	A	730.52	365.76	14.54	503.34	478.34	353.26	$[M+H^+]^{1+}$	
L	D	774.51	387.76	12.79	503.34	522.33	397.25	$[M+H^+]^{1+}$	
L	E	788.52	394.76	13.11	503.34	536.34	411.26	$[M+H^+]^{1+}$	
L	F	806.54	403.77	16.72	503.34	554.36	429.28	$[M+H^+]^{1+}$	
L	I	772.56	386.78	16.90	503.34	520.38	395.30	$[M+H^+]^{1+}$	average integral of II, IL, LI, LI
L	K	787.57	394.29	9.94	503.34	535.39	410.31	$[M+H^+]^{1+}$	
L	L	772.56	386.78	17.22	503.34	520.38	395.30	$[M+H^+]^{1+}$	average integral of II, IL, LI, LI
L	M	790.52	395.76	15.72	503.34	538.34	413.26	$[M+H^+]^{1+}$	
L	N	773.52	387.26	12.04	503.34	521.34	396.26	$[M+H^+]^{1+}$	
L	Q	787.53	394.27	12.22	503.34	535.35	410.27	$[M+H^+]^{1+}$	
L	R	815.58	408.29	10.03	503.34	563.40	438.32	$[M+H^+]^{1+}$	
L	S	746.51	373.76	12.39	503.34	494.33	369.25	b4	
L	T	760.52	380.76	13.36	503.34	508.34	383.26	$[M+H^+]^{1+}$	
L	V	758.54	379.77	16.50	503.34	506.36	381.28	b4	
L	W	845.55	423.28	16.62	503.34	593.37	468.29	$[M+H^+]^{1+}$	average integral of IW, LW
L	Y	822.54	411.77	14.63	503.34	570.36	445.28	y4	
V	A	716.50	358.75	13.53	489.32	478.34	353.26	$[M+H^+]^{1+}$	
V	D	760.49	380.75	12.15	489.32	522.33	397.25	$[M+H^+]^{1+}$	
V	E	774.50	387.75	12.31	489.32	536.34	411.26	$[M+H^+]^{1+}$	
V	F	792.52	396.76	15.72	489.32	554.36	429.28	$[M+H^+]^{1+}$	
V	I	758.54	379.77	16.18	489.32	520.38	395.30	y4	average integral of VI, VL
V	K	773.55	387.28	9.38	489.32	535.39	410.31	$[M+H^+]^{1+}$	
V	L	758.54	379.77	16.18	489.32	520.38	395.30	y4	average integral of VI, VL
V	M	776.50	388.75	14.61	489.32	538.34	413.26	y4	
V	N	759.50	380.25	11.31	489.32	521.34	396.26	$[M+H^+]^{1+}$	
V	Q	773.51	387.26	11.49	489.32	535.35	410.27	$[M+H^+]^{1+}$	
V	R	801.56	401.28	9.42	489.32	563.40	438.32	$[M+H^+]^{1+}$	
V	S	732.49	366.75	11.71	489.32	494.33	369.25	$[M+H^+]^{1+}$	
V	T	746.50	373.75	12.39	489.32	508.34	383.26	b4	
V	V	744.52	372.76	15.36	489.32	506.36	381.28	$[M+H^+]^{1+}$	
V	W	831.53	416.27	15.74	489.32	593.37	468.29	$[M+H^+]^{1+}$	
V	Y	808.52	404.76	13.68	489.32	570.36	445.28	$[M+H^+]^{1+}$	

Table S4. Characterization data of L4

β3-amino acid		Detected peaks			MS2 fragment ions			Pull down assay	
2nd	5th	$[M+H^+]^{1+}$	$[M+2H^+]^{2+}$	Rt (min)	b4	y4	y3	Detected ion	Remark
N	A	731.72	366.36	10.73	504.30	478.34	353.26	$[M+H^+]^{1+}$	
N	D	775.77	388.39	10.93	504.30	522.33	397.25	$[M+H^+]^{1+}$	
N	E	789.68	395.34	10.82	504.30	536.34	411.26	$[M+H^+]^{1+}$	
N	F	807.85	404.43	12.43	504.30	554.36	429.28	$[M+H^+]^{1+}$	
N	I	773.84	387.42	12.19	504.30	520.38	395.30	$[M+H^+]^{1+}$	average integral of NI, NL
N	K	788.67	394.84	8.63	504.30	535.39	410.31	$[M+2H^+]^{2+}$	
N	L	773.87	387.44	12.31	504.30	520.38	395.30	$[M+H^+]^{1+}$	average integral of NI, NL
N	M	791.82	396.41	11.53	504.30	538.34	413.26	$[M+H^+]^{1+}$	
N	N	774.80	387.90	10.33	504.30	521.34	396.26	$[M+H^+]^{1+}$	
N	Q	788.73	394.87	10.38	504.30	535.35	410.27	$[M+H^+]^{1+}$	
N	R	816.82	408.91	8.63	504.30	563.40	438.32	$[M+2H^+]^{2+}$	
N	S	747.47	374.24	10.46	504.30	494.33	369.25	y4	
N	T	761.81	381.41	10.65	504.30	508.34	383.26	y4	
N	V	759.81	380.41	11.69	504.30	506.36	381.28	$[M+H^+]^{1+}$	
N	W	846.73	423.87	12.64	504.30	593.37	468.29	$[M+H^+]^{1+}$	
N	Y	823.76	412.38	11.24	504.30	570.36	445.28	$[M+H^+]^{1+}$	
Q	A	745.83	373.42	10.96	518.31	478.34	353.26	$[M+H^+]^{1+}$	
Q	D	789.78	395.39	10.94	518.31	522.33	397.25	$[M+H^+]^{1+}$	
Q	E	803.70	402.35	11.02	518.31	536.34	411.26	$[M+H^+]^{1+}$	
Q	F	821.79	411.40	12.43	518.31	554.36	429.28	$[M+H^+]^{1+}$	
Q	I	787.88	394.44	12.25	518.31	520.38	395.30	$[M+H^+]^{1+}$	average integral of QI, QL
Q	K	802.75	401.88	8.85	518.31	535.39	410.31	$[M+2H^+]^{2+}$	
Q	L	787.88	394.44	12.35	518.31	520.38	395.30	$[M+H^+]^{1+}$	average integral of QI, QL
Q	M	805.84	403.42	11.66	518.31	538.34	413.26	$[M+H^+]^{1+}$	
Q	N	788.73	394.87	10.45	518.31	521.34	396.26	$[M+H^+]^{1+}$	
Q	Q	802.72	401.86	10.66	518.31	535.35	410.27	$[M+H^+]^{1+}$	
Q	R	830.89	415.95	8.89	518.31	563.40	438.32	$[M+2H^+]^{2+}$	
Q	S	761.81	381.41	10.65	518.31	494.33	369.25	y4	
Q	T	775.78	388.39	10.85	518.31	508.34	383.26	$[M+H^+]^{1+}$	
Q	V	773.84	387.42	11.83	518.31	506.36	381.28	$[M+H^+]^{1+}$	
Q	W	860.82	430.91	12.84	518.31	593.37	468.29	$[M+H^+]^{1+}$	
Q	Y	837.73	419.37	11.32	518.31	570.36	445.28	$[M+H^+]^{1+}$	
S	A	704.77	352.89	10.95	477.29	478.34	353.26	$[M+H^+]^{1+}$	
S	D	748.79	374.90	10.97	477.29	522.33	397.25	$[M+H^+]^{1+}$	
S	E	762.83	381.92	10.94	477.29	536.34	411.26	$[M+H^+]^{1+}$	
S	F	780.77	390.89	12.69	477.29	554.36	429.28	$[M+H^+]^{1+}$	
S	I	746.77	373.89	12.53	477.29	520.38	395.30	$[M+H^+]^{1+}$	average integroal of SI, SL
S	K	761.80	381.40	8.70	477.29	535.39	410.31	$[M+2H^+]^{2+}$	
S	L	746.77	373.89	12.60	477.29	520.38	395.30	$[M+H^+]^{1+}$	average integroal of SI, SL
S	M	764.48	382.74	11.79	477.29	538.34	413.26	$[M+H^+]^{1+}$	
S	N	747.72	374.36	10.42	477.29	521.34	396.26	b4	
S	Q	761.81	381.41	10.52	477.29	535.35	410.27	y4	
S	R	789.77	395.39	8.67	477.29	563.40	438.32	$[M+2H^+]^{2+}$	
S	S	720.74	360.87	10.59	477.29	494.33	369.25	$[M+H^+]^{1+}$	
S	T	734.78	367.89	10.75	477.29	508.34	383.26	$[M+H^+]^{1+}$	
S	V	732.75	366.88	11.94	477.29	506.36	381.28	$[M+H^+]^{1+}$	
S	W	819.80	410.40	12.97	477.29	593.37	468.29	$[M+H^+]^{1+}$	
S	Y	796.87	398.94	11.36	477.29	570.36	445.28	$[M+H^+]^{1+}$	
T	A	718.84	359.92	11.11	491.30	478.34	353.26	$[M+H^+]^{1+}$	
T	D	762.83	381.92	11.06	491.30	522.33	397.25	$[M+H^+]^{1+}$	
T	E	776.67	388.84	11.08	491.30	536.34	411.26	$[M+H^+]^{1+}$	
T	F	794.73	397.87	10.61	491.30	554.36	429.28	$[M+H^+]^{1+}$	
T	I	760.86	380.93	13.08	491.30	520.38	395.30	$[M+H^+]^{1+}$	average integral of TI, TL
T	K	775.63	388.32	8.68	491.30	535.39	410.31	$[M+2H^+]^{2+}$	
T	L	760.86	380.93	13.08	491.30	520.38	395.30	$[M+H^+]^{1+}$	average integral of TI, TL
T	M	778.75	389.88	12.25	491.30	538.34	413.26	$[M+H^+]^{1+}$	
T	N	761.81	381.41	10.52	491.30	521.34	396.26	y4	
T	Q	775.79	388.40	10.60	491.30	535.35	410.27	$[M+H^+]^{1+}$	
T	R	803.79	402.40	8.71	491.30	563.40	438.32	$[M+2H^+]^{2+}$	
T	S	734.73	367.87	10.65	491.30	494.33	369.25	$[M+H^+]^{1+}$	
T	T	748.78	374.89	10.88	491.30	508.34	383.26	$[M+H^+]^{1+}$	
T	V	746.83	373.92	12.37	491.30	506.36	381.28	$[M+H^+]^{1+}$	
T	W	833.84	417.42	13.51	491.30	593.37	468.29	$[M+H^+]^{1+}$	
T	Y	810.67	405.84	11.68	491.30	570.36	445.28	$[M+H^+]^{1+}$	

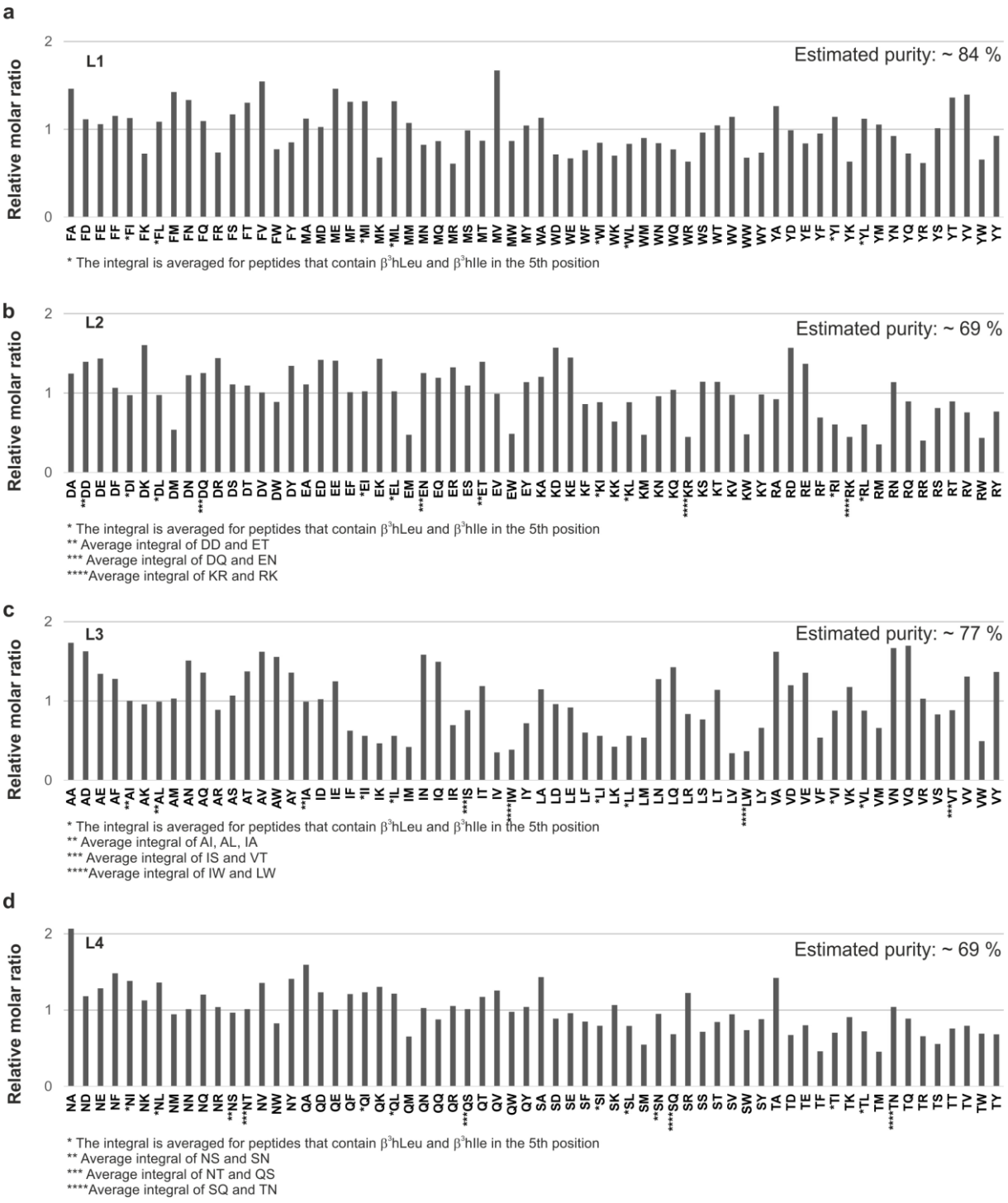

Figure S1. Estimation of equimolarity and purity of the 64-membered sub-libraries.

a) L1 **b)** L2 **c)** L3 **d)** L4. Estimations were based on peak area integrations of HPLC-MS measurements. Equimolarity was estimated using the following formula: AUCcompound / (AUCtotal /64). The relative value of 1 indicates equimolar concentration. Purity was estimated using the following formula: AUCcompound / AUCtotal *100. Single letter amino acid codes are corresponding to the homologous β^3-amino acid used in position 2 and 5 of the foldamers.

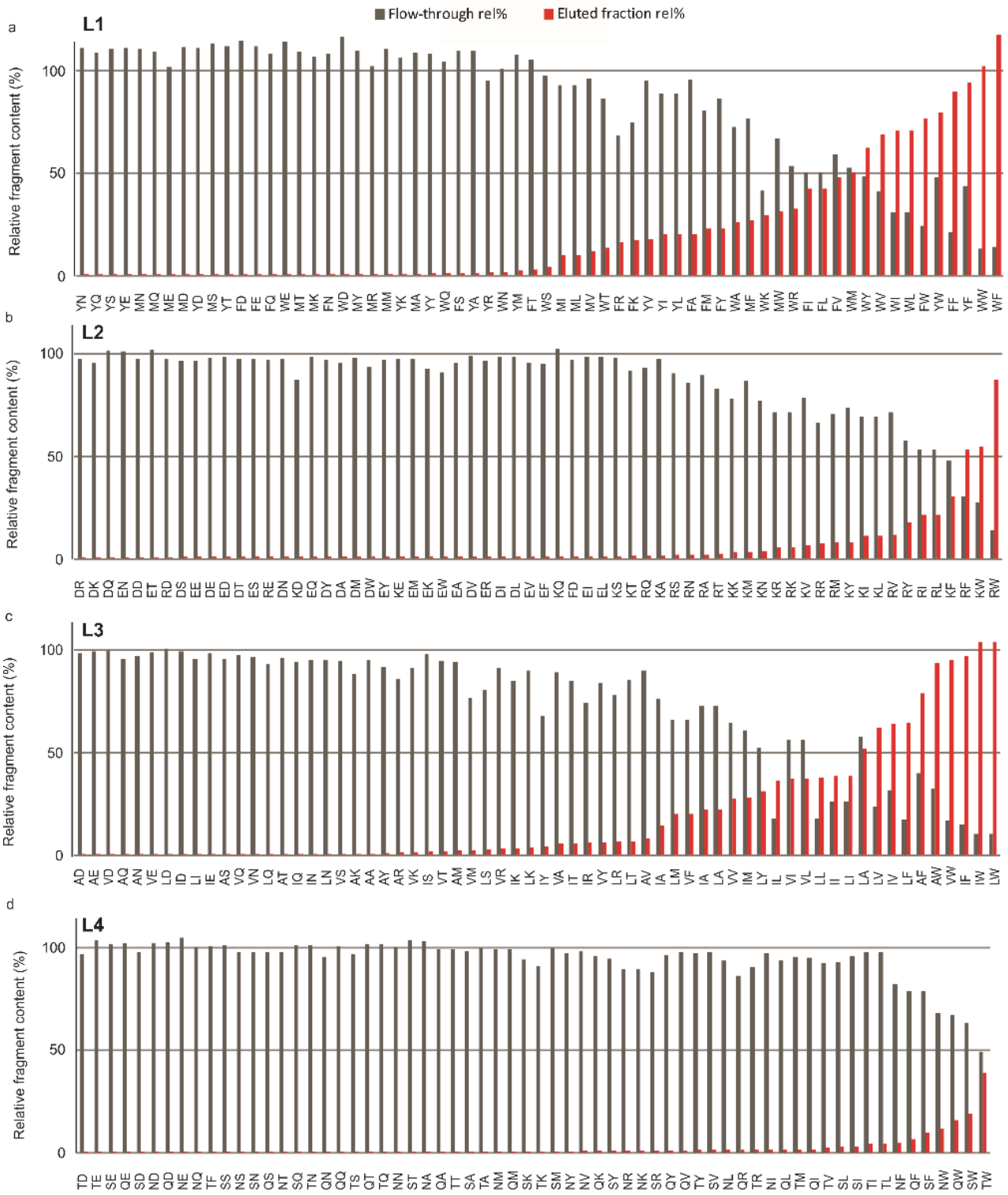

Figure S2. Results of the pulldown assay.

Relative content of the fragments was calculated on the basis of HPLC-MS peak integration using the following formula: $AUC_{fragment}/AUC_{control}$ *100 in the flow-through (grey bars) and in the eluted samples (red bars) for **a** L1, **b** L2, **c** L3 and **d** L4 sub-libraries. AUC determination

for overlapping peaks were according to Table S1-4. Single letter amino acid codes are corresponding to the homologous β^3-amino acid used in position 2 and 5 of the foldamers.

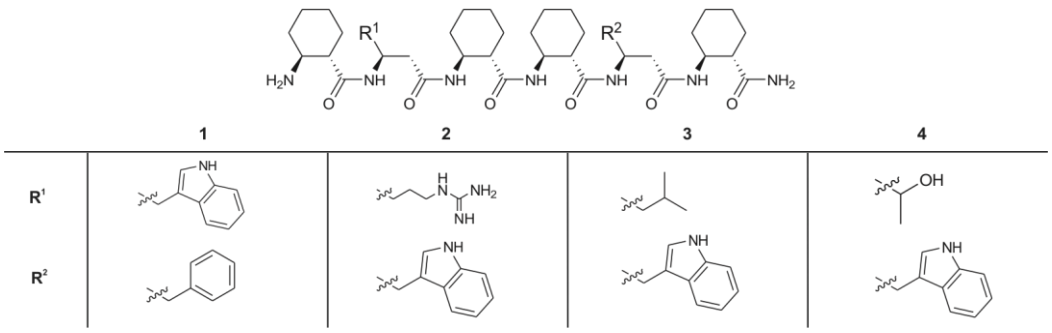

Figure S3. Chemical structure of the selected foldameric recognition segment candidates (1-4). Side-chains in positions 2 (R^1) and 5 (R^2) are indicated.

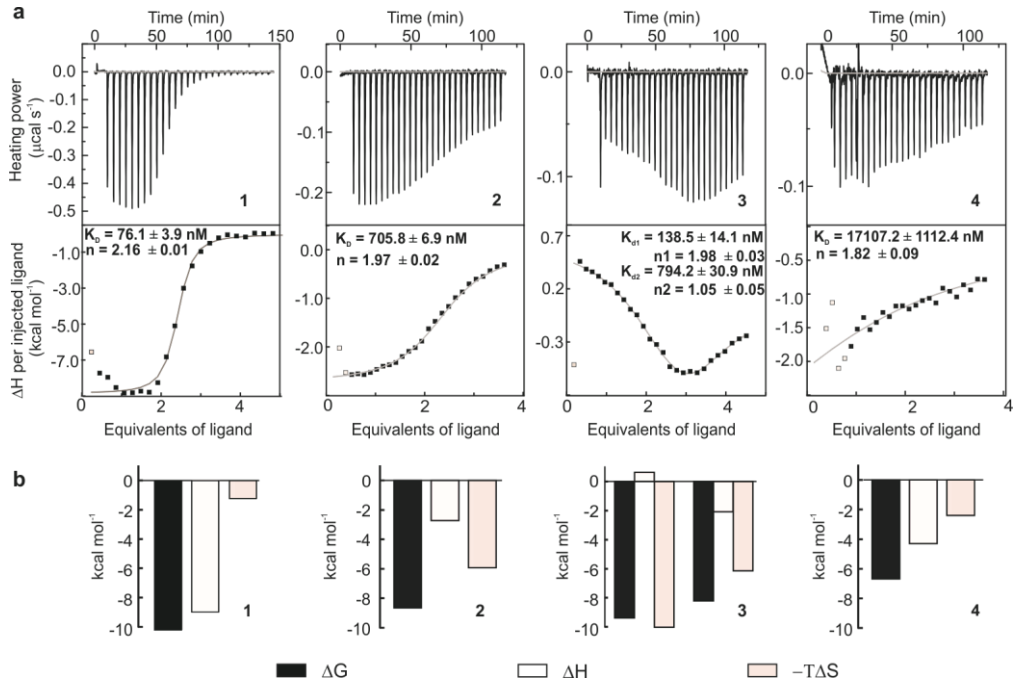

Figure S4. ITC titration data for 1-4. a) ITC titration raw data (upper) and integrated enthalpograms with fitted curves and parameters (lower). b) Thermodynamic parameters derived from the ITC titration curves for folded fragments **1-4**.

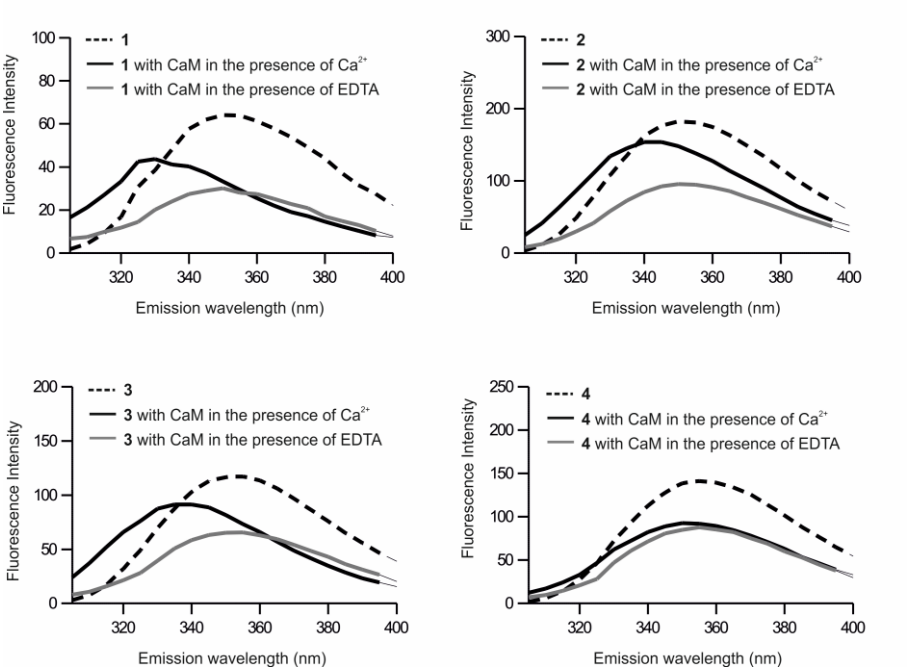

Figure S5. Fluorescence blue-shift measurements.

Fluorescence emission spectra in the range 300-400 nm for the fragments in 0.2 μM concentration (dashed line), in the presence of 0.2 μM CaM and 1 mM $CaCl_2$ (solid, black line) or 5 mM EDTA (solid grey line). The emission maximum corresponding to the β^3-*h*Trp residue exhibited a blue shift upon addition of CaM only in the presence of Ca^{2+}, which indicated Ca^{2+}-dependent interaction between the fragments and CaM.

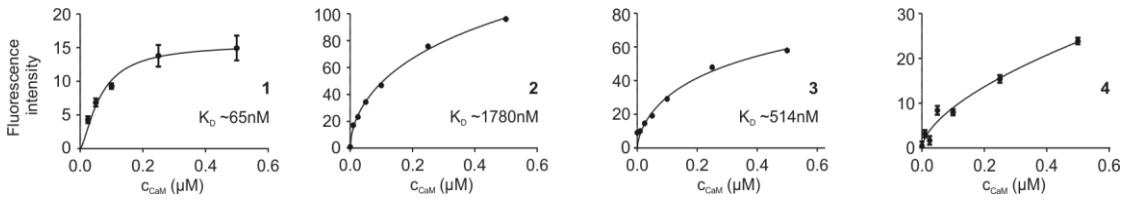

Figure S6. Estimated K_D values from Trp fluorescence measurements.

Observed and fitted titration curves for the Trp fluorescence blue-shifts and the estimated K_D values. Fluorescence intensity was monitored at 330 nm.

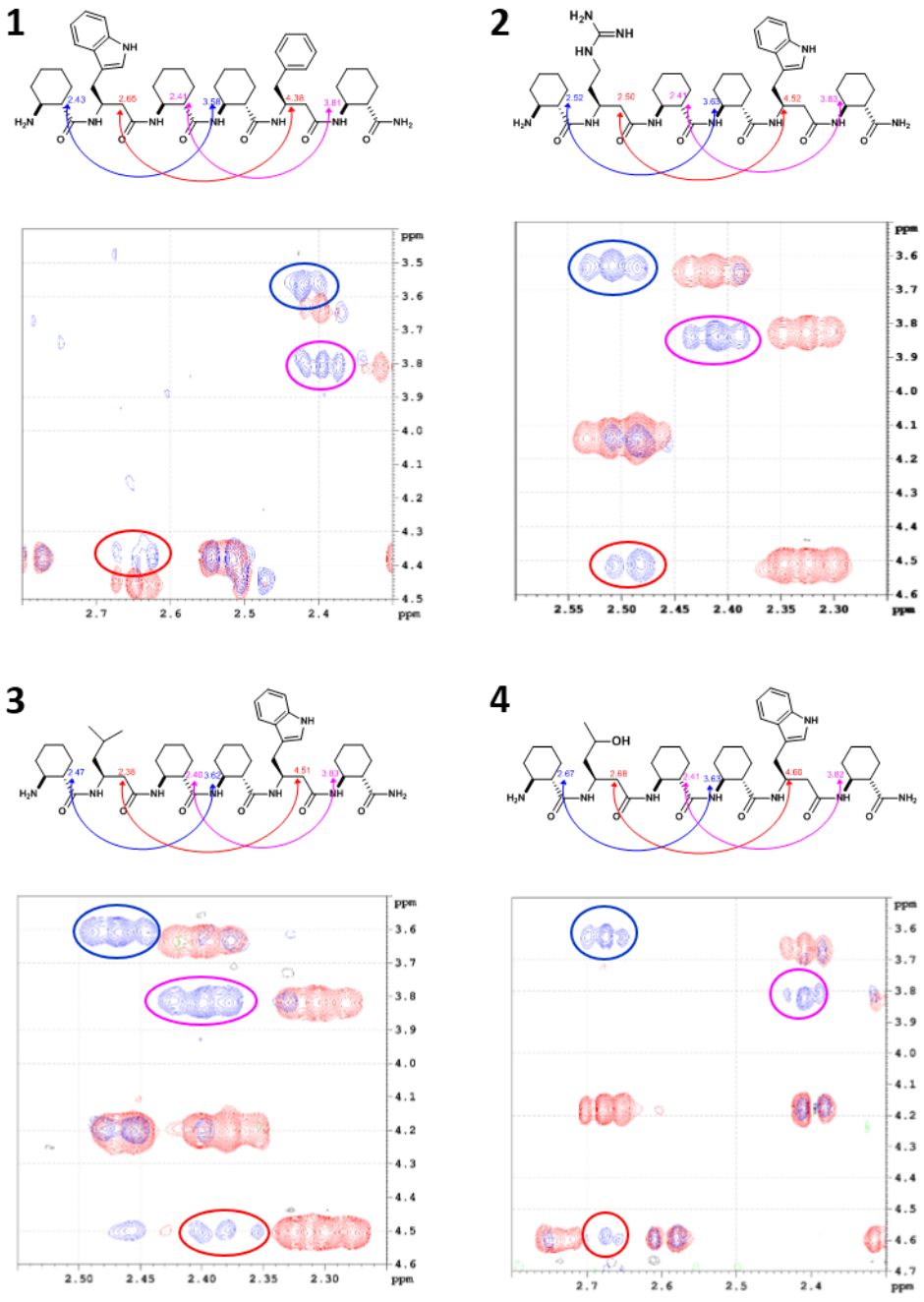

Figure S7. ROESY spectra for 1-4

NOE interactions showing the helicity of compounds **1-4**. Overlaid TOCSY (red) and ROESY (blue) spectra for compounds **1-4** in the absence of the protein. Colour-coded chemical shift assignment and detected i – i+3 type long-range interactions, characteristic for the H14 helix, are indicated on the structures. Peptides were dissolved in 20 mM pH 7.0 d_{18}-HEPES, at a concentration of 90-500 μM. NMR experiments were performed at 25 °C.

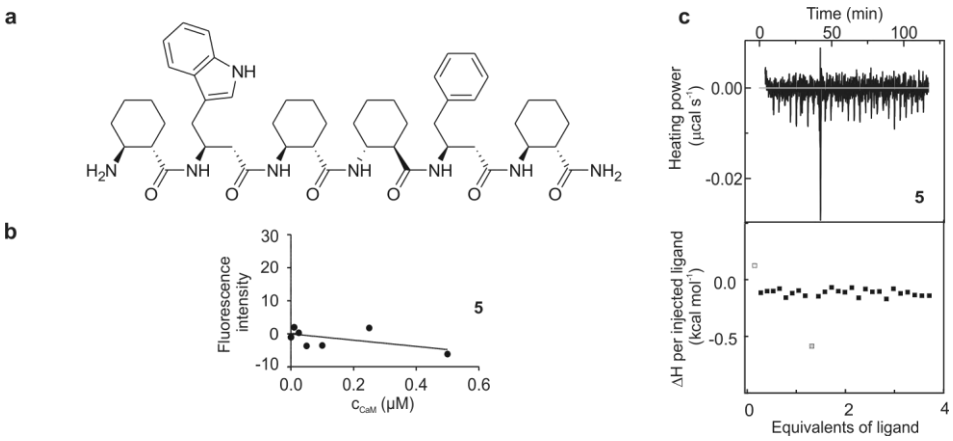

Figure S8. Structure and binding data for the non-helical control peptide

a) Structure of the non-helical control derivative (**5**). b) Result of the fluorescence titration experiment c) ITC titration raw data (upper) and integrated enthalpogram (lower).

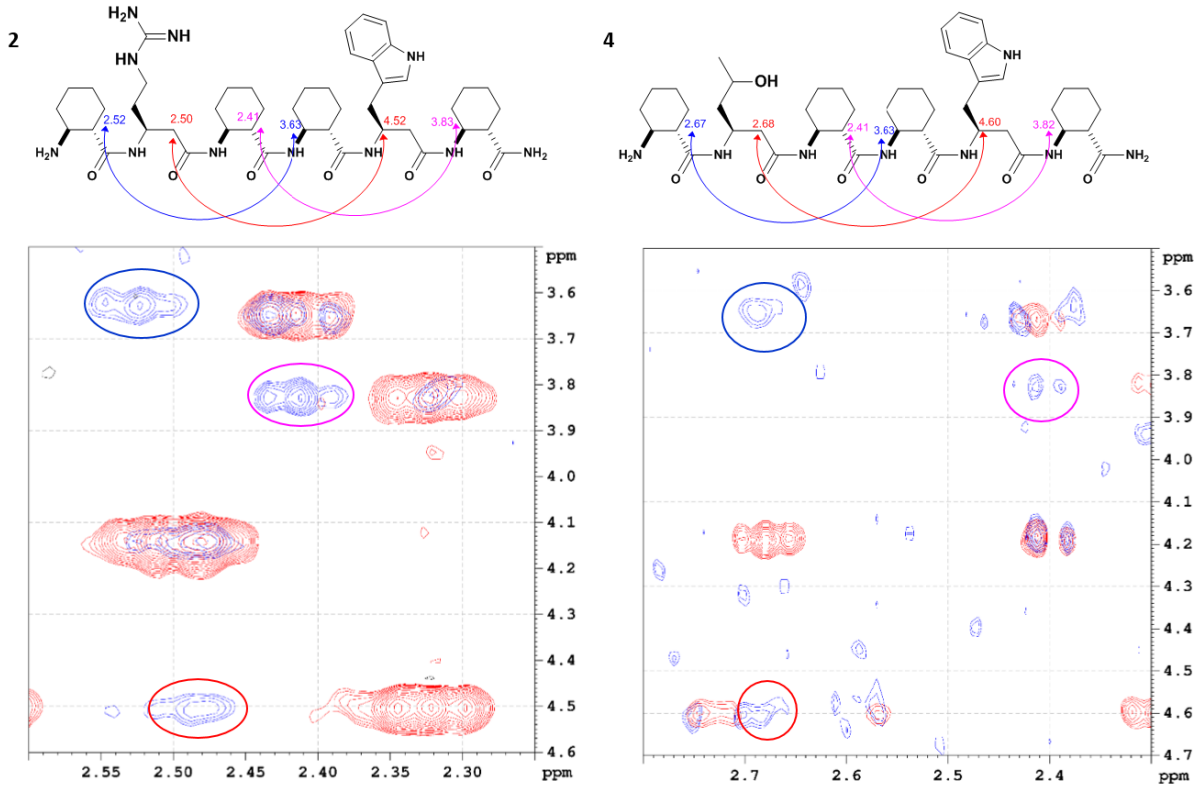

Figure S9. trNOE spectra for 2 and 4

Transferred NOE interactions showing the helicity of the CaM-bound compounds **2** and **4**; overlaid TOCSY (red) and NOESY spectra acquired with a mixing time of 150 ms (blue). While free ligands have short correlation times and slow NOE build-up (400-800 ms), protein-sized systems and bound ligands have long correlation times and NOE builds up rapidly (50-150 ms). The cross-peaks in the 2D NOESY spectra acquired with a mixing time of 150 ms represents the structure of the bound peptides (transferred NOE), which appeared to be a H14 helix. Spectra were acquired under the same conditions as described above but CaM was added to the sample (ca. 50 x ligand excess was applied).

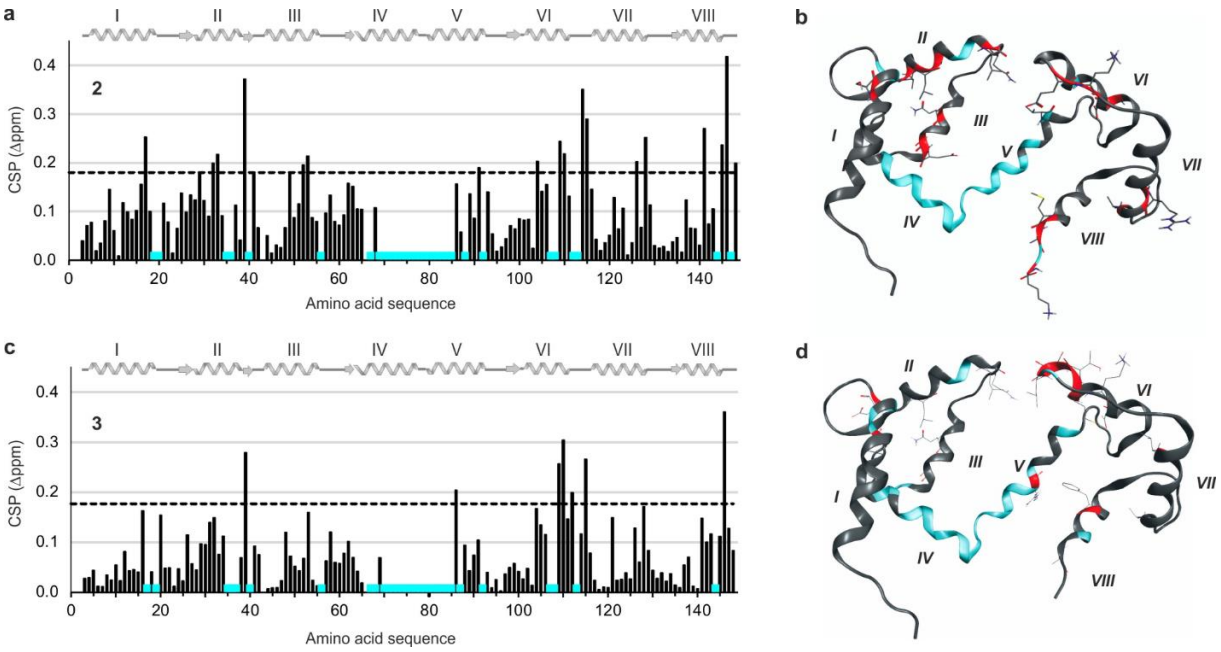

Figure S10. NMR CSP determination upon ligand binding. a Chemical shift perturbations (CSP) of CaM in the presence of 3 equivalents of **2**. **b** Residues with CSPs above the threshold (red) and the highest resonance broadening (cyan) mapped to the ribbon representation of CaM (PDB code: 2K0E[2]). **c** CSPs of CaM in the presence of 3 equivalents of **3**. **d** Residues with CSPs above the threshold (red) and the highest resonance broadening (cyan) mapped to the ribbon representation of CaM. Residues with extreme resonance broadening (completely disappeared) are marked with a cyan line. The CaM secondary structure is indicated above the diagrams. The CSP values were calculated using the formula $[(\Delta\delta(^{1}H))^2 + 0.14*(\Delta\delta(^{15}N))^2]^{1/2}$. A broken line indicates the mean+standard deviation of the CSP values for the individual titrations, which are used as a threshold.

Table S5. Characterization data of the members of DCL

DCL members		Calculated					Detected peaks	
monomer I	monomer II	MW	$[MH^+]^{1+}$	$[M+2H^+]^{2+}$	$[M+3H^+]^{3+}$	$[M+4H^+]^{4+}$	Rt(min)	Detected ion
6	11	2160.75	2161.75	1081.38	721.25	541.19	13.64	$[M+3H^+]^{3+}$
6	10	2171.77	2172.77	1086.89	724.92	543.94	13.69	$[M+3H^+]^{3+}$
6	9	2199.79	2200.79	1100.9	734.26	550.95	13.74	$[M+3H^+]^{3+}$
6	GSH	1400.48	1401.48	701.24	467.83	351.12	13.96	$[M+2H^+]^{2+}$
6	16	2171.73	2172.73	1086.87	724.91	543.93	15.01	$[M+2H^+]^{2+}$
6	15	2130.68	2131.68	1066.34	711.23	533.67	15.11	$[M+2H^+]^{2+}$
6	17	2144.71	2145.71	1073.36	715.9	537.18	15.41	$[M+2H^+]^{2+}$
6	-	1096.39	1097.39	549.2	366.46	275.1	15.51	$[MH^+]^{1+}$
6	8	2167.74	2168.74	1084.87	723.58	542.94	15.73	$[M+2H^+]^{2+}$
6	7	2229.81	2230.81	1115.91	744.27	558.45	16.5	$[M+2H^+]^{2+}$
6	6	2190.78	2191.78	1096.39	731.26	548.7	16.58	$[M+2H^+]^{2+}$
6	13	2142.73	2143.73	1072.37	715.24	536.68	16.6	$[M+2H^+]^{2+}$
6	14	2117.72	2118.72	1059.86	706.91	530.43	17	$[M+2H^+]^{2+}$
6	12	2156.76	2157.76	1079.38	719.92	540.19	17.06	$[M+2H^+]^{2+}$
7	11	2199.78	2200.78	1100.89	734.26	550.95	13.62	$[M+3H^+]^{3+}$
7	10	2210.8	2211.8	1106.4	737.93	553.7	13.64	$[M+3H^+]^{3+}$
7	9	2238.82	2239.82	1120.41	747.27	560.71	13.77	$[M+3H^+]^{3+}$
7	GSH	1439.51	1440.51	720.76	480.84	360.88	13.9	$[M+2H^+]^{2+}$
7	16	2210.76	2211.76	1106.38	737.92	553.69	14.95	$[M+2H^+]^{2+}$
7	15	2169.71	2170.71	1085.86	724.24	543.43	15.05	$[M+2H^+]^{2+}$
7	-	1135.42	1136.42	568.71	379.47	284.86	15.35	$[MH+]^{1+}$
7	17	2183.74	2184.74	1092.87	728.91	546.94	15.35	$[M+2H+]^{2+}$
7	8	2206.77	2207.77	1104.39	736.59	552.69	15.68	$[M+2H^+]^{2+}$
7	7	2268.84	2269.84	1135.42	757.28	568.21	16.49	$[M+2H^+]^{2+}$
7	13	2181.76	2182.76	1091.88	728.25	546.44	16.52	$[M+2H^+]^{2+}$
7	14	2156.75	2157.75	1079.38	719.92	540.19	16.93	$[M+2H^+]^{2+}$
7	12	2195.79	2196.79	1098.9	732.93	549.95	17.01	$[M+2H^+]^{2+}$
8	GSH	1377.44	1378.44	689.72	460.15	345.36	12.64	$[M+3H^+]^{3+}$
8	11	2137.71	2138.71	1069.86	713.57	535.43	12.87	$[M+3H^+]^{3+}$
8	10	2148.73	2149.73	1075.37	717.24	538.18	12.92	$[M+3H^+]^{3+}$
8	9	2176.75	2177.75	1089.38	726.58	545.19	12.98	$[M+3H^+]^{3+}$
8	-	1073.35	1074.35	537.68	358.78	269.34	14.05	$[MH^+]^{1+}$
8	16	2148.69	2149.69	1075.35	717.23	538.17	14.1	$[M+3H^+]^{3+}$
8	15	2107.64	2108.64	1054.82	703.55	527.91	14.21	$[M+2H^+]^{2+}$
8	17	2121.67	2122.67	1061.84	708.22	531.42	14.5	$[M+2H^+]^{2+}$
8	8	2144.7	2145.7	1073.35	715.9	537.18	14.88	$[M+2H^+]^{2+}$
8	13	2119.69	2120.69	1060.85	707.56	530.92	15.75	$[M+2H^+]^{2+}$
8	14	2094.68	2095.68	1048.34	699.23	524.67	16.14	$[M+2H^+]^{2+}$
8	12	2133.72	2134.72	1067.86	712.24	534.43	16.22	$[M+2H^+]^{2+}$
9	GSH	1409.49	1410.49	705.75	470.83	353.37	9.97	$[M+2H^+]^{2+}$
9	-	1105.4	1106.4	553.7	369.47	277.35	10.75	$[M+2H^+]^{2+}$
9	11	2169.76	2170.76	1085.88	724.25	543.44	11.3	$[M+4H^+]4+$
9	10	2180.78	2181.78	1091.39	727.93	546.2	11.33	$[M+4H^+]4+$
9	9	2208.8	2209.8	1105.4	737.27	553.2	11.42	$[M+4H^+]4+$
9	16	2180.74	2181.74	1091.37	727.91	546.19	12.22	$[M+3H^+]^{3+}$
9	15	2139.69	2140.69	1070.85	714.23	535.92	12.26	$[M+3H^+]^{3+}$
9	17	2153.72	2154.72	1077.86	718.91	539.43	12.55	$[M+3H^+]^{3+}$
9	13	2151.74	2152.74	1076.87	718.25	538.94	13.71	$[M+3H^+]^{3+}$
9	14	2126.73	2127.73	1064.37	709.91	532.68	14.09	$[M+3H^+]^{3+}$
9	12	2165.77	2166.77	1083.89	722.92	542.44	14.19	$[M+3H^+]^{3+}$

10	GSH	1381.47	1382.47	691.74	461.49	346.37	9.9	$[M+2H^+]^{2+}$
10	-	1077.38	1078.38	539.69	360.13	270.35	10.65	$[M+2H^+]^{2+}$
10	11	2141.74	2142.74	1071.87	714.91	536.44	11.23	$[M+4H^+]4+$
10	10	2152.76	2153.76	1077.38	718.59	539.19	11.3	$[M+4H^+]4+$
10	16	2152.72	2153.72	1077.36	718.57	539.18	12.12	$[M+3H^+]^{3+}$
10	15	2111.63	2112.63	1056.82	704.88	528.91	12.17	$[M+3H^+]^{3+}$
10	17	2125.7	2126.7	1063.85	709.57	532.43	12.49	$[M+3H^+]^{3+}$
10	14	2098.71	2099.71	1050.36	700.57	525.68	14.02	$[M+3H^+]^{3+}$
10	13	2123.68	2124.68	1062.84	708.89	531.92	14.07	$[M+3H+]^{3+}$
10	12	2137.75	2138.75	1069.88	713.58	535.44	14.12	$[M+3H^+]^{3+}$
11	GSH	1370.45	1371.45	686.23	457.82	343.61	9.79	$[M+2H^+]^{2+}$
11	-	1066.36	1067.36	534.18	356.45	267.59	10.58	$[M+2H^+]^{2+}$
11	11	2130.72	2131.72	1066.36	711.24	533.68	11.19	$[M+4H^+]4+$
11	16	2141.7	2142.7	1071.85	714.9	536.43	12.09	$[M+3H^+]^{3+}$
11	15	2100.65	2101.65	1051.33	701.22	526.16	12.15	$[M+3H^+]^{3+}$
11	17	2114.68	2115.68	1058.34	705.89	529.67	12.47	$[M+3H^+]^{3+}$
11	13	2112.7	2113.7	1057.35	705.23	529.18	13.62	$[M+3H^+]^{3+}$
11	14	2087.69	2088.69	1044.85	696.9	522.92	14.02	$[M+3H^+]^{3+}$
11	12	2126.73	2127.73	1064.37	709.91	532.68	14.1	$[M+3H^+]^{3+}$
12	GSH	1366.46	1367.46	684.23	456.49	342.62	14.6	$[M+2H^+]^{2+}$
12	16	2137.71	2138.71	1069.86	713.57	535.43	15.48	$[M+2H^+]^{2+}$
12	15	2096.66	2097.66	1049.33	699.89	525.17	15.61	$[M+2H^+]^{2+}$
12	17	2111.67	2112.67	1056.84	704.89	528.92	15.89	$[M+2H^+]^{2+}$
12	-	1062.37	1063.37	532.19	355.12	266.59	16.18	$[MH^+]^{1+}$
12	13	2108.71	2109.71	1055.36	703.9	528.18	17.12	$[M+2H^+]^{2+}$
12	14	2084.61	2085.61	1043.31	695.87	522.15	17.53	$[M+2H^+]^{2+}$
12	12	2123.72	2124.72	1062.86	708.91	531.93	17.59	$[M+2H^+]^{2+}$
13	GSH	1352.43	1353.43	677.22	451.81	339.11	13.81	$[M+2H^+]^{2+}$
13	16	2122.74	2123.74	1062.37	708.58	531.69	14.97	$[M+2H^+]^{2+}$
13	15	2082.63	2083.63	1042.32	695.21	521.66	15.1	$[M+2H^+]^{2+}$
13	-	1048.34	1049.34	525.17	350.45	263.09	15.36	$[MH^+]^{1+}$
13	17	2096.66	2097.66	1049.33	699.89	525.17	15.37	$[M+3H^+]^{3+}$
13	13	2094.68	2095.68	1048.34	699.23	524.67	16.61	$[M+2H^+]^{2+}$
14	GSH	1327.42	1328.42	664.71	443.47	332.86	14.4	$[M+2H^+]^{2+}$
14	16	2098.67	2099.67	1050.34	700.56	525.67	15.4	$[M+2H^+]^{2+}$
14	15	2057.62	2058.62	1029.81	686.87	515.41	15.5	$[M+2H^+]^{2+}$
14	17	2071.65	2072.65	1036.83	691.55	518.91	15.78	$[M+2H^+]^{2+}$
14	-	1023.33	1024.33	512.67	342.11	256.83	16.14	$[MH^+]^{1+}$
14	13	2069.67	2070.67	1035.84	690.89	518.42	17.04	$[M+2H^+]^{2+}$
14	14	2044.66	2045.66	1023.33	682.55	512.17	17.5	$[M+2H^+]^{2+}$
15	GSH	1340.38	1341.38	671.19	447.79	336.1	11.21	$[M+2H^+]^{2+}$
15	-	1036.29	1037.29	519.15	346.43	260.07	12.47	$[MH^+]^{1+}$
15	16	2110.69	2111.69	1056.35	704.56	528.67	13.34	$[M+2H^+]^{2+}$
15	15	2070.58	2071.58	1036.29	691.19	518.65	13.43	$[M+2H^+]^{2+}$
16	GSH	1381.43	1382.43	691.72	461.48	346.36	11.19	$[M+2H^+]^{2+}$
16	-	1077.34	1078.34	539.67	360.11	270.34	12.36	$[MH^+]^{1+}$
16	16	2152.68	2153.68	1077.34	718.56	539.17	13.24	$[M+2H^+]^{2+}$
17	GSH	1354.41	1355.41	678.21	452.47	339.6	11.71	$[M+2H^+]^{2+}$
17	-	1050.32	1051.32	526.16	351.11	263.58	13.04	$[MH^+]^{1+}$
17	16	2125.66	2126.66	1063.83	709.55	532.42	13.68	$[M+2H^+]^{2+}$
17	15	2083.7	2084.7	1042.85	695.57	521.93	13.75	$[M+3H^+]^{3+}$
17	17	2098.64	2099.64	1050.32	700.55	525.66	14.04	$[M+3H^+]^{3+}$

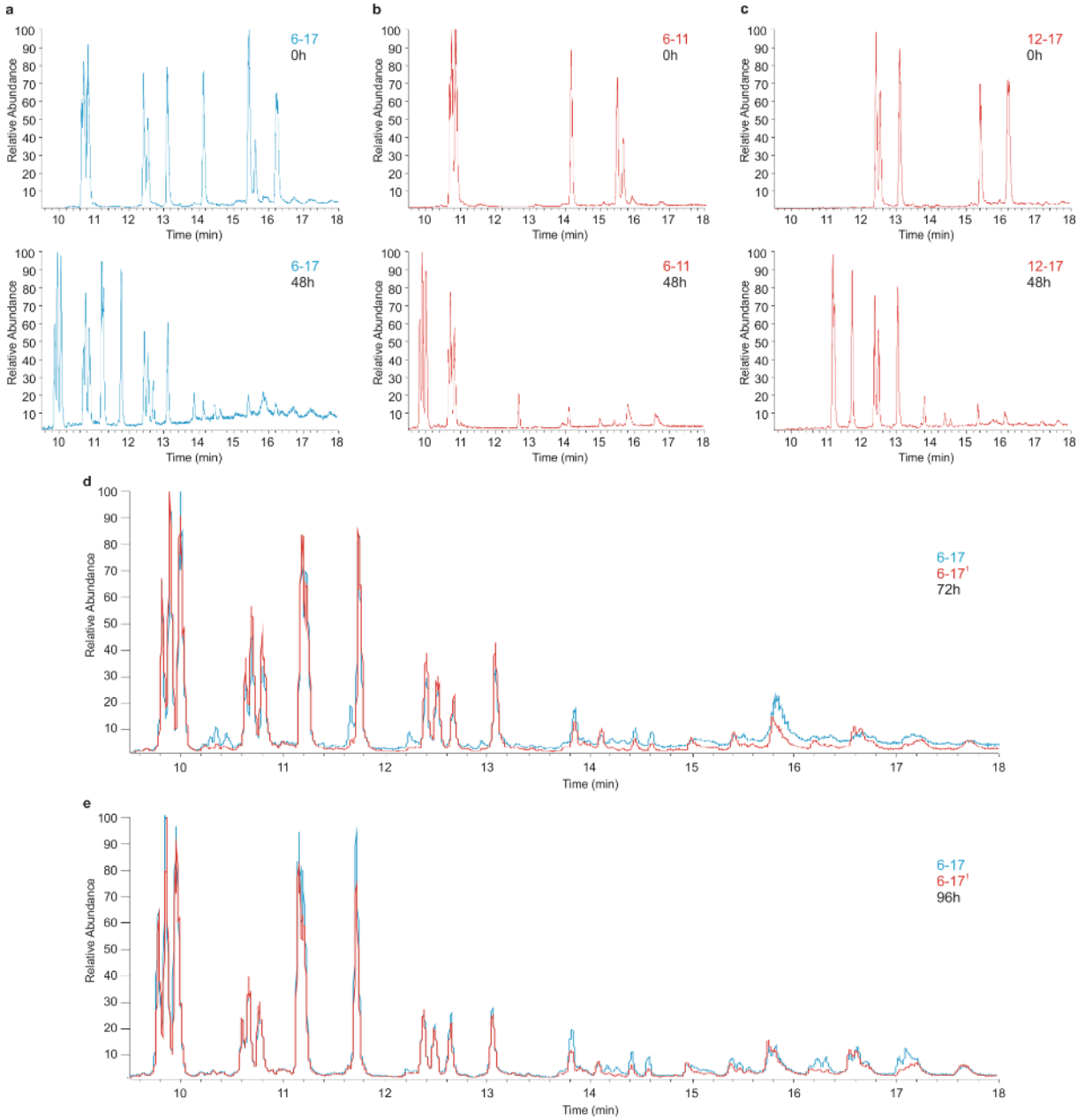

Figure S11. Assessing thermodynamic equilibrium. Partial MS-detected HPLC chromatograms for DCLs of different mixture compositions at 0 h and pre-equilibrated at 48 h: library containing **6-17** at 10 μM for each members (**a**), **6-11** at 20 μM for each members (**b**) and **12-17** at 20 μM for each members (**c**). The pre-equilibrated mixtures **b** and **c** were pooled and the product composition was analyzed after 72 h (**d**) and 96 h (**e**). The HPLC results obtained for the pre-equilibrated library are given with red curves, and the analysis for the control library is given in blue. After 96 h, only slight differences could be detected between pre-equilibrated and pooled sample (red) and the control sample (blue). This showed that thermodynamic equilibrium has been reached after 96 h independently of the starting conditions.

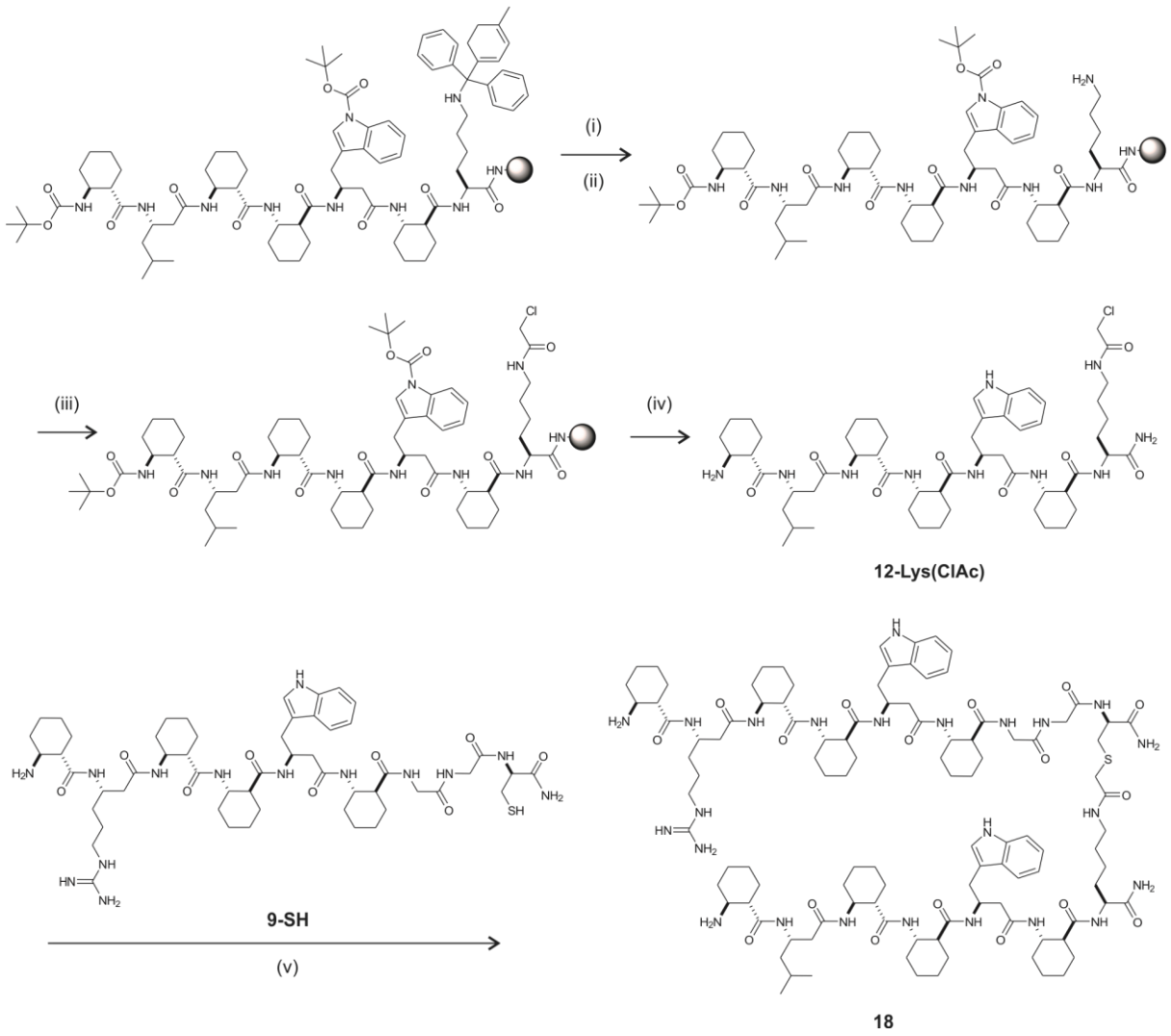

Figure S12. Synthesis of 18. Reaction condition: (i) AcOH/TFE/DCM (2:1:7); (ii) 5% DIEA in DMF, 30 min, RT; (iii) chloroacetic acid/DCC/HOAt, 3 h, RT; (iv) TFA/H_2O/TIS (92:5:3), 3 h, RT; (v) 0.1 M Tris buffer (pH=8.2), overnight, RT.

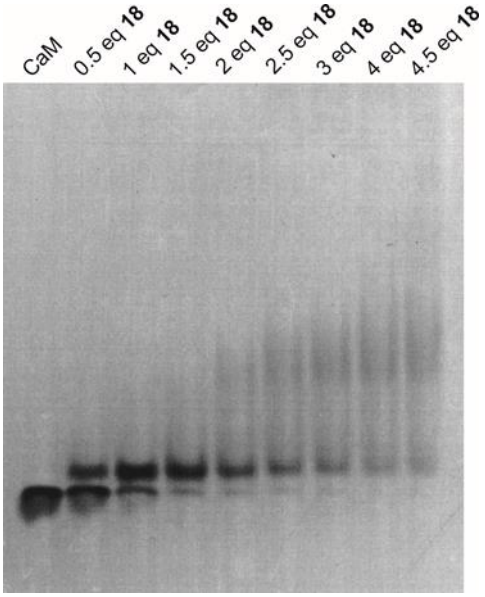

Figure S13. Native gel electrophoresis of CaM after addition of different amount of **18**. CaM concentration was 100 μM in pH 7.0, 20 mM HEPES buffer containing 30 mM $CaCl_2$ and 10 % DMSO. Foldamer equivalents are indicated on the top., The two bands appear assigned to pure CaM and the stoichiometric complex of CaM-**18** up to a CaM:**18** ratio of 1. Increasing equivalents of **18** decreased the intensity of the bands, and smears appear indicating formation of complexes with varying compositions. This observation supported cross-linking interaction mode of **18** at high concentrations. Due to the weak binding nature, this interaction mode does not play roles at submicromolar concentrations.

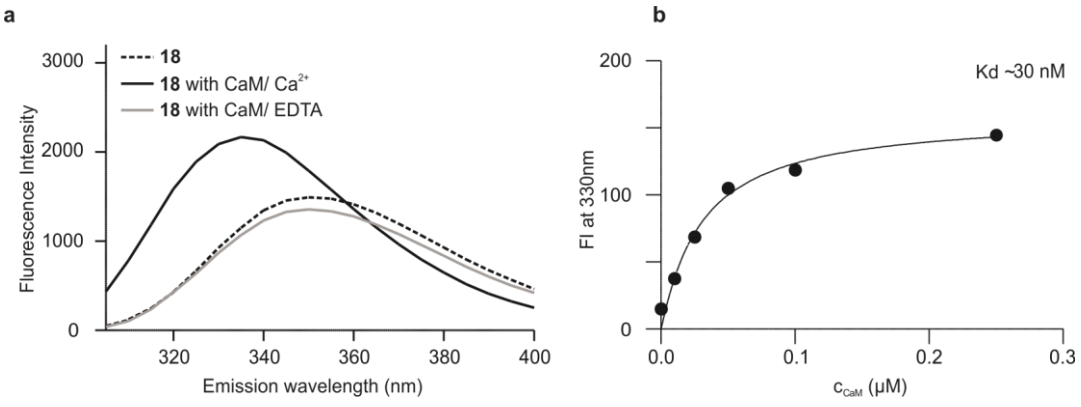

Figure S14. Fluorescence titration experiment of 18. a) observed blue shift upon the addition of CaM to **18** in the presence of Ca^{2+}. **b)** fitted titration curve and the estimated dissociation constant in the inset.

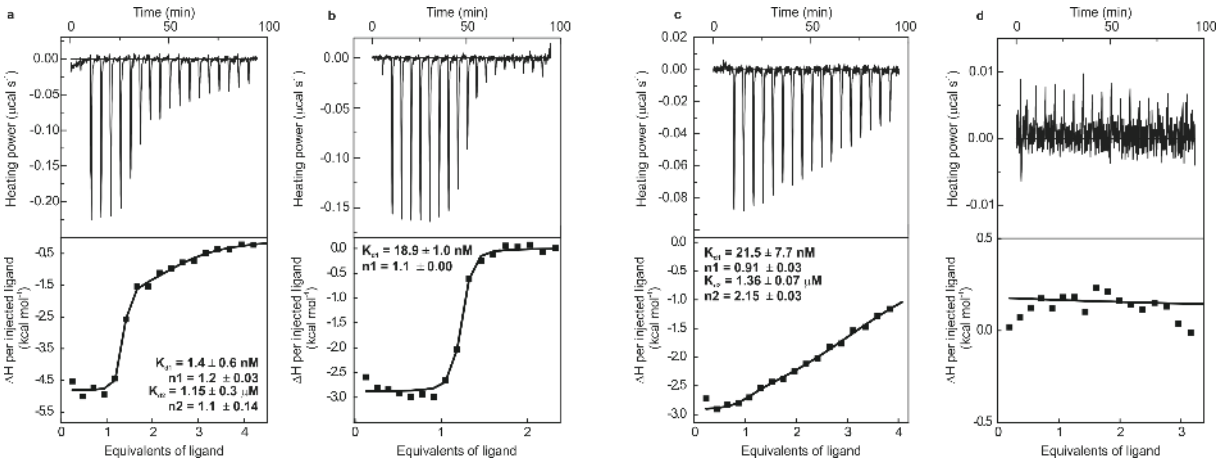

Figure S15. ITC competitive and control titrations for 18 measured at 35 °C. Raw data (upper) and integrated peaks with fitted values (lower) with indicated K_D and stoichiometry. **18** titrated to 3.5 μM CaM in the cell (**a)**, TRPV1-CT_{15} titrated to 10 μM CaM (**b**); competition experiment for **18** titrated to CaM:TRPV1-CT_{15} 1:2 sample (**c**) and TRPV1-CT_{15} titrated to CaM:**18** 1:2 sample (**d**). All titrations were performed in pH 7.0 20 mM HEPES, with 30 mM $CaCl_2$.

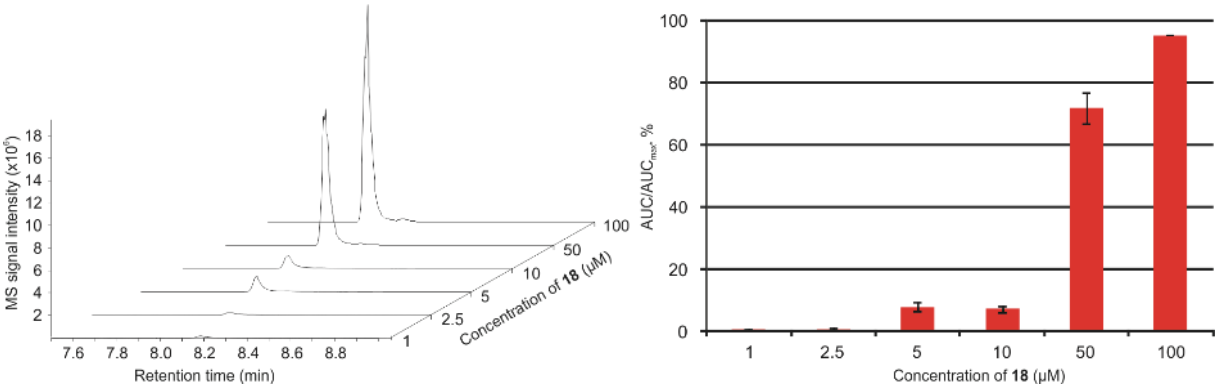

Figure S16. Competition pull-down assay. TRPV-CT_{15} saturated, immobilized CaM was titrated with increasing concentrations of **18**, which exhibited a concentration-dependent elution of the TRPV1 fragment from CaM, which supported the competition between the two compounds. **a** Partial HPLC-MS spectra of the eluted TRPV-CT_{15} (m/z: 899-901) in the presence of different competitor concentration. **b** Relative AUC values measured for TRPV1-CT_{15}, where AUC_{max} was given by complete elution of TRPV-CT_{15} with EDTA. Estimated total concentration of CaM was 60 μM on the basis of the capacity of the resin, which resulted in a steep elution at 50 μM TRPV-CT_{15} concentration and corresponded to 1:1 CaM:TRPV-CT_{15} complex.

Peptide characterization data

Lyophilized peptides were analyzed by ESI-MS and analytical HPLC measurements on an Aeris Widepore XB-C18 4.6 x 250 mm column (Phenomenex) with a gradient from 5% 0.1% TFA/water (A) to 80% 0.1% TFA/20% water/80% ACN (B)over 25 min at a flow rate of 1.2 ml min^{-1}, using UV detection at 220 nm.. Peptide purity was >95% according to analytical HPLC measurements.

Table S6. Summary of ESI-MS data

Number	Compound	Molecular weight		Expected m/z values (based on monoisotopic mass)		Detected m/z
		average	monoisotopic			
1	WF	879.1408	878.5418	$[M+1H]^{1+}$	879.5491	579.5834
				$[M+2H]^{2+}$	440.2782	440.3333
2	RW	888.1526	887.5745	$[M+1H]^{1+}$	888.5818	888.5834
				$[M+2H]^{2+}$	444.7945	444.9167
3	LW	845.1246	844.5575	$[M+1H]^{1+}$	845.5648	845.5834
				$[M+2H]^{2+}$	423.2860	423.3333
4	TW	833.0708	832.5211	$[M+1H]^{1+}$	833.5284	833.5903
				$[M+2H]^{2+}$	417.2678	417.4483
5	control	879.1408	878.5418	$[M+1H]^{1+}$	879.5491	879.6112
				$[M+2H]^{2+}$	440.2782	440.3747
6	WF-GGC	1096.3863	1095.5939	$[M+1H]^{1+}$	1096.6012	1096.5000
				$[M+2H]^{2+}$	548.8042	548.8333
7	WW-GGC	1135.4224	1134.6048	$[M+1H]^{1+}$	1135.6121	1135.5834
				$[M+2H]^{2+}$	568.3097	568.3333
8	YF-GGC	1073.3497	1072.5780	$[M+1H]^{1+}$	1073.5853	1073.5834
				$[M+2H]^{2+}$	537.2963	537.4167
9	RW-GGC	1105.3982	1104.6266	$[M+1H]^{1+}$	1105.6339	1105.5834
				$[M+2H]^{2+}$	553.3206	553.4157
10	KW-GGC	1077.3848	1076.6205	$[M+1H]^{1+}$	1077.6278	1077.5834
				$[M+2H]^{2+}$	539.3175	539.5000
11	RF-GGC	1066.3621	1065.6157	$[M+1H]^{1+}$	1066.6230	1066.5834
				$[M+2H]^{2+}$	533.8151	553.9167
12	LW-GGC	1062.3701	1061.6096	$[M+1H]^{1+}$	1062.6169	1062.6667
				$[M+2H]^{2+}$	531.8121	531.9167
13	VW-GGC	1048.3435	1047.5939	$[M+1H]^{1+}$	1048.6012	1048.6168
				$[M+2H]^{2+}$	524.8042	525.0317
14	IF-GGC	1023.3341	1022.5987	$[M+1H]^{1+}$	1023.6060	1023.6667
				$[M+2H]^{2+}$	512.3066	512.5000
15	SW-GGC	1036.2898	1035.5576	$[M+1H]^{1+}$	1036.5649	1036.5834
				$[M+2H]^{2+}$	518.7861	518.8333
16	QW-GGC	1077.3417	1076.5841	$[M+1H]^{1+}$	1077.5914	1077.5000
				$[M+2H]^{2+}$	539.2993	539.3333
17	TW-GGC	1050.3164	1049.5732	$[M+1H]^{1+}$	1050.5805	1050.5834
				$[M+2H]^{2+}$	525.7939	525.9167
9-12	RW-LW	2118.7158	2117.2740	$[M+2H]^{2+}$	1059.6423	1059.6600
				$[M+3H]^{3+}$	706.7639	706.8000

TRPV1$_{784-798}$		1798.0990	1797.0162	**$[M+2H]^{2+}$**	899.5081	899.9639
				$[M+3H]^{3+}$	600.0054	600.6056

Compound **1**

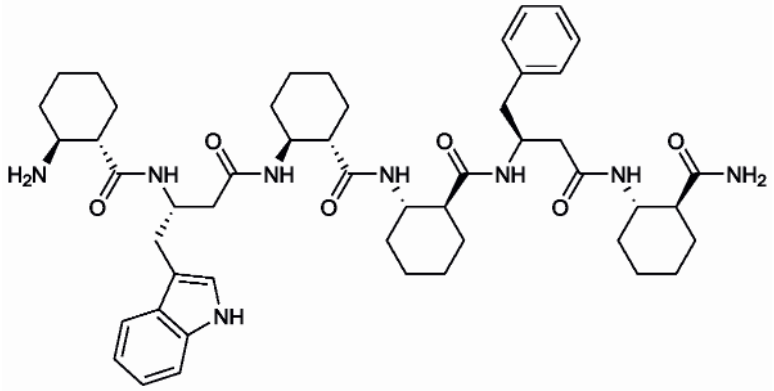
H2N
NH
O
NH2
NH

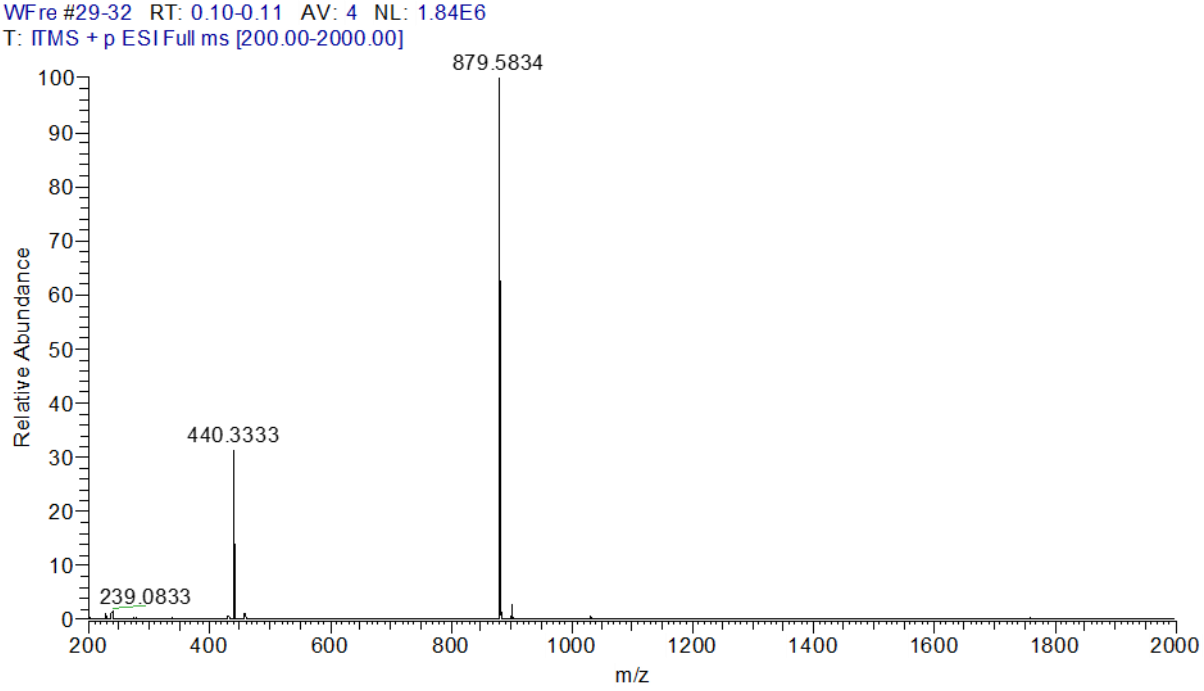
WFre #29-32 RT: 0.10-0.11 AV: 4 NL: 1.84E6
T: ITMS + p ESI Full ms [200.00-2000.00]
879.5834
440.3333
239.0833
Relative Abundance
m/z

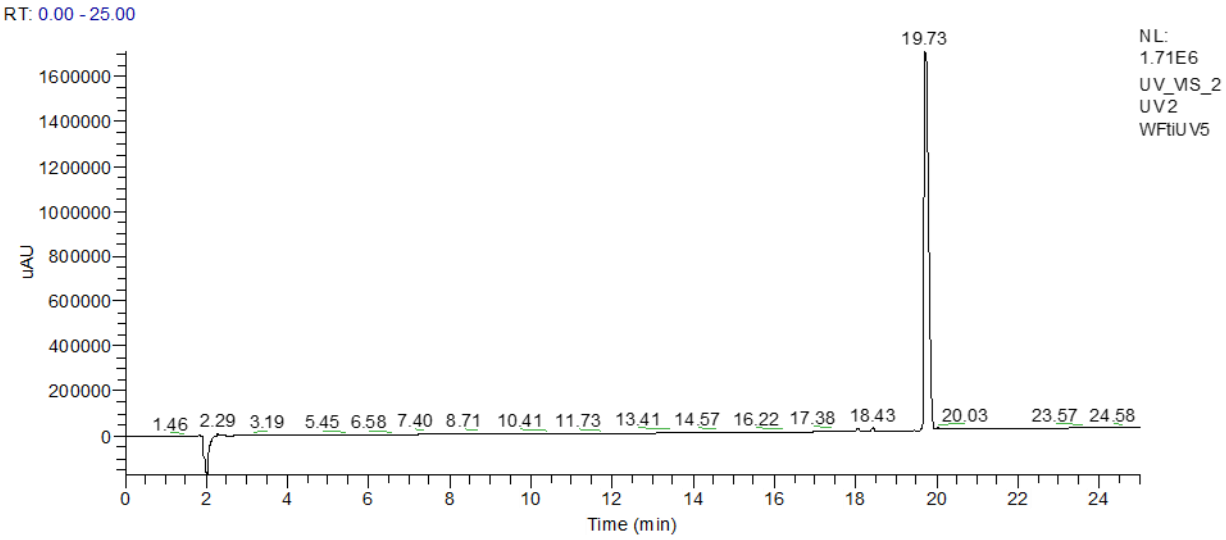
RT: 0.00 - 25.00
19.73
NL:
1.71E6
UV_VIS_2
UV2
WFtiUV5
uAU
1.46 2.29 3.19 5.45 6.58 7.40 8.71 10.41 11.73 13.41 14.57 16.22 17.38 18.43 20.03 23.57 24.58
Time (min)

Compound **2**

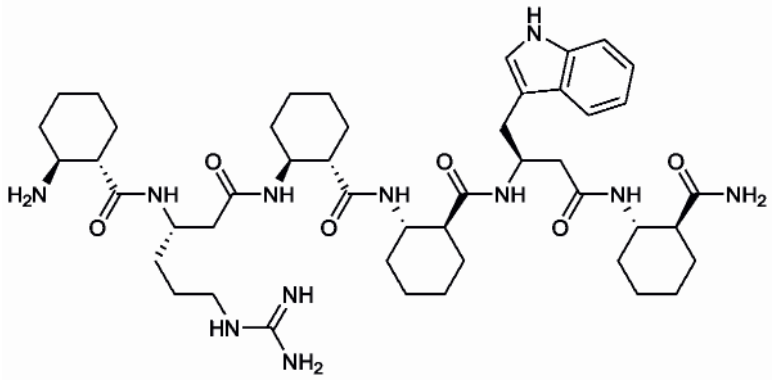

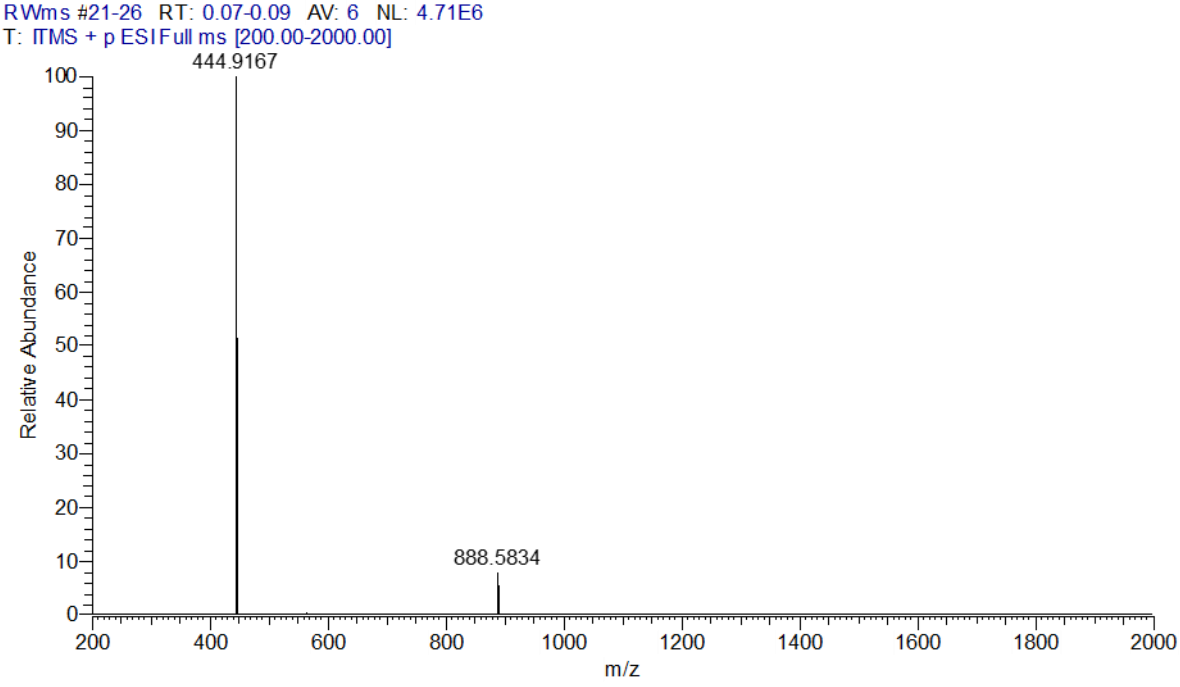
RWms #21-26 RT: 0.07-0.09 AV: 6 NL: 4.71E6
T: ITMS + p ESI Full ms [200.00-2000.00]
444.9167
888.5834
Relative Abundance
m/z

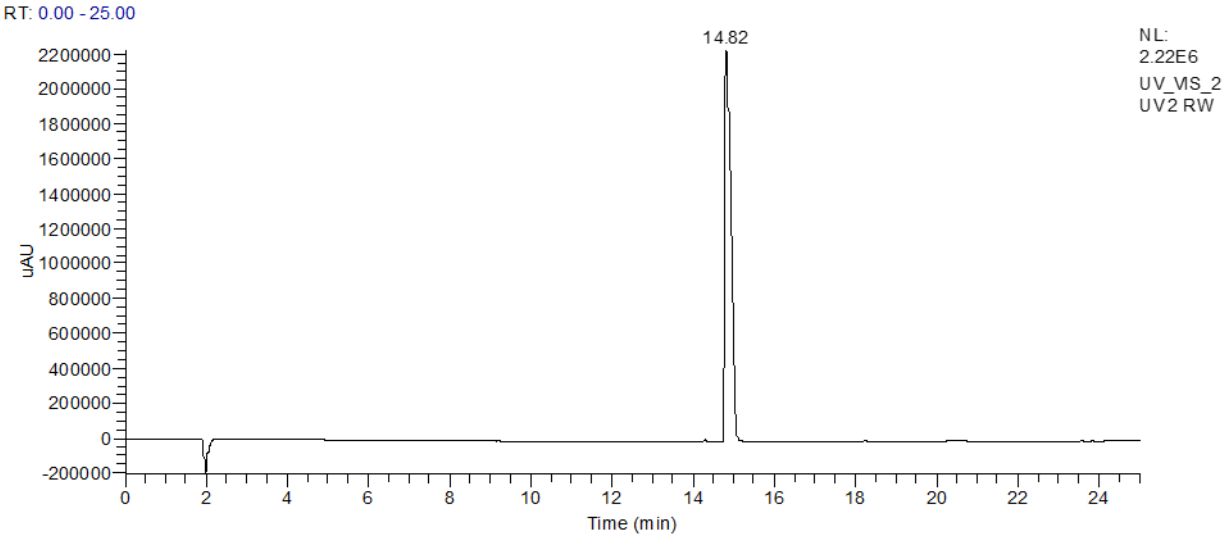
RT: 0.00 - 25.00
14.82
NL:
2.22E6
UV_VIS_2
UV2 RW
uAU
Time (min)

Compound **3**

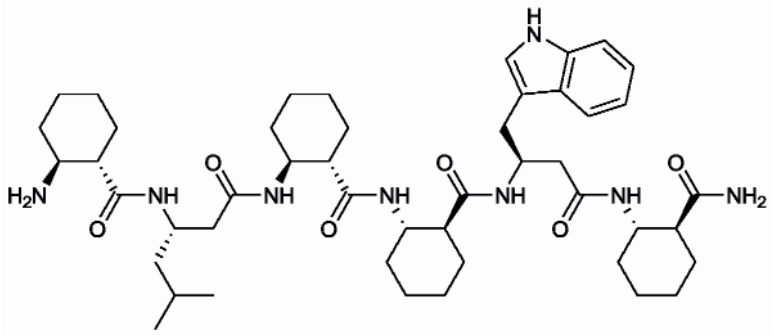
H
N
H2N
NH
NH
NH
NH
NH
NH2
O

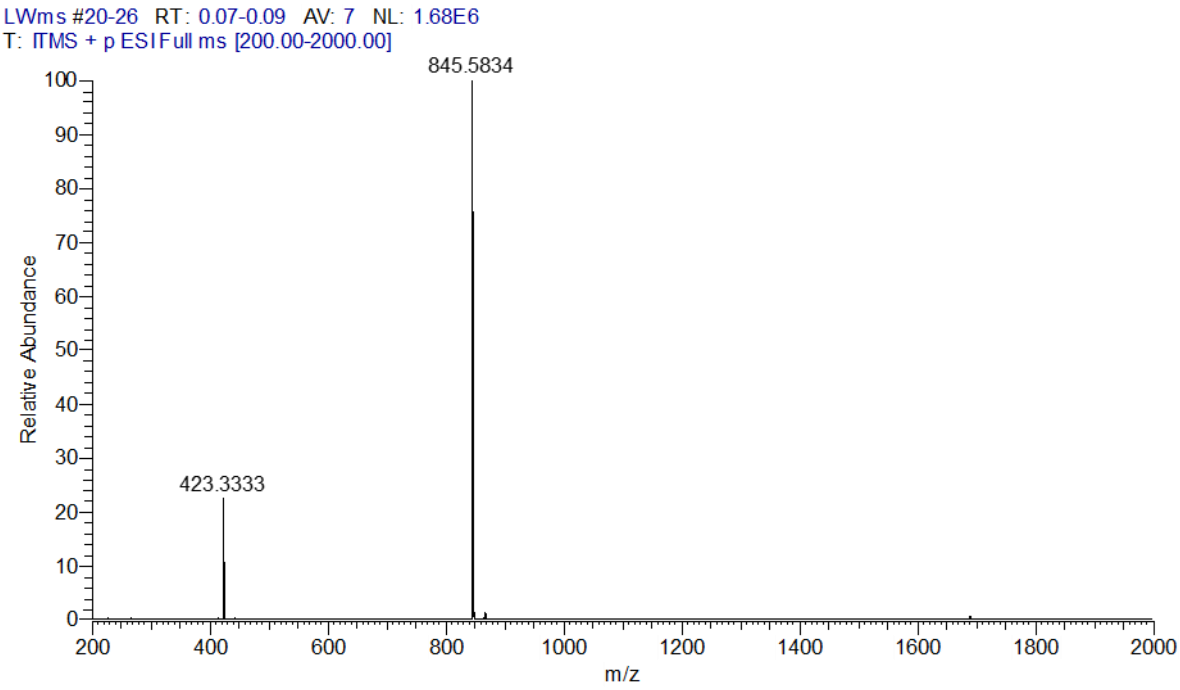
LWms #20-26 RT: 0.07-0.09 AV: 7 NL: 1.68E6
T: ITMS + p ESI Full ms [200.00-2000.00]
845.5834
423.3333
Relative Abundance
m/z
100
90
80
70
60
50
40
30
20
10
0
200
400
600
800
1000
1200
1400
1600
1800
2000

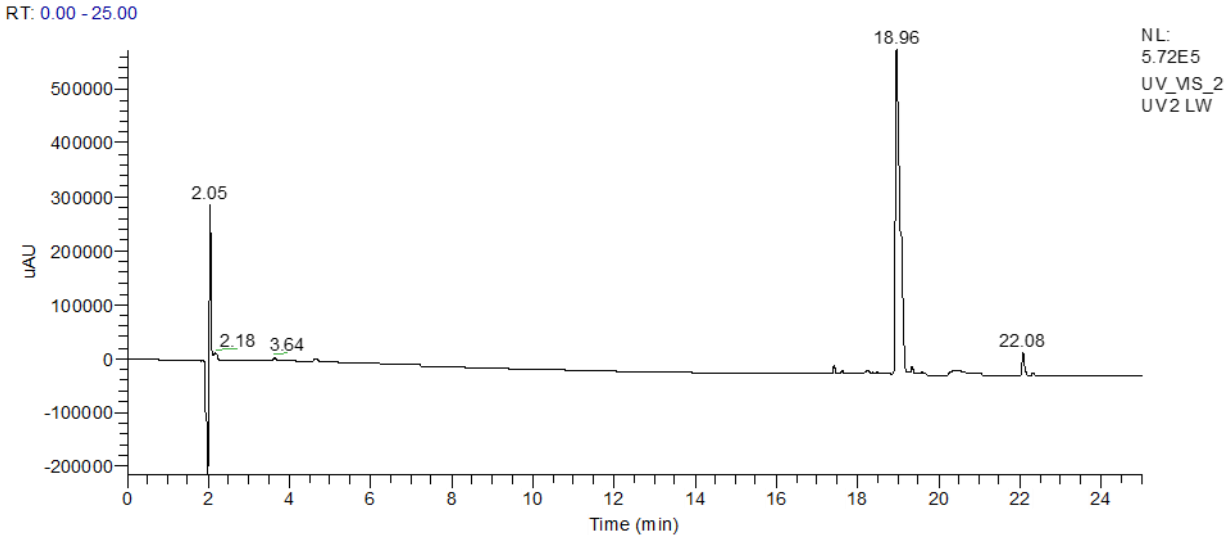
RT: 0.00 - 25.00
NL:
5.72E5
UV_VIS_2
UV2 LW
18.96
2.05
2.18
3.64
22.08
uAU
500000
400000
300000
200000
100000
0
-100000
-200000
0
2
4
6
8
10
12
14
16
18
20
22
24
Time (min)

Compound **4**

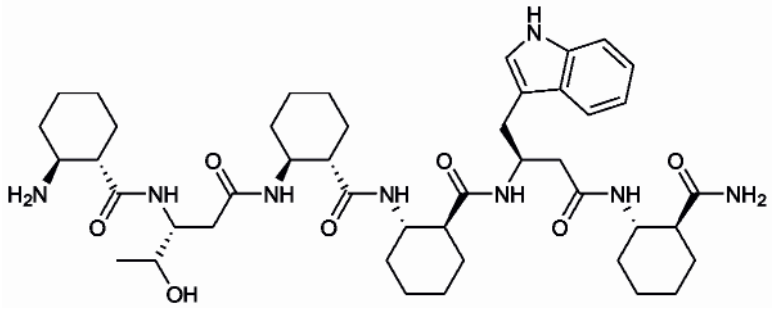

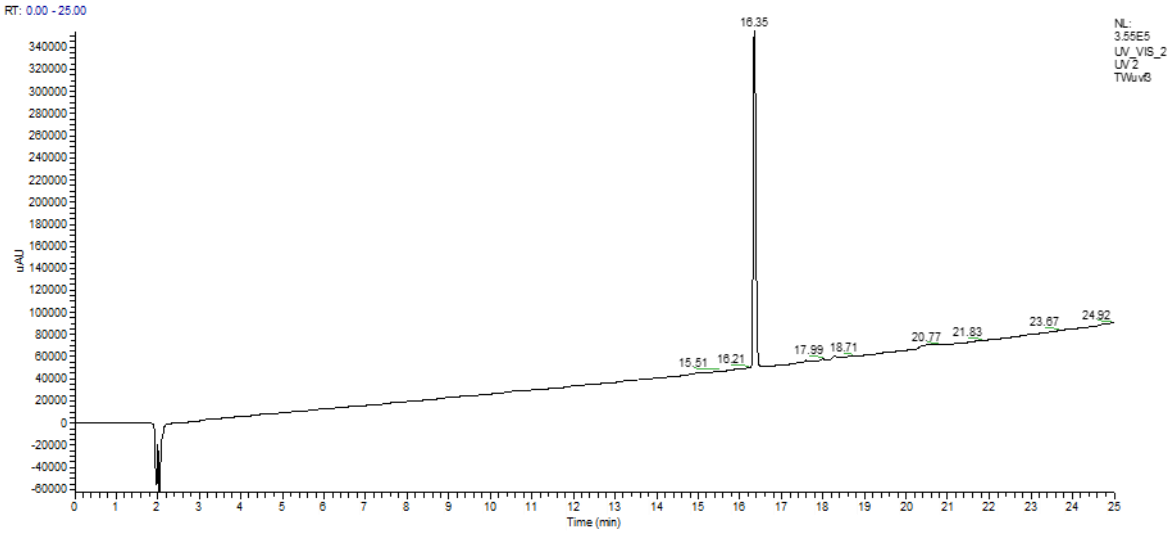
RT: 0.00 - 25.00
NL:
3.55E5
UV_VIS_2
UV 2
TWuv8
uAU
Time (min)
16.35
15.51
16.21
17.99
18.71
20.77
21.83
23.67
24.92

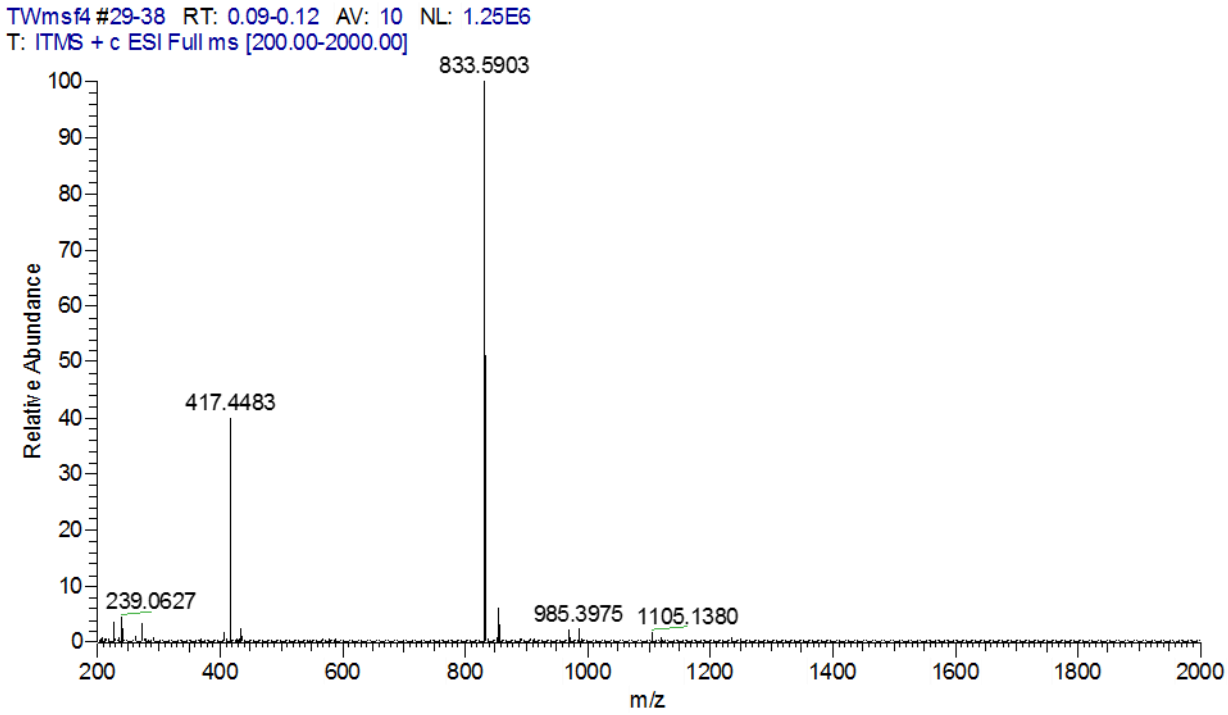
TWmsf4 #29-38 RT: 0.09-0.12 AV: 10 NL: 1.25E6
T: ITMS + c ESI Full ms [200.00-2000.00]
833.5903
417.4483
239.0627
985.3975
1105.1380
Relative Abundance
m/z

Compound **5**

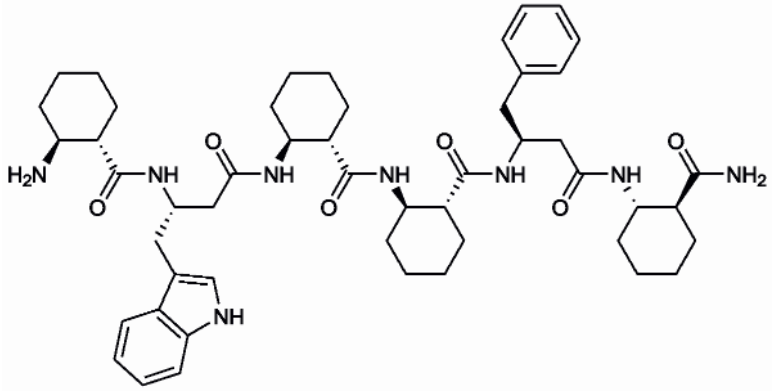
H2N
NH
NH
NH
NH
NH
NH2
NH

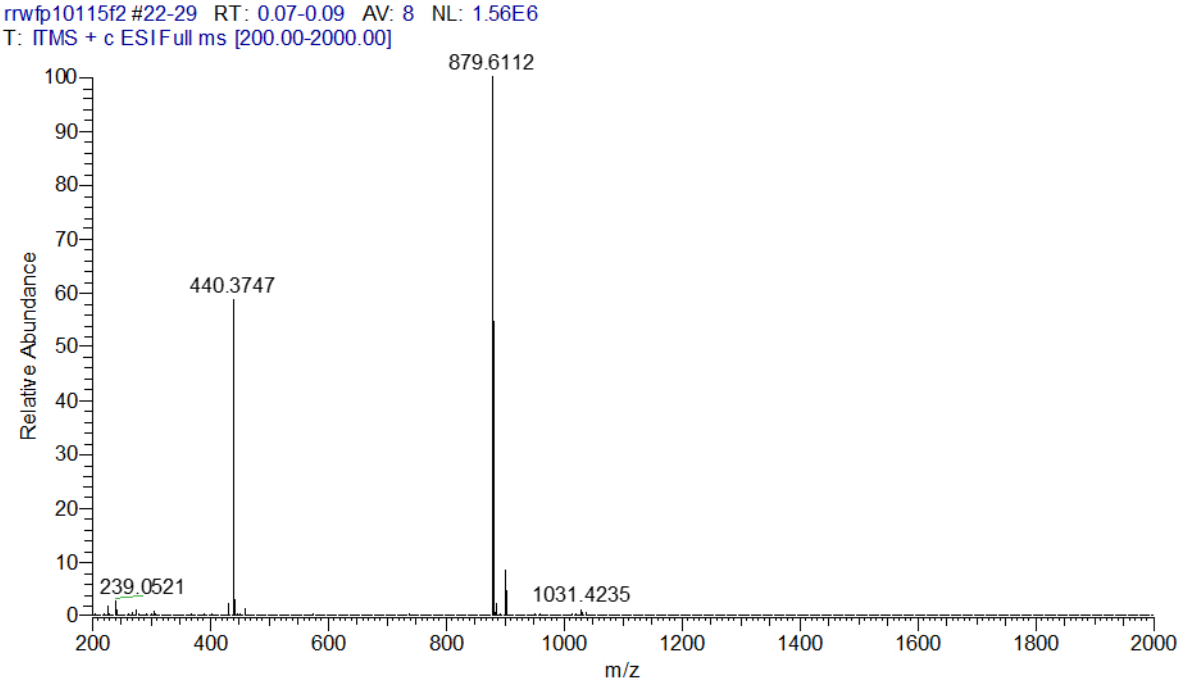
rrwfp10115f2 #22-29 RT: 0.07-0.09 AV: 8 NL: 1.56E6
T: ITMS + c ESI Full ms [200.00-2000.00]
879.6112
440.3747
239.0521
1031.4235
Relative Abundance
m/z

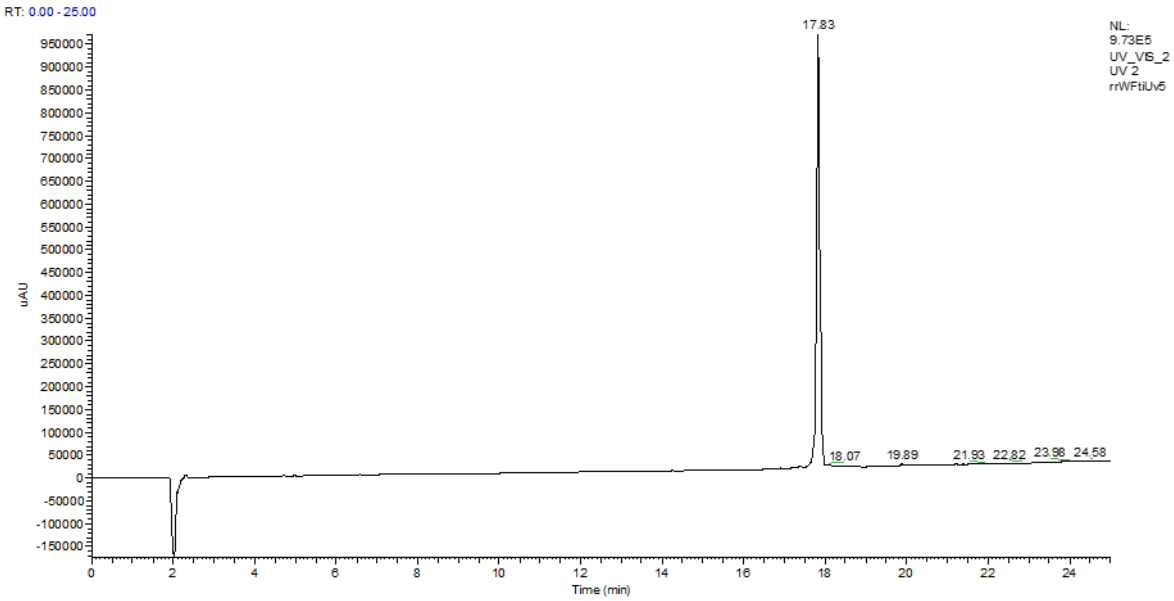
RT: 0.00 - 25.00
17.83
NL:
9.73E5
UV_VIS_2
UV 2
rrWFtiUv5
uAU
18.07
19.89
21.93
22.82
23.98
24.58
Time (min)

Compound **6**

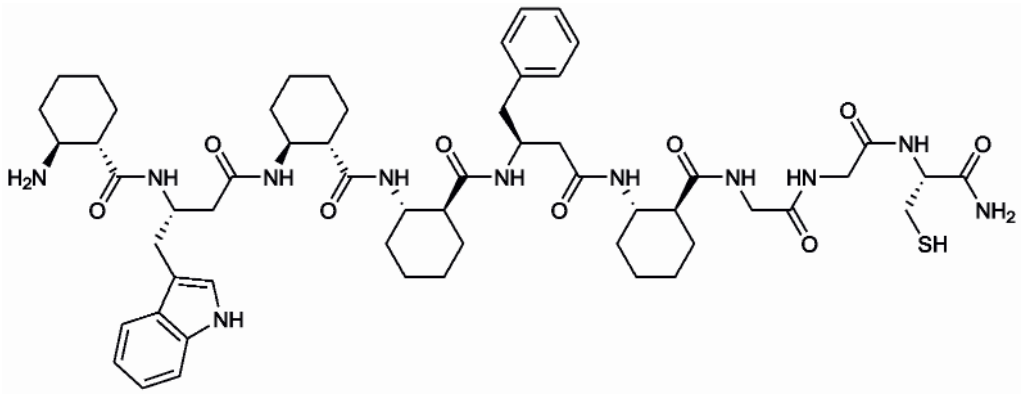
H2N
NH
O
NH2
SH
HN
NH

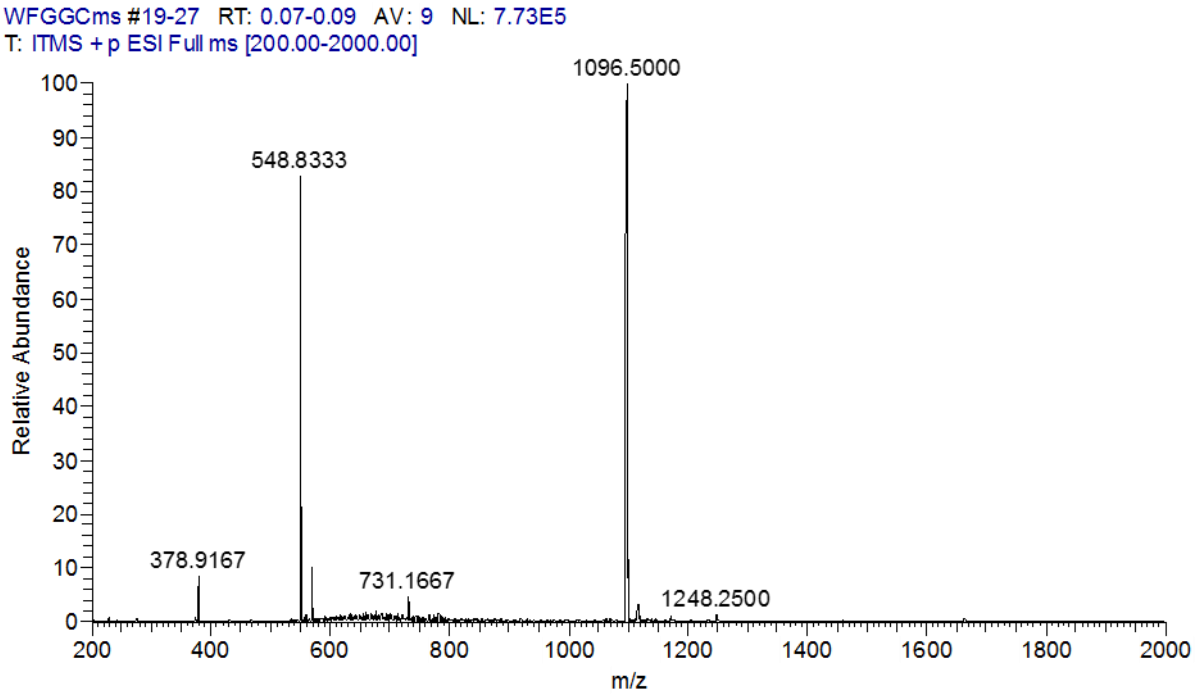
WFGGCms #19-27 RT: 0.07-0.09 AV: 9 NL: 7.73E5
T: ITMS + p ESI Full ms [200.00-2000.00]
1096.5000
548.8333
378.9167
731.1667
1248.2500
Relative Abundance
m/z

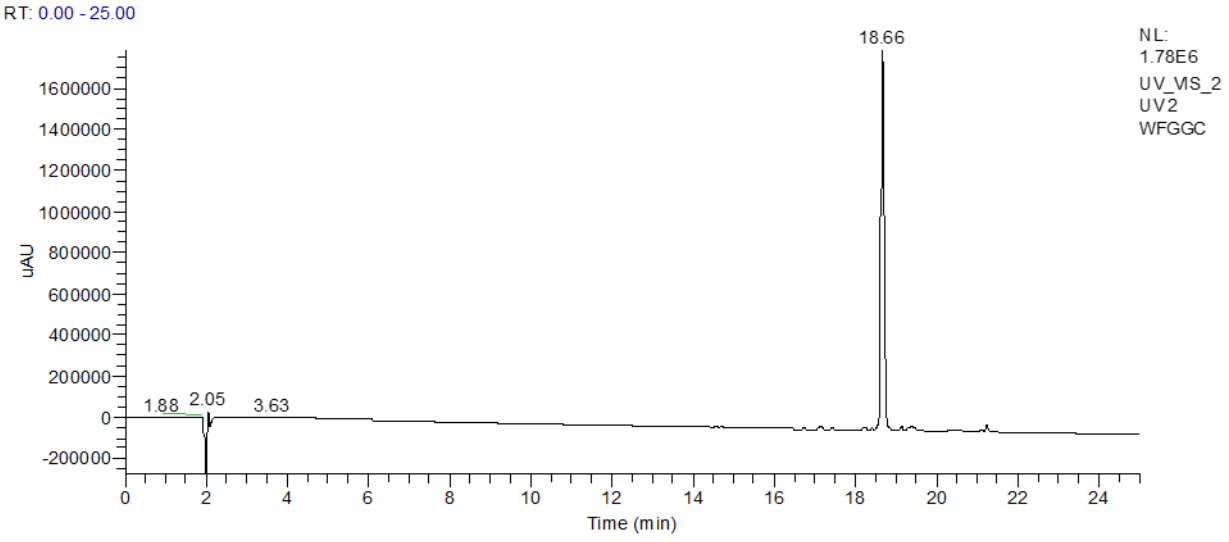
RT: 0.00 - 25.00
18.66
NL:
1.78E6
UV_VIS_2
UV2
WFGGC
uAU
1.88
2.05
3.63
Time (min)

Compound **7**

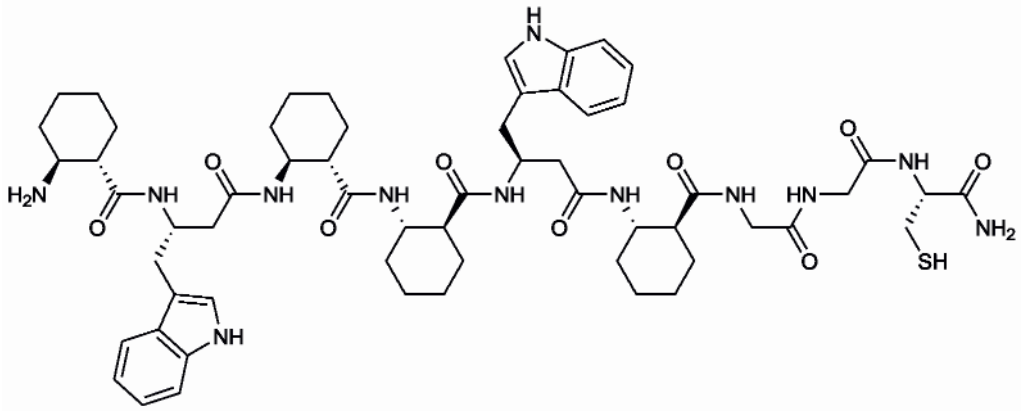

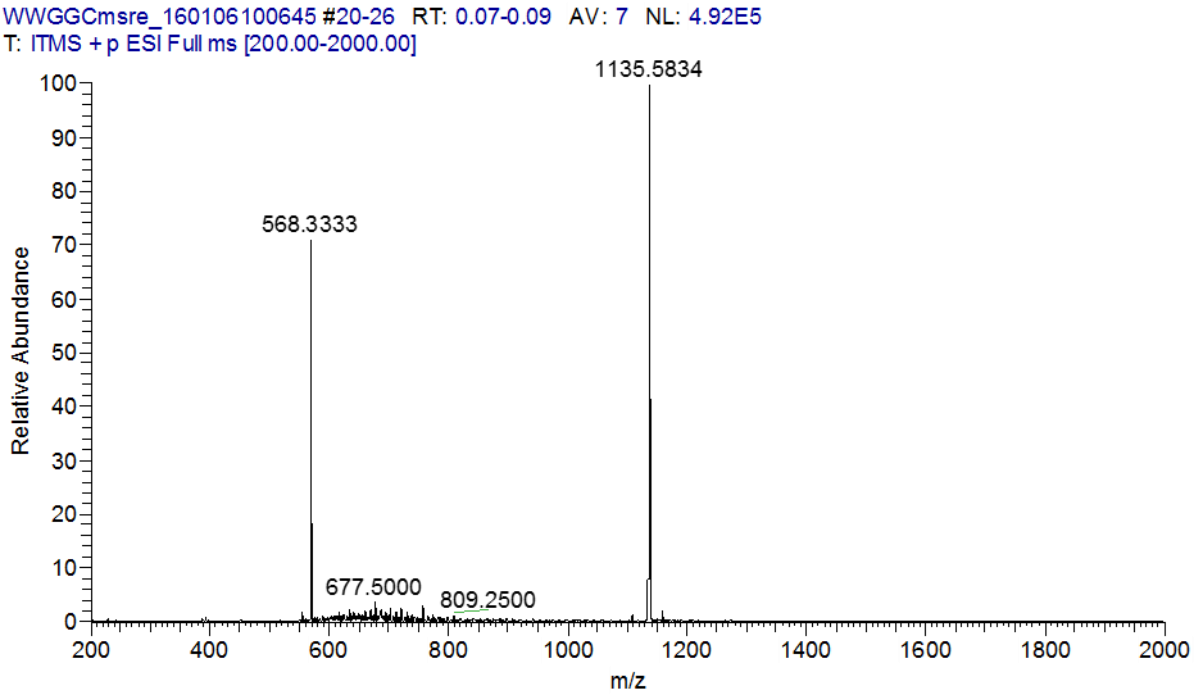
WWGGCmsre_160106100645 #20-26 RT: 0.07-0.09 AV: 7 NL: 4.92E5
T: ITMS + p ESI Full ms [200.00-2000.00]
1135.5834
568.3333
677.5000
809.2500
Relative Abundance
m/z

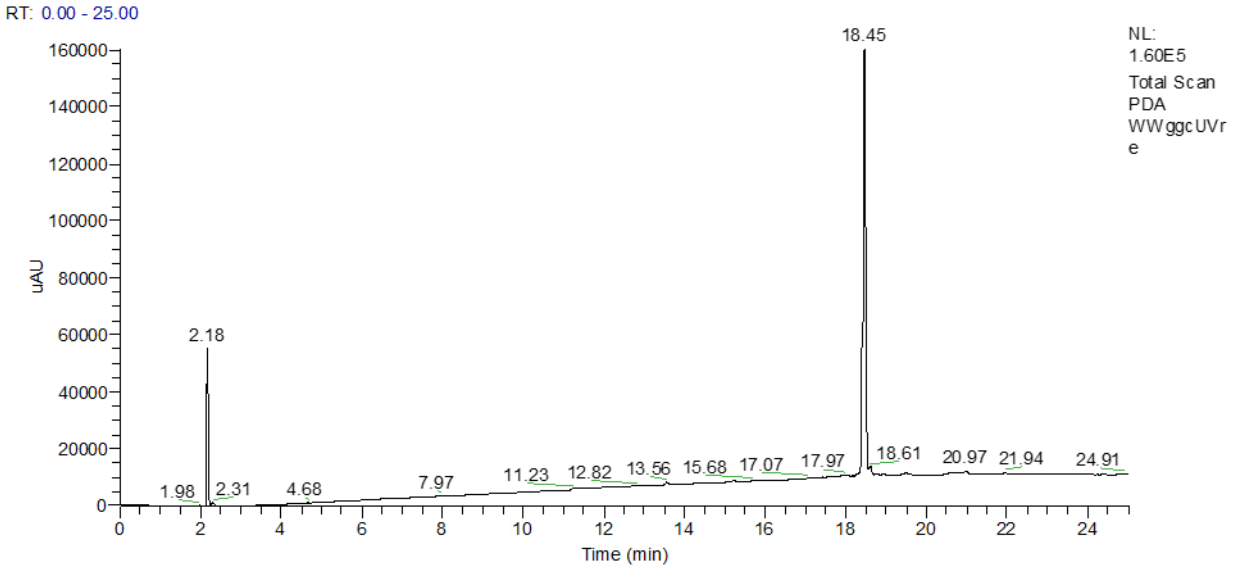
RT: 0.00 - 25.00
NL:
1.60E5
Total Scan
PDA
WWggcUVr
e
uAU
Time (min)
18.45
2.18
1.98
2.31
4.68
7.97
11.23
12.82
13.56
15.68
17.07
17.97
18.61
20.97
21.94
24.91

Compound **8**

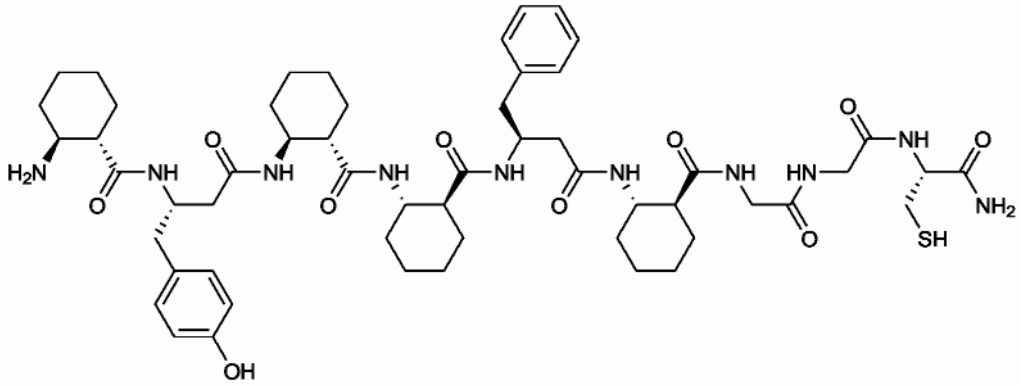
H2N
NH
NH
NH
NH
NH
NH
HN
NH
NH2
SH
OH

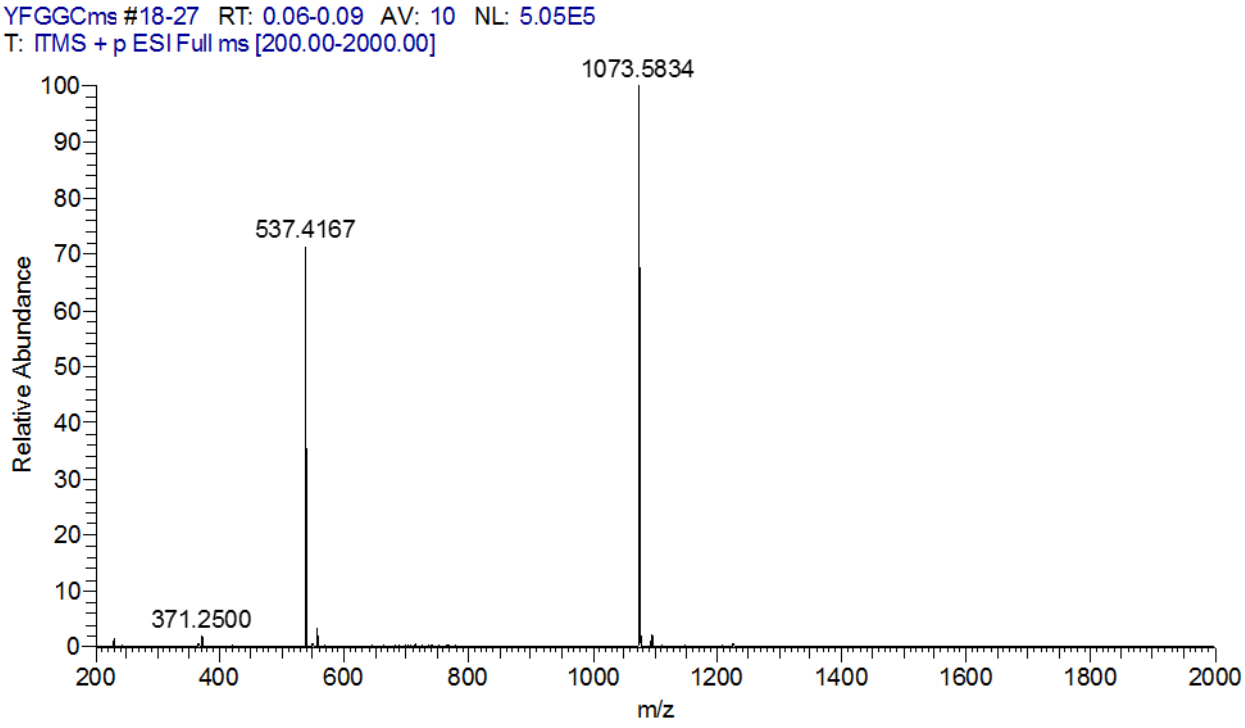
YFGGCms #18-27 RT: 0.06-0.09 AV: 10 NL: 5.05E5
T: ITMS + p ESI Full ms [200.00-2000.00]
1073.5834
537.4167
371.2500
Relative Abundance
m/z

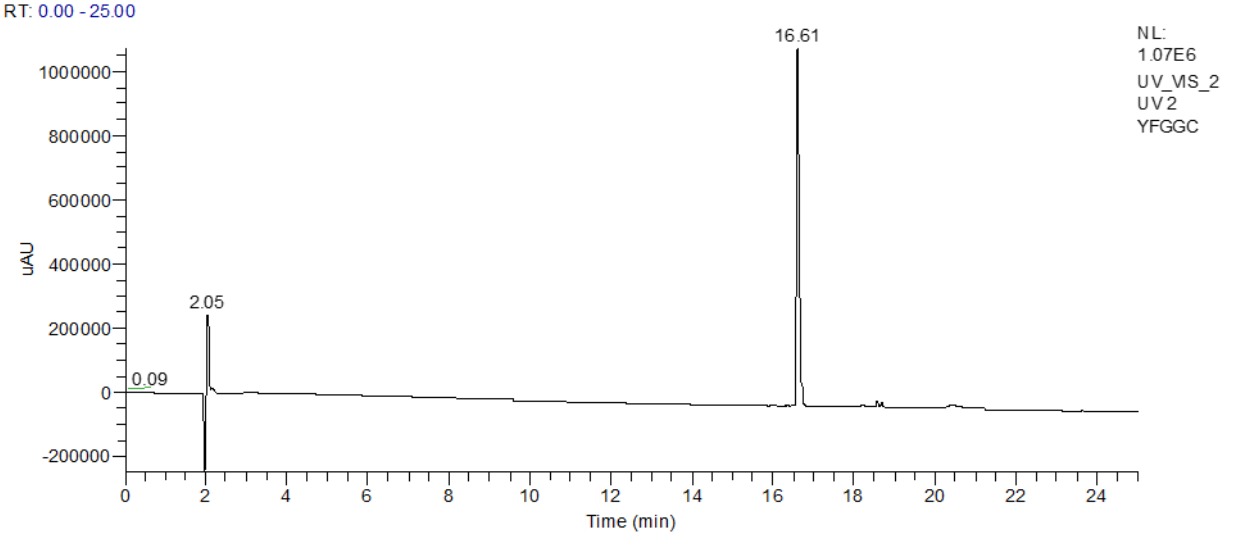
RT: 0.00 - 25.00
16.61
NL:
1.07E6
UV_VIS_2
UV2
YFGGC
2.05
0.09
uAU
Time (min)

Compound **9**

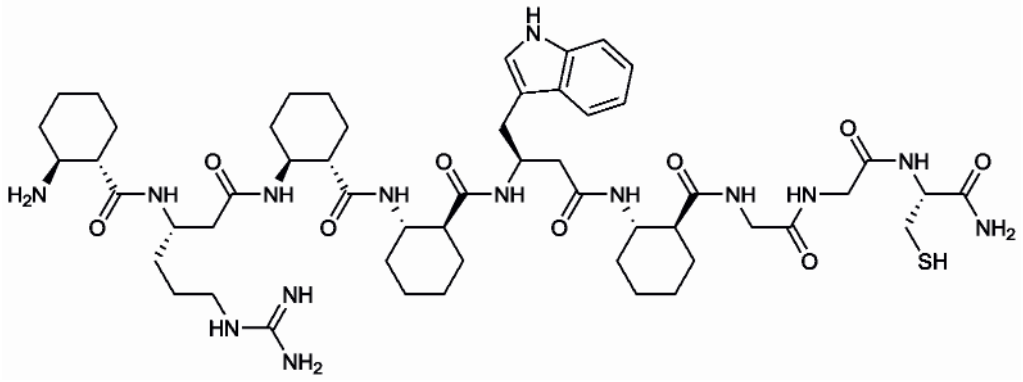

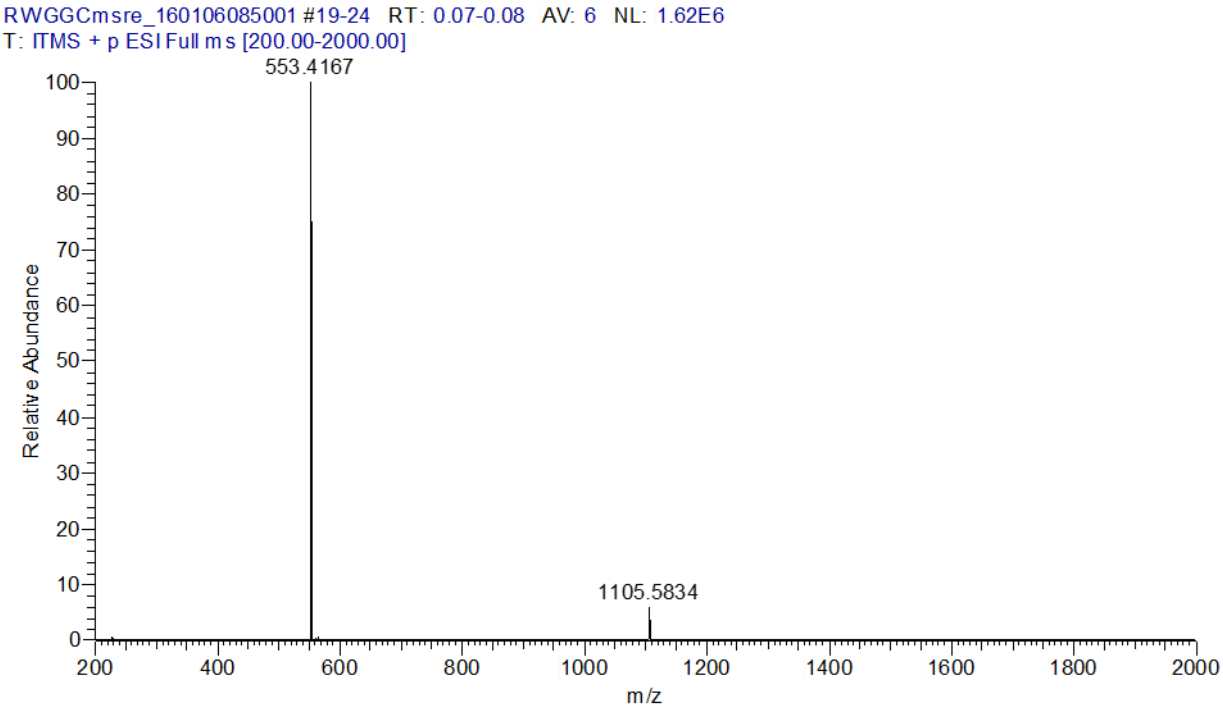
RWGGCmsre_160106085001 #19-24 RT: 0.07-0.08 AV: 6 NL: 1.62E6
T: ITMS + p ESI Full ms [200.00-2000.00]
553.4167
1105.5834
Relative Abundance
m/z
100
90
80
70
60
50
40
30
20
10
0
200
400
600
800
1000
1200
1400
1600
1800
2000

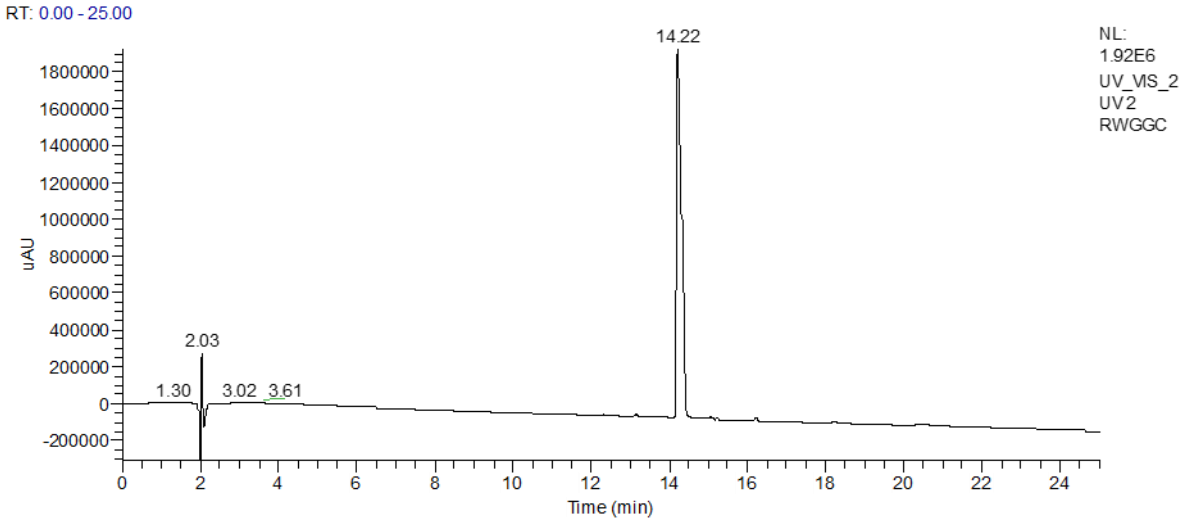
RT: 0.00 - 25.00
NL:
1.92E6
UV_VIS_2
UV2
RWGGC
14.22
2.03
1.30
3.02
3.61
uAU
1800000
1600000
1400000
1200000
1000000
800000
600000
400000
200000
0
-200000
0
2
4
6
8
10
12
14
16
18
20
22
24
Time (min)

Compound **10**

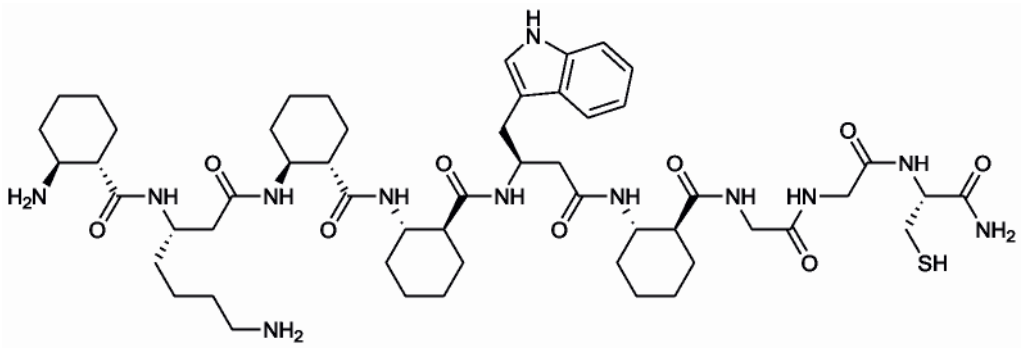

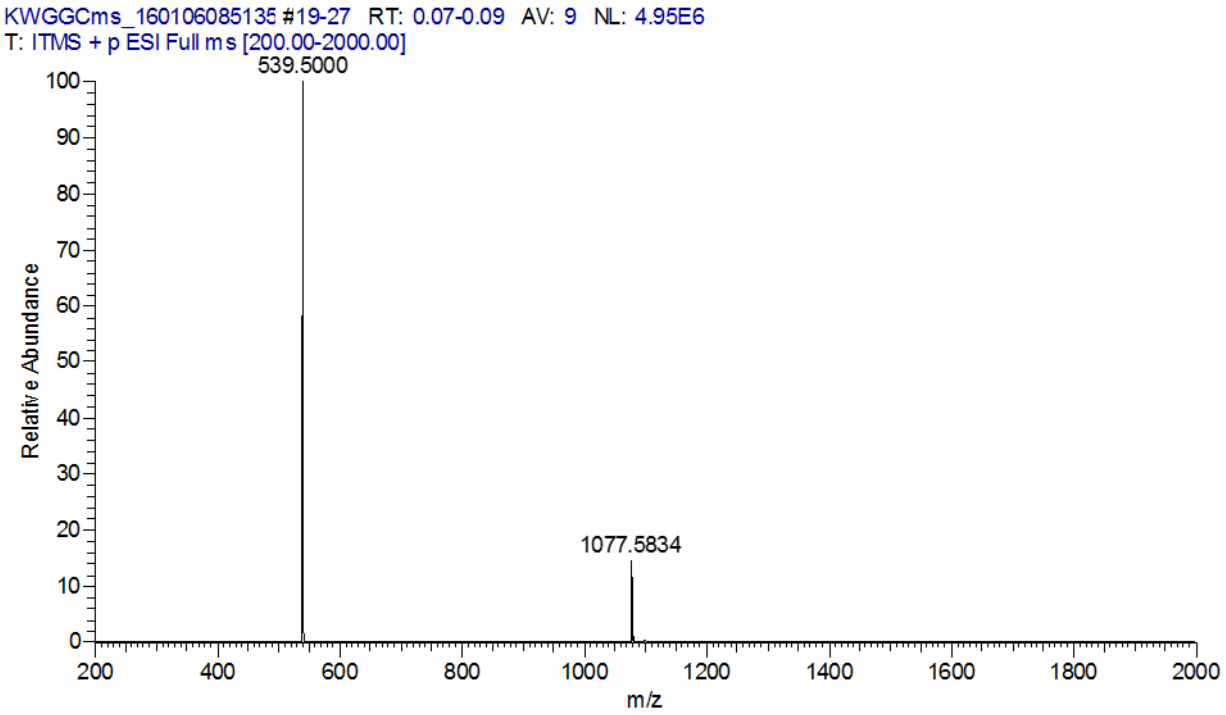
KWGGCms_160106085135 #19-27 RT: 0.07-0.09 AV: 9 NL: 4.95E6
T: ITMS + p ESI Full ms [200.00-2000.00]
539.5000
1077.5834
Relative Abundance
m/z

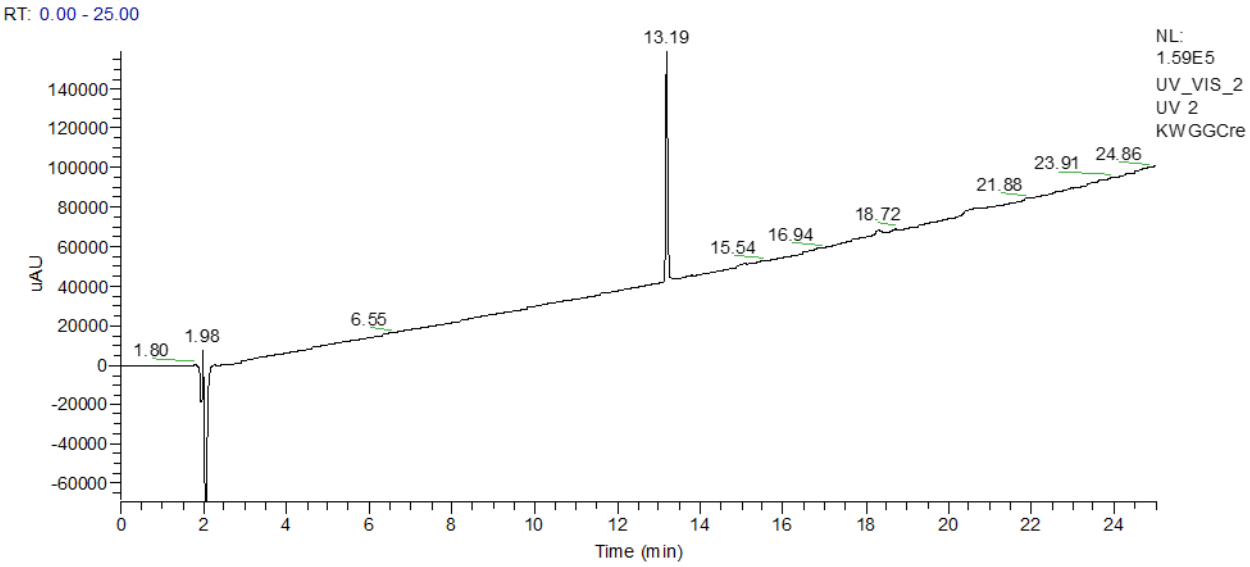
RT: 0.00 - 25.00
NL:
1.59E5
UV_VIS_2
UV 2
KWGGCre
13.19
1.80
1.98
6.55
15.54
16.94
18.72
21.88
23.91
24.86
uAU
Time (min)

Compound **11**

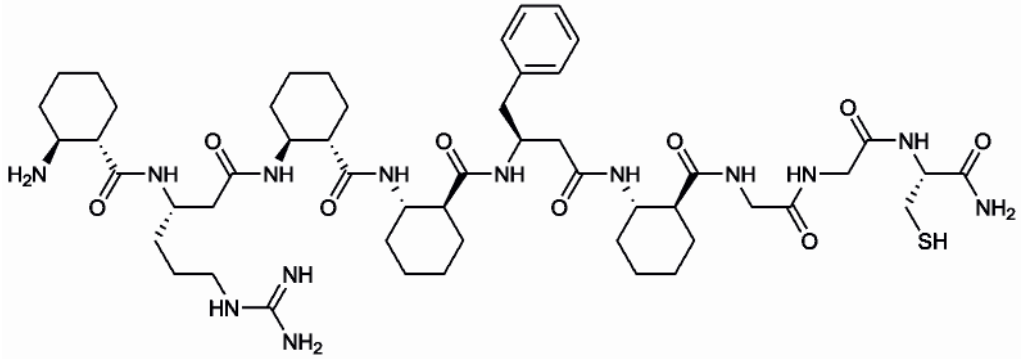

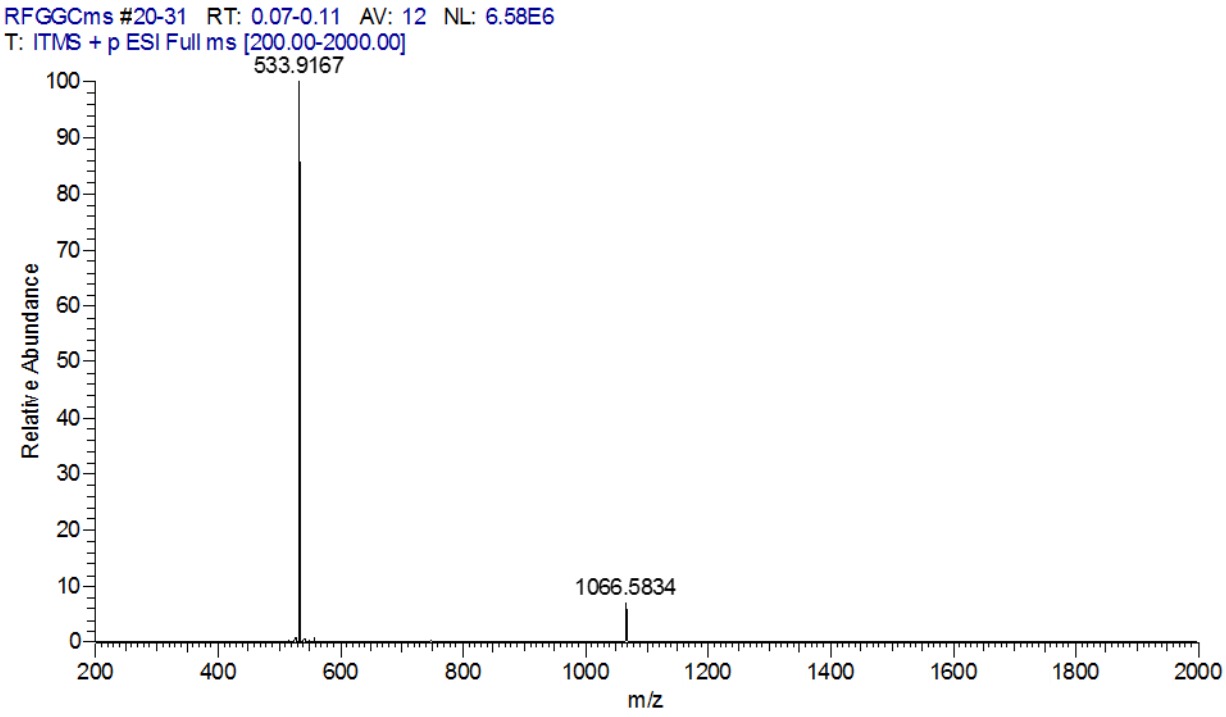
RFGGCms #20-31 RT: 0.07-0.11 AV: 12 NL: 6.58E6
T: ITMS + p ESI Full ms [200.00-2000.00]
533.9167
1066.5834
Relative Abundance
m/z
100
90
80
70
60
50
40
30
20
10
0
200
400
600
800
1000
1200
1400
1600
1800
2000

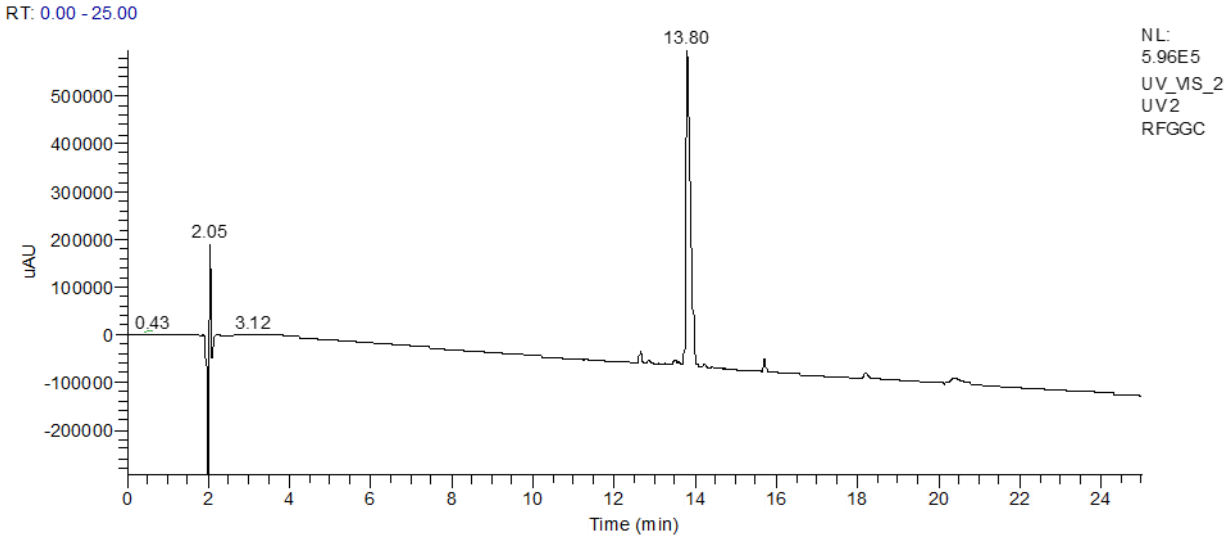
RT: 0.00 - 25.00
NL:
5.96E5
UV_VIS_2
UV2
RFGGC
13.80
2.05
0.43
3.12
uAU
500000
400000
300000
200000
100000
0
-100000
-200000
0
2
4
6
8
10
12
14
16
18
20
22
24
Time (min)

Compound **12**

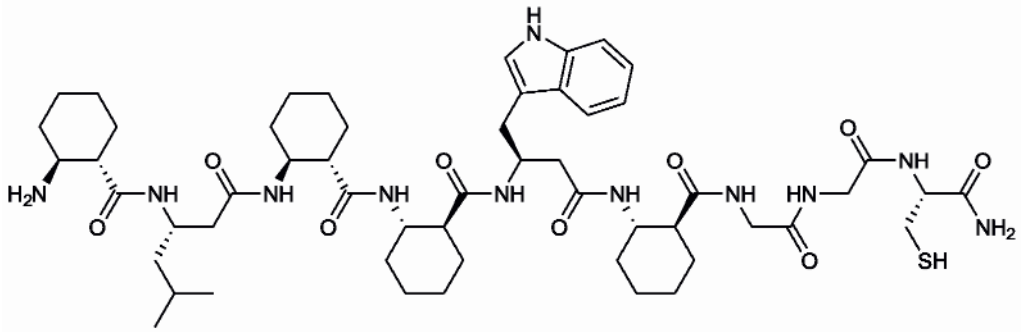

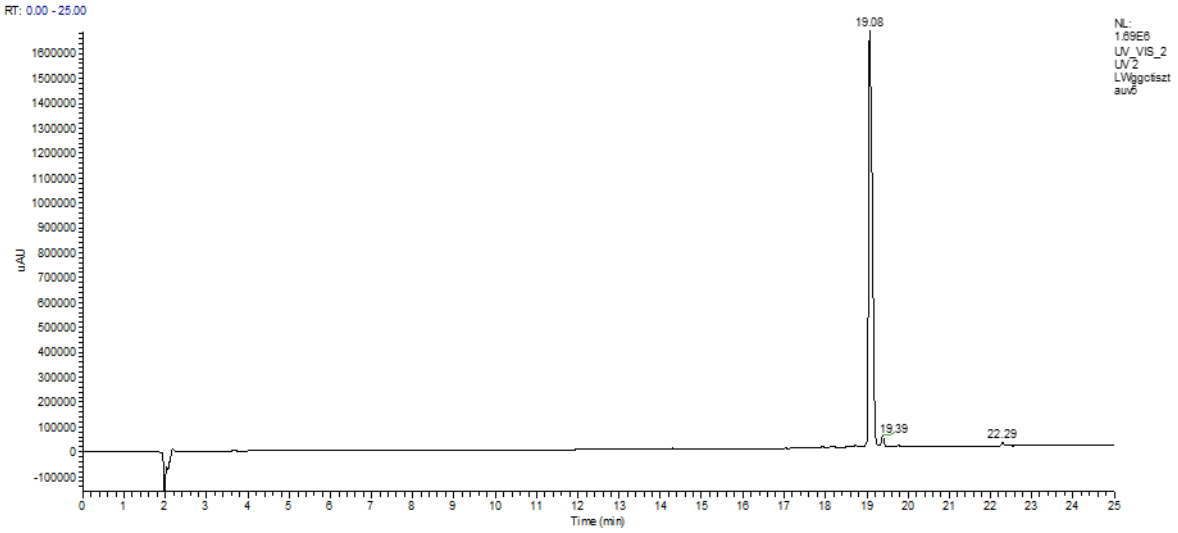

LWggc_160107083237 #20-25 RT: 0.07-0.09 AV: 6 NL: 7.08E5
T: ITMS + p ESI Full ms [200.00-2000.00]

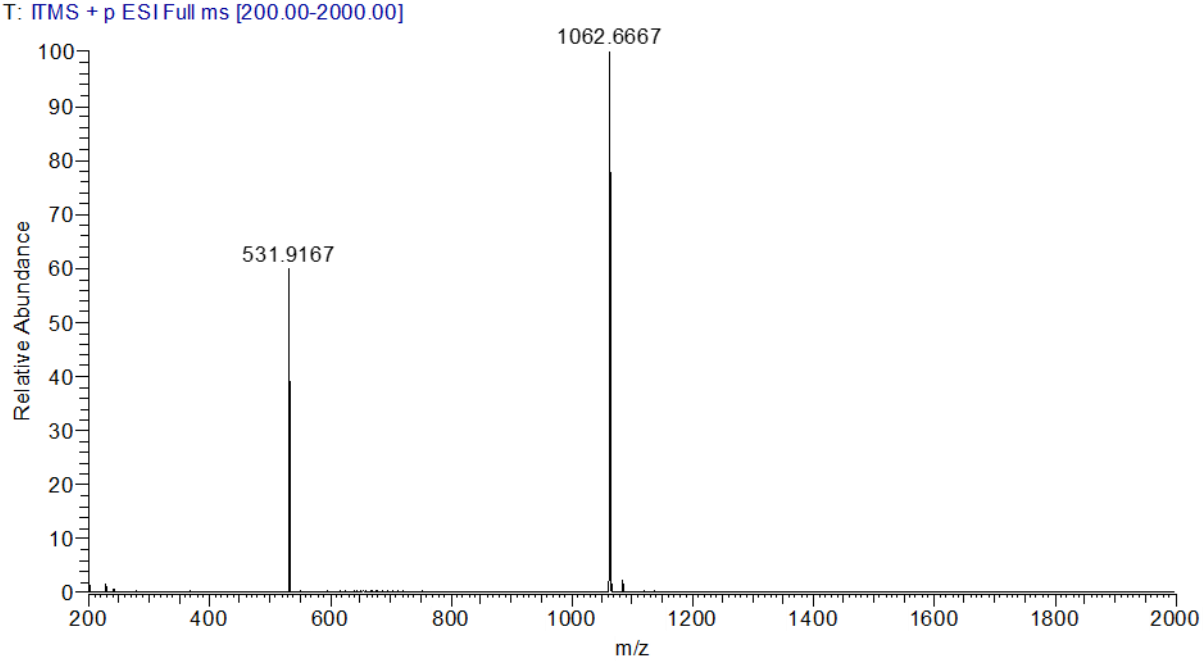

Compound **13**

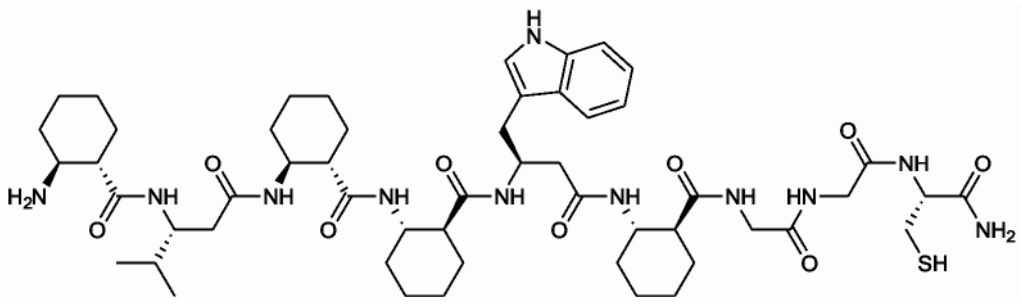

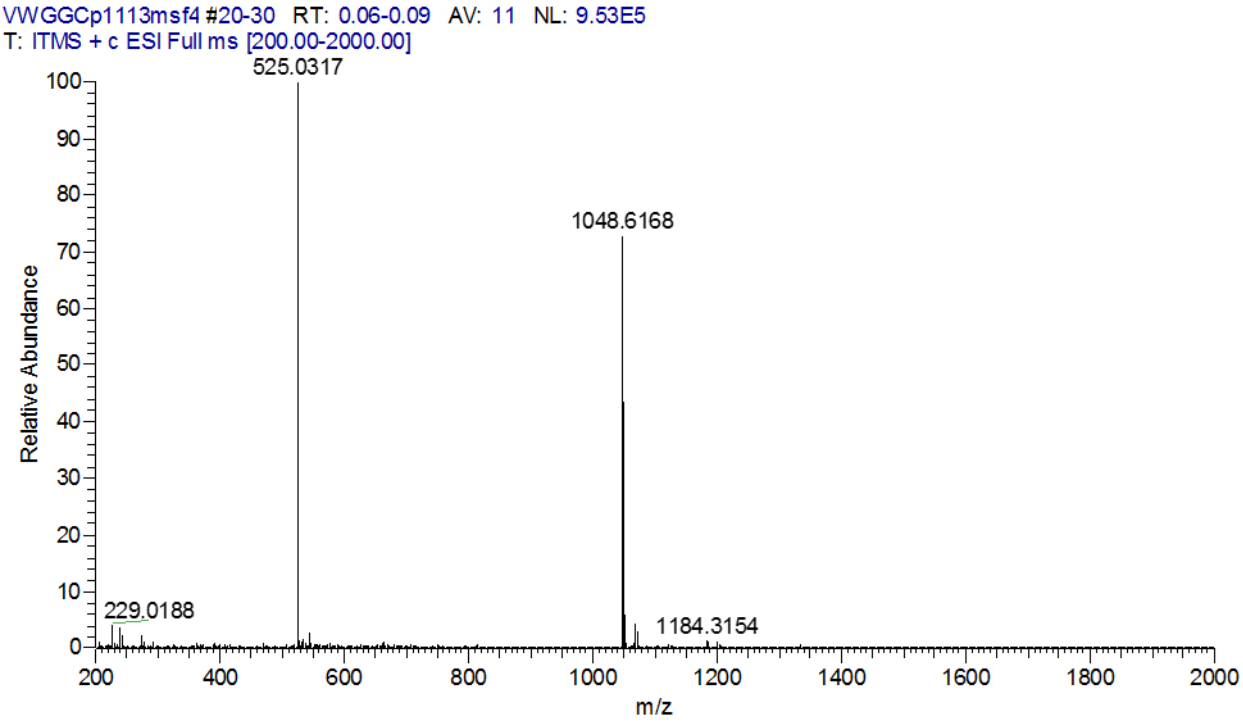
VWGGCp1113msf4 #20-30 RT: 0.06-0.09 AV: 11 NL: 9.53E5
T: ITMS + c ESI Full ms [200.00-2000.00]
525.0317
1048.6168
229.0188
1184.3154
Relative Abundance
m/z

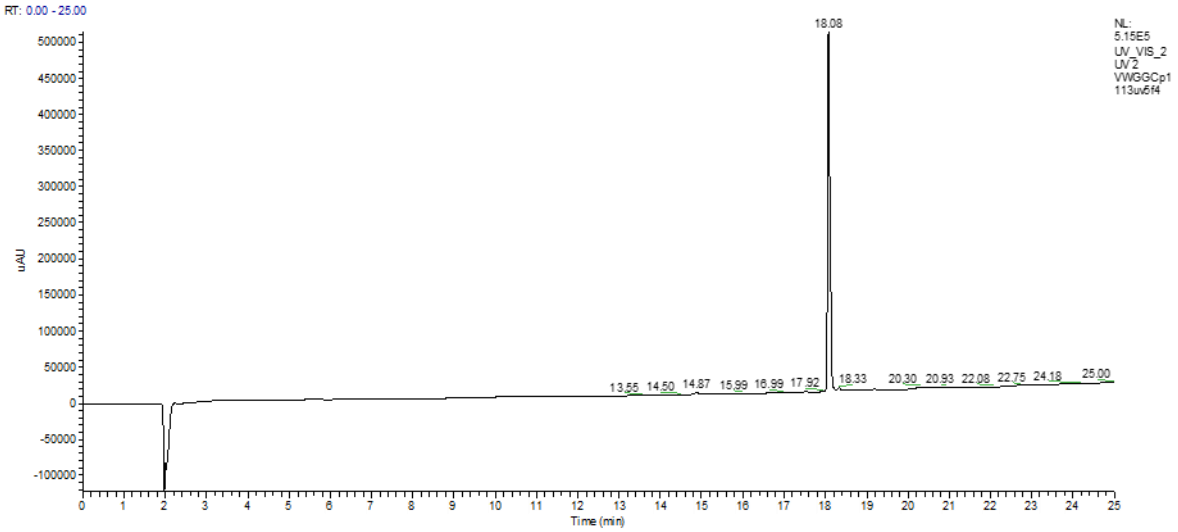
RT: 0.00 - 25.00
18.08
NL:
5.15E5
UV_VIS_2
UV 2
VWGGCp1
113uv5f4
uAU
Time (min)

Compound **14**

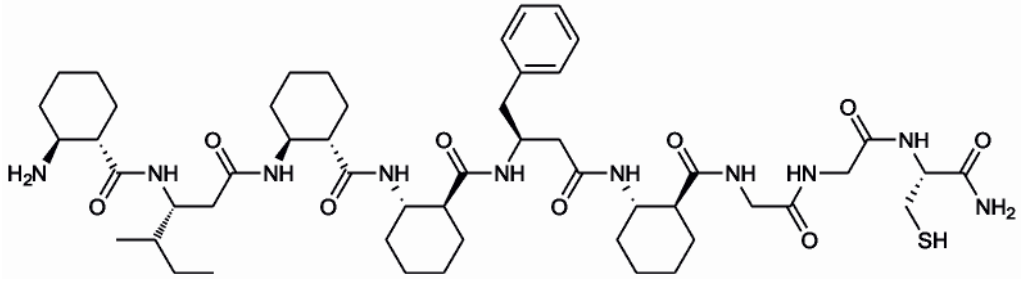

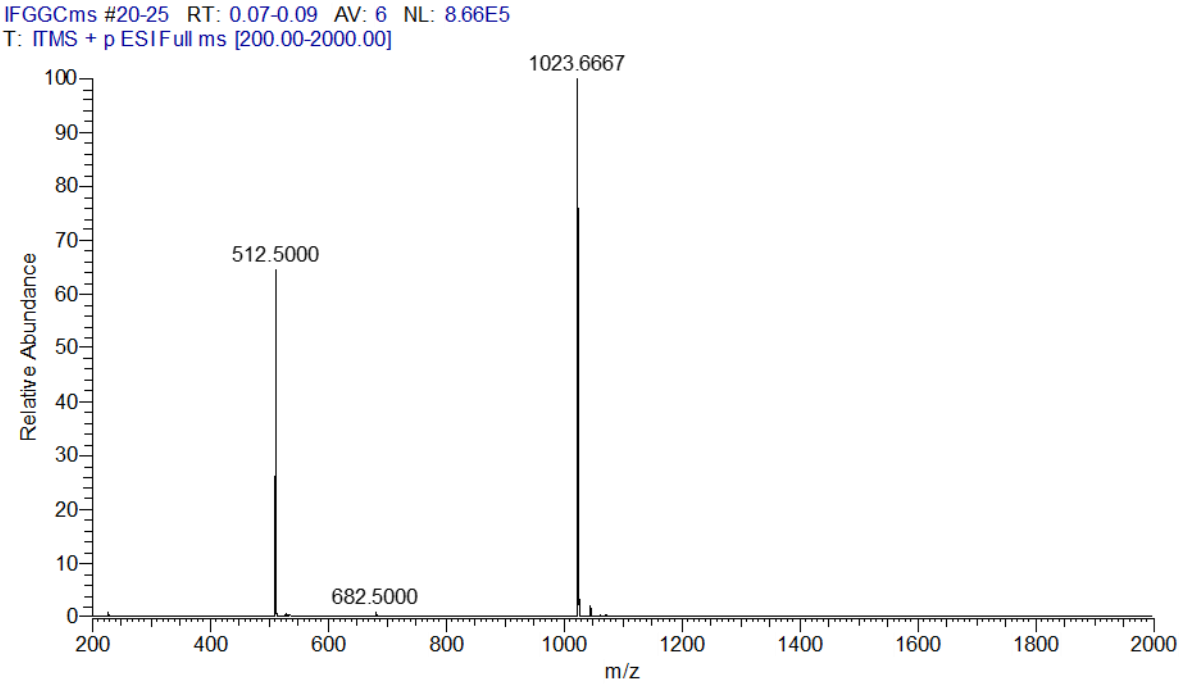
IFGGCms #20-25 RT: 0.07-0.09 AV: 6 NL: 8.66E5
T: ITMS + p ESI Full ms [200.00-2000.00]
1023.6667
512.5000
682.5000
Relative Abundance
m/z

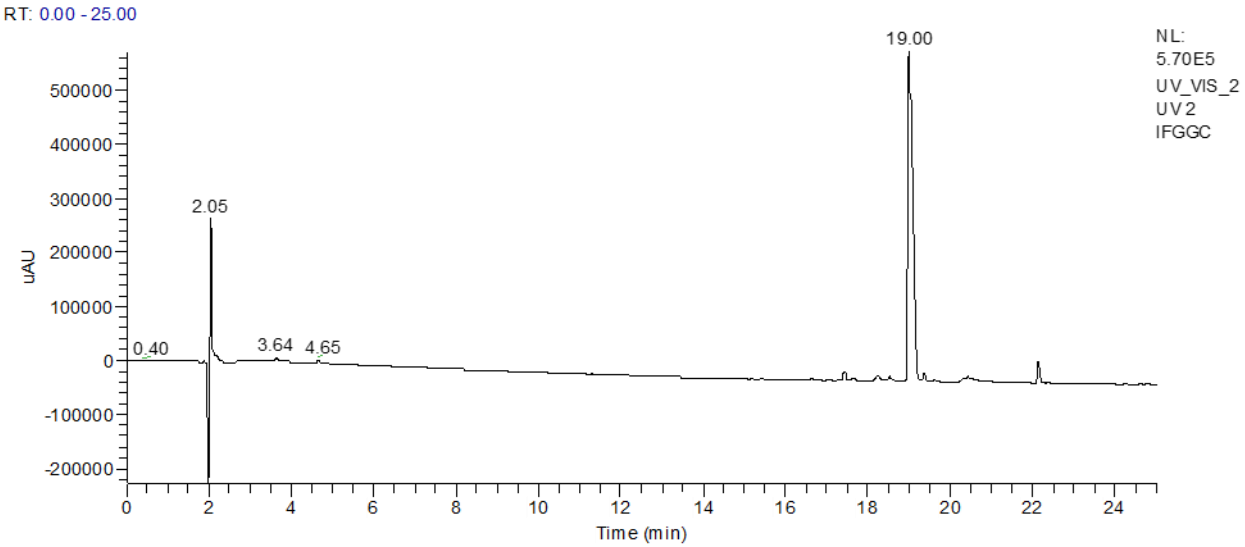
RT: 0.00 - 25.00
19.00
NL:
5.70E5
UV_VIS_2
UV 2
IFGGC
2.05
0.40
3.64
4.65
uAU
Time (min)

Compound **15**

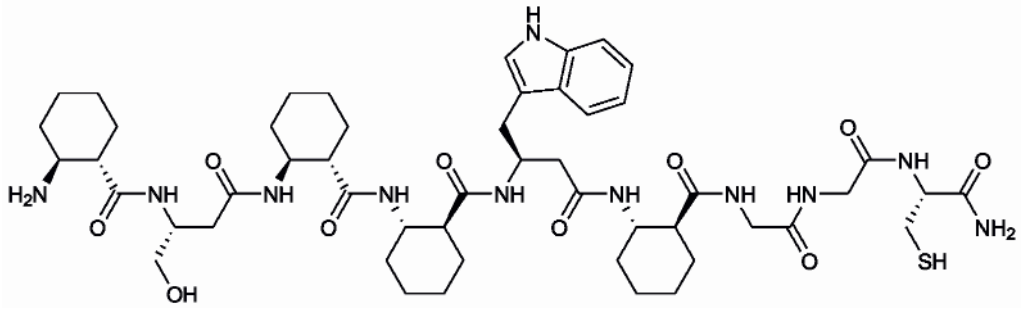

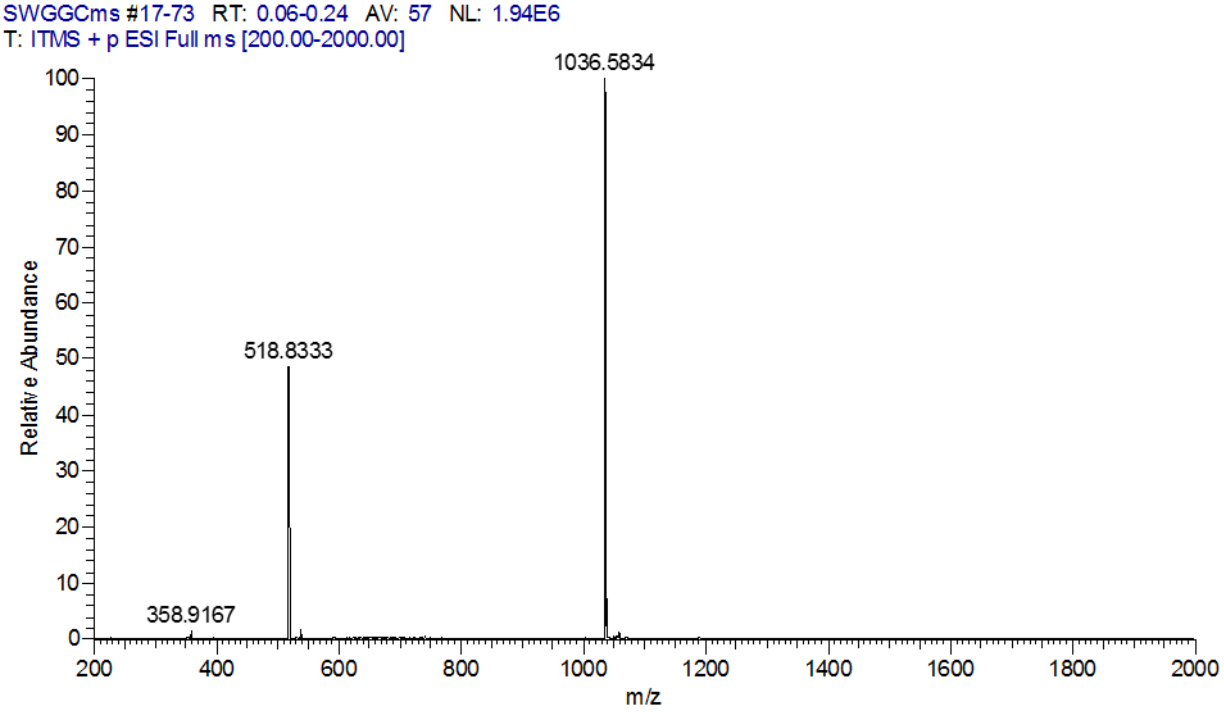
SWGGCms #17-73 RT: 0.06-0.24 AV: 57 NL: 1.94E6
T: ITMS + p ESI Full ms [200.00-2000.00]
1036.5834
518.8333
358.9167
Relative Abundance
m/z

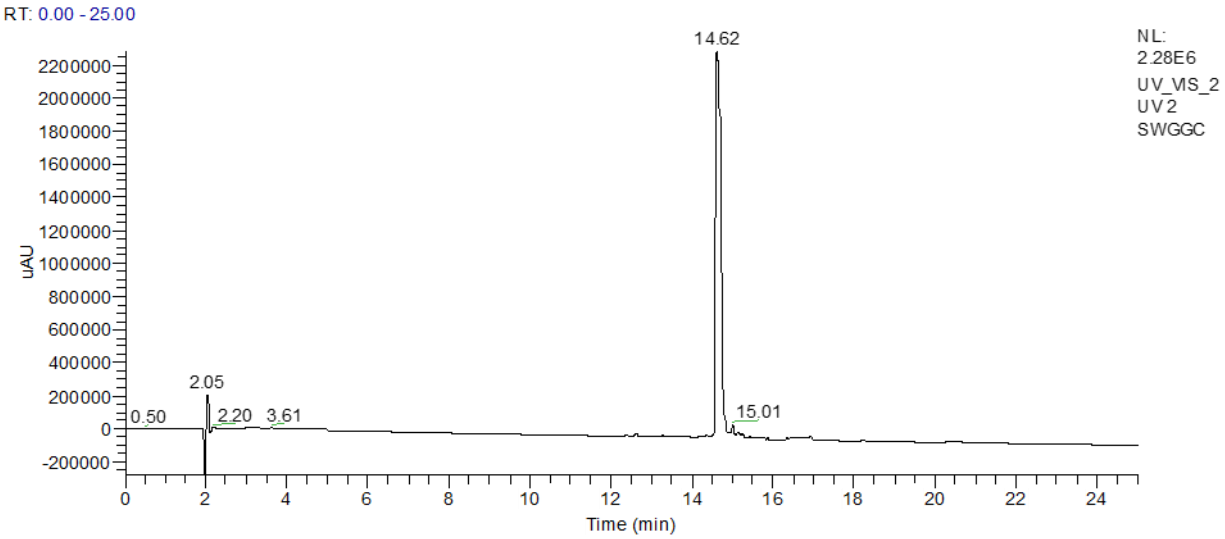
RT: 0.00 - 25.00
14.62
NL:
2.28E6
UV_VIS_2
UV2
SWGGC
2.05
0.50
2.20
3.61
15.01
uAU
Time (min)

Compound **16**

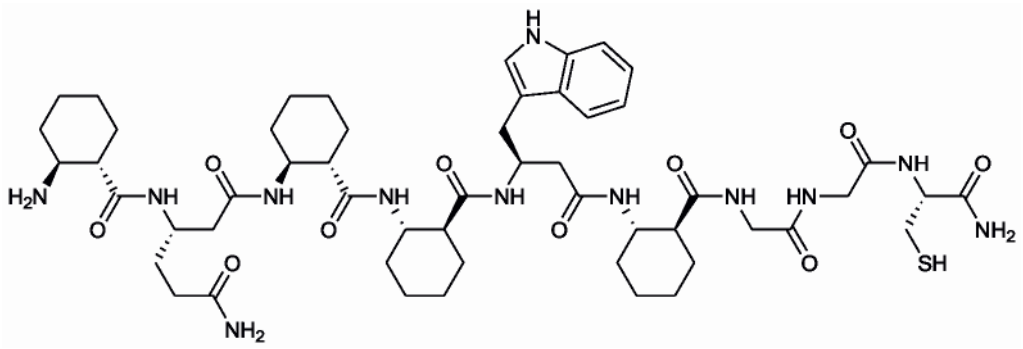

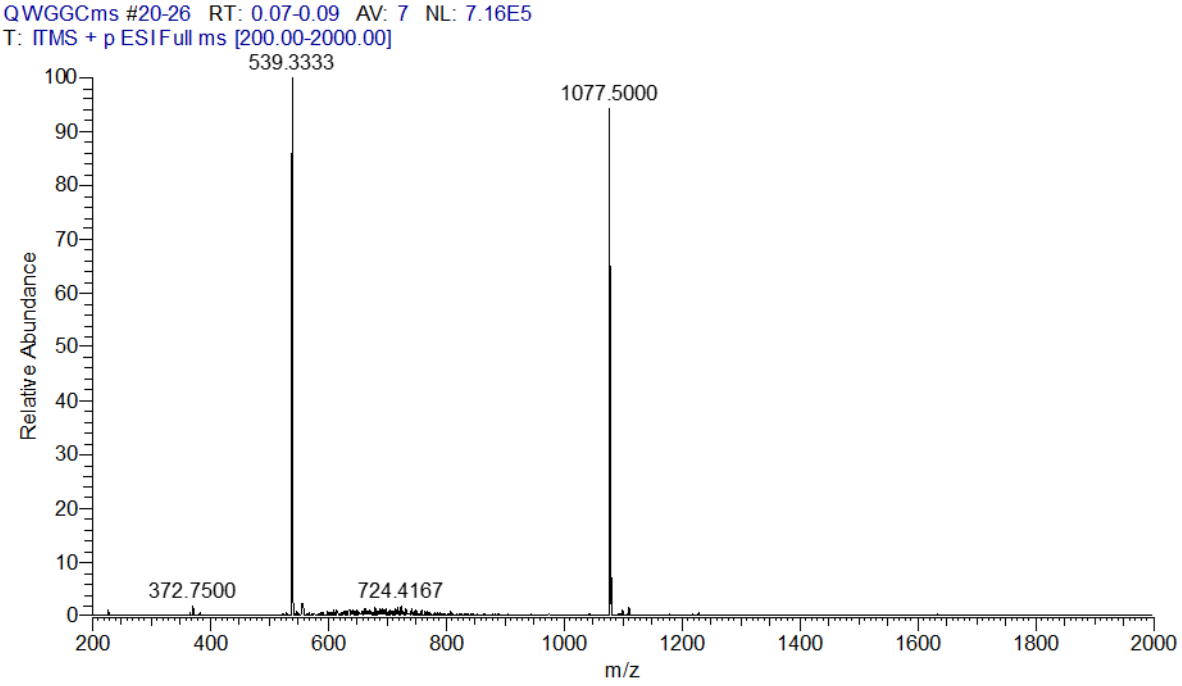
QWGGCms #20-26 RT: 0.07-0.09 AV: 7 NL: 7.16E5
T: ITMS + p ESI Full ms [200.00-2000.00]
539.3333
1077.5000
372.7500
724.4167
Relative Abundance
m/z

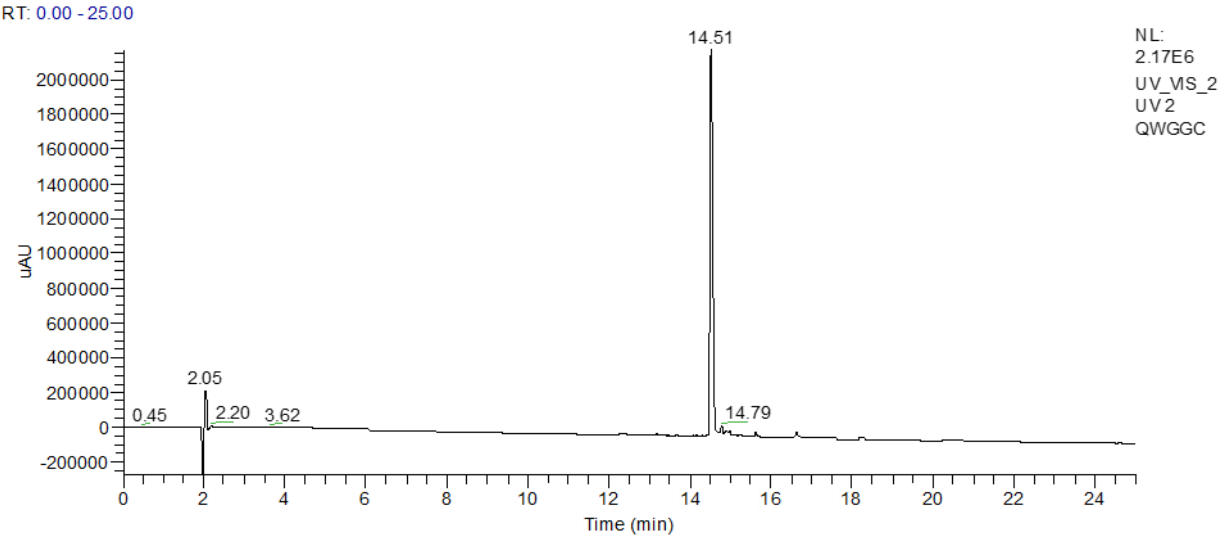
RT: 0.00 - 25.00
14.51
NL:
2.17E6
UV_VIS_2
UV2
QWGGC
2.05
0.45
2.20
3.62
14.79
uAU
Time (min)

Compound **17**

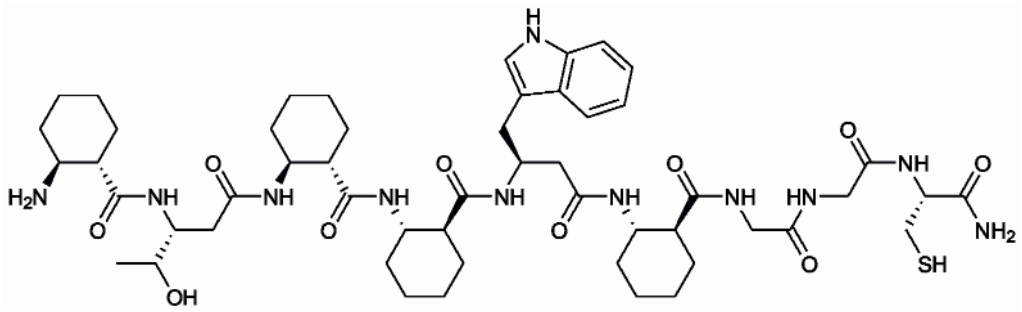

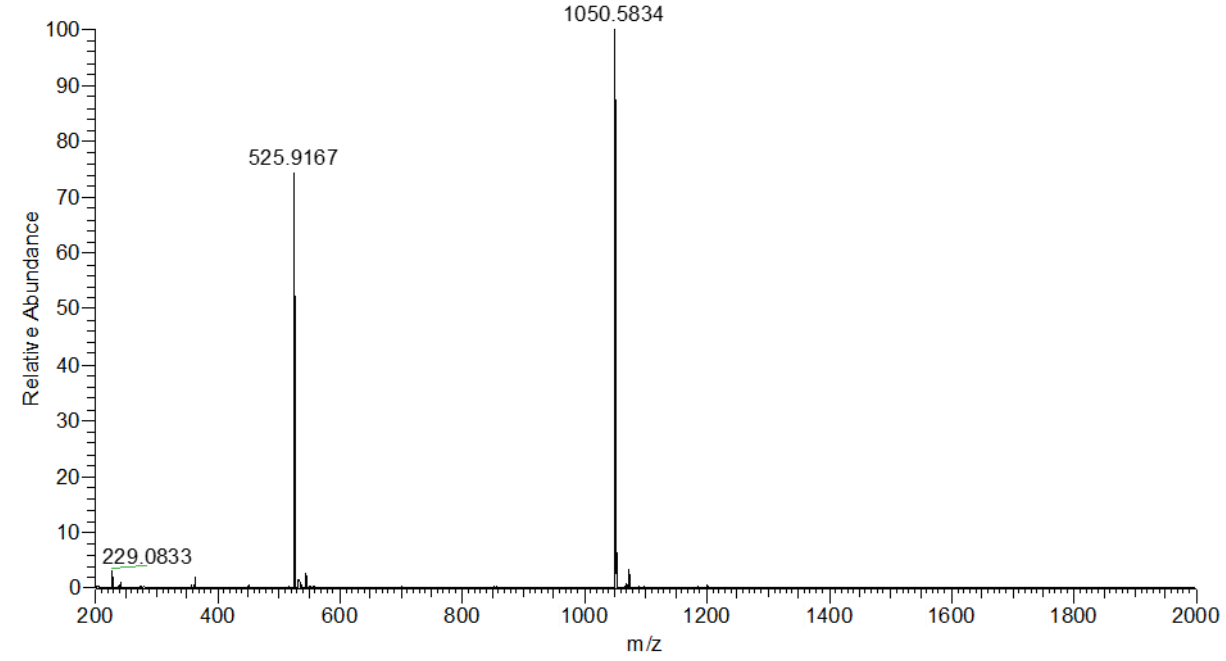
TWGGCms #18-25 RT: 0.06-0.09 AV: 8 NL: 3.16E5
T: ITMS + p ESI Full ms [200.00-2000.00]
1050.5834
525.9167
229.0833
Relative Abundance
m/z

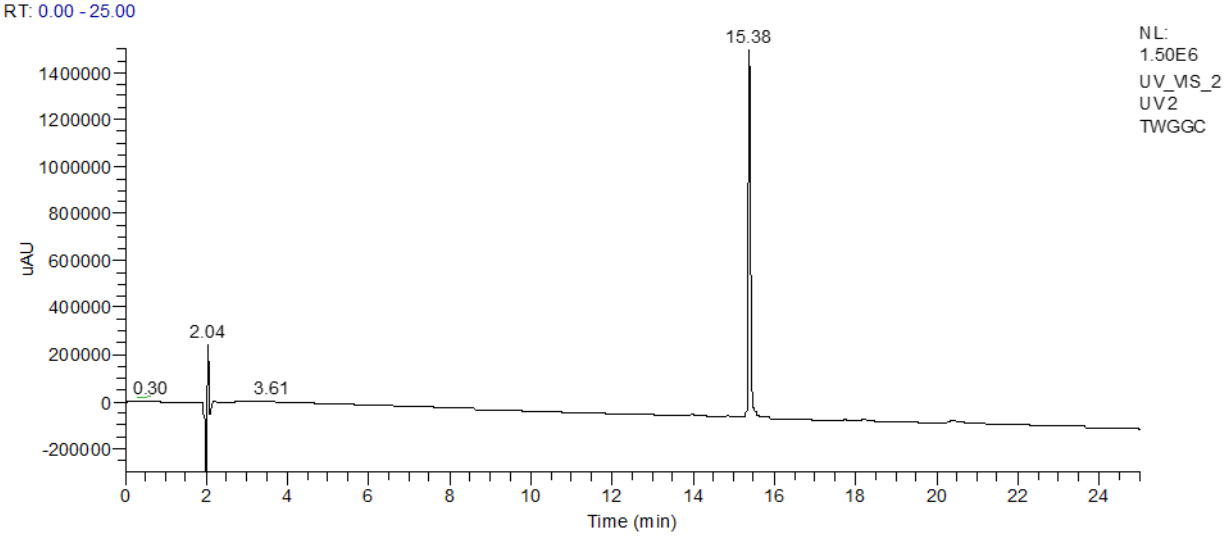
RT: 0.00 - 25.00
15.38
NL:
1.50E6
UV_VIS_2
UV2
TWGGC
2.04
0.30
3.61
uAU
Time (min)

Compound **18**

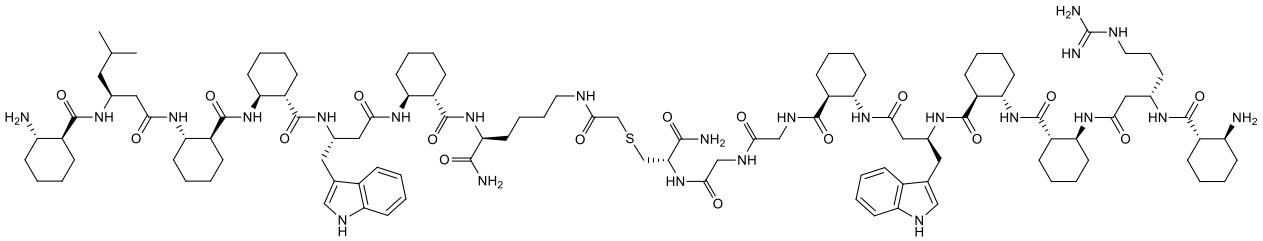

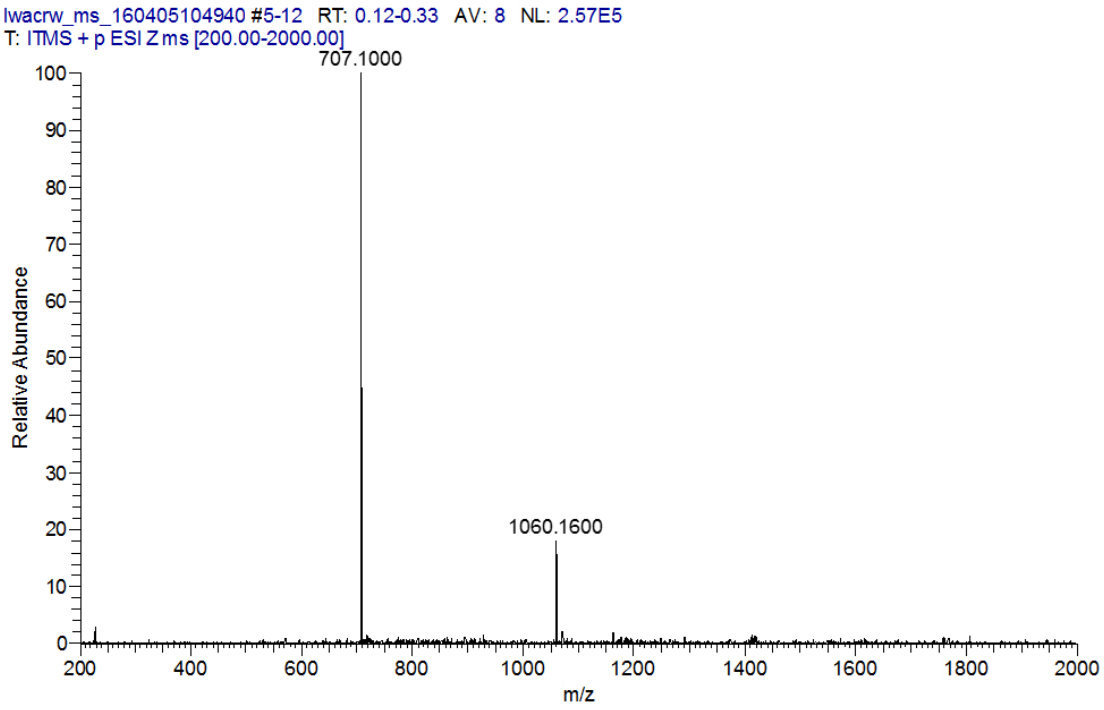
lwacrw_ms_160405104940 #5-12 RT: 0.12-0.33 AV: 8 NL: 2.57E5
T: ITMS + p ESI Z ms [200.00-2000.00]
707.1000
1060.1600
Relative Abundance
m/z

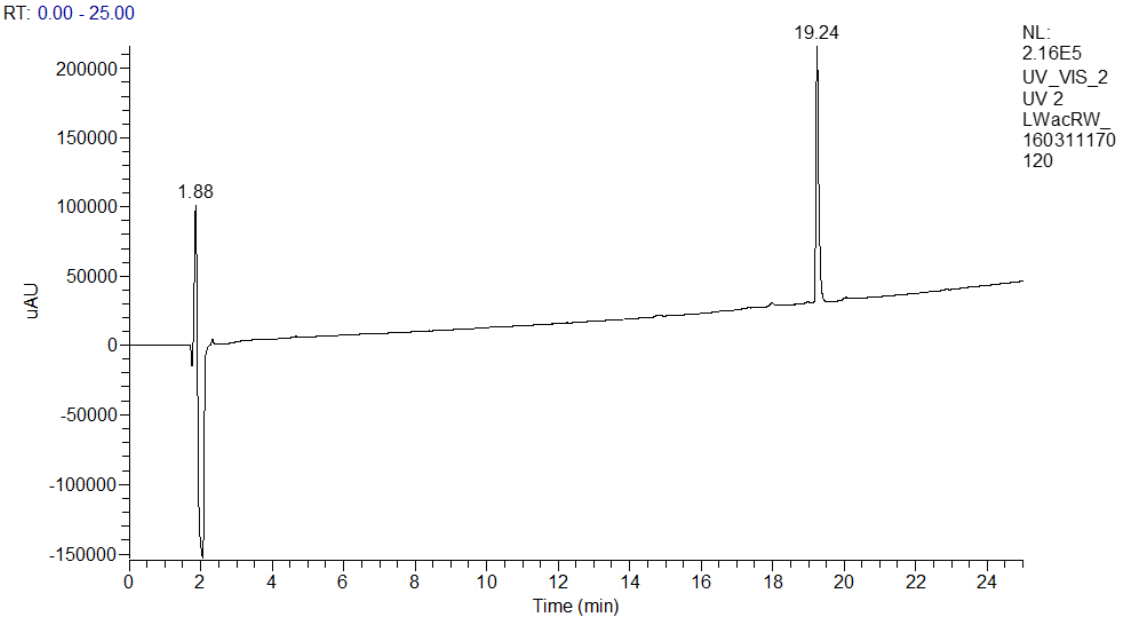
RT: 0.00 - 25.00
19.24
1.88
NL:
2.16E5
UV_VIS_2
UV 2
LWacRW_
160311170
120
uAU
Time (min)

TRPV1$_{784\text{-}798}$

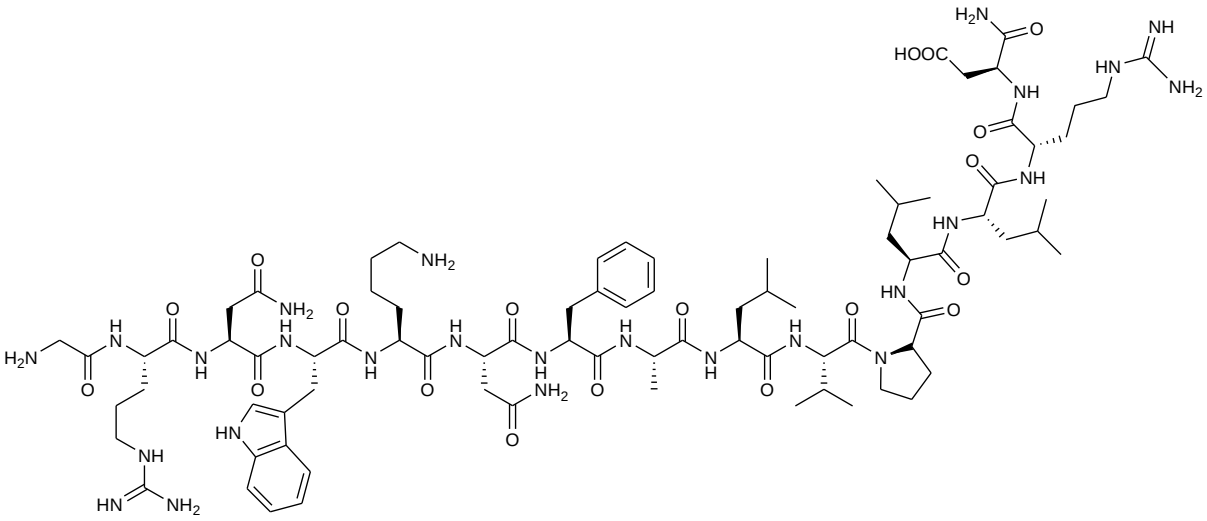

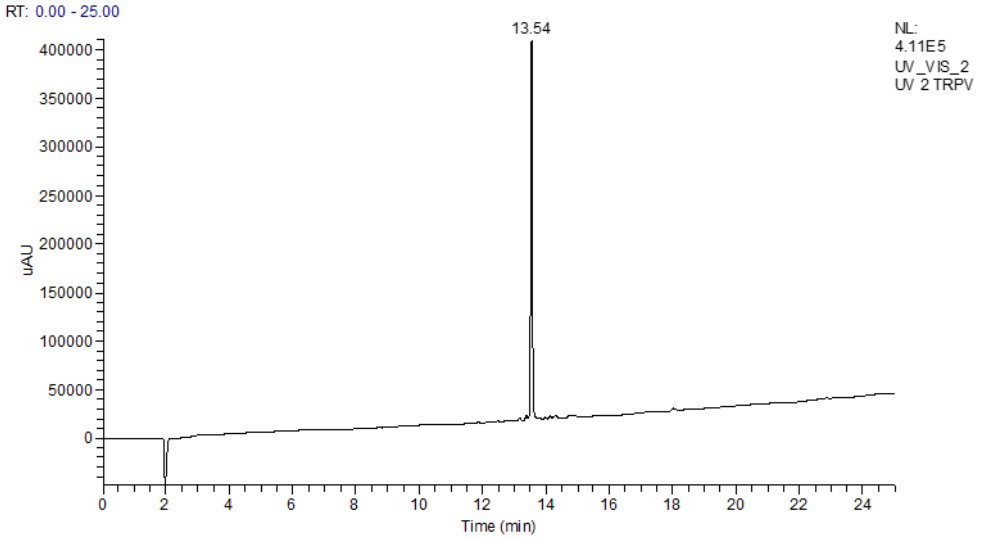

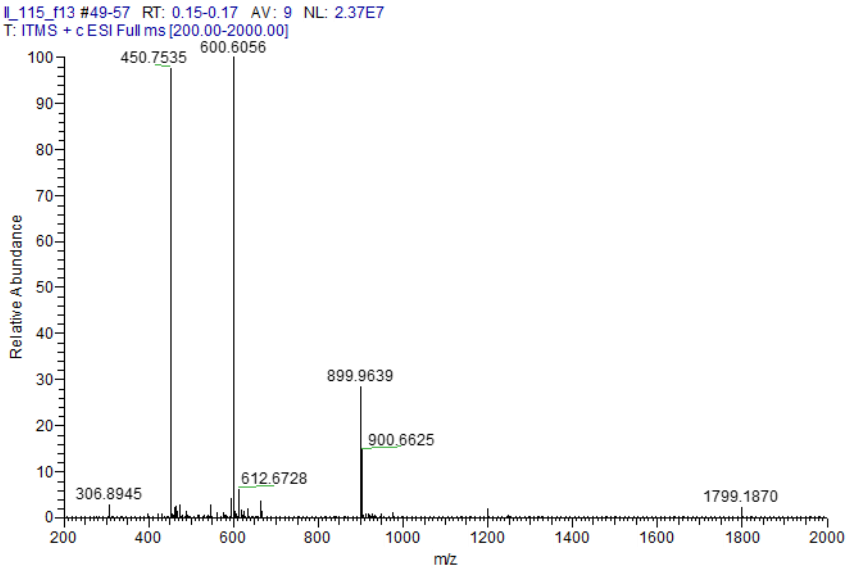
ll_115_f13 #49-57 RT: 0.15-0.17 AV: 9 NL: 2.37E7
T: ITMS + c ESI Full ms [200.00-2000.00]
450.7535
600.6056
899.9639
900.6625
612.6728
306.8945
1799.1870
Relative Abundance
m/z

References

1 Boutin, J. A. *et al.* Limitations of the coupling of amino acid mixtures for the preparation of equimolar peptide libraries. *Mol. Divers.* **3**, 43-60 (1997).

2 Gsponer, J. *et al.* A coupled equilibrium shift mechanism in calmodulin-mediated signal transduction. *Structure* **16**, 736-746 (2008).